REPORT DOCUMENTATION PAGE

AFRL-SR-AR-TR-03-

0342

1. AGENCY USE ONLY *(Leave blank)*	2. REPORT DATE	3. REPORT TYPE AND DATES COVERED
	14 AUG 03	FINAL REPORT - 01 SEP 95 - 31 MAY 02

4. TITLE AND SUBTITLE
AIR FORCE FAST CENTER FOR LIGHTWEIGHT STRUCTURAL MATERIALS AND PROCESSING

5. FUNDING NUMBERS
F49620-95-1-0512
62228D
4276/AS

6. AUTHOR(S)
DR PAUL O. BINEY
DR JIANREN ZHOU
DR LAURA CARSON

7. PERFORMING ORGANIZATION NAME(S) AND ADDRESS(ES)
PRAIRIE VIEW A&M UNIVERSITY FAST CENTER
P.O. BOX 4208
PRAIRIE VIEW, TX 77446

8. PERFORMING ORGANIZATION REPORT NUMBER

9. SPONSORING/MONITORING AGENCY NAME(S) AND ADDRESS(ES)
AFOSR/NL
4015 WILSON BLVD., SUITE 713
ARLINGTON, VA 22203-1954

10. SPONSORING/MONITORING AGENCY REPORT NUMBER

11. SUPPLEMENTARY NOTES

12a. DISTRIBUTION AVAILABILITY STATEMENT
APPROVE FOR PUBLIC RELEASE: DISTRIBUTION UNLIMITED.

12b. DISTRIBUTION CODE

13. ABSTRACT *(Maximum 200 words)*

The sixth year of the FAST Center at Prairie View A&M University was mainly devoted to the continuation of research in polymer processing and characterization, and mechanical and microstructural characterization, and a study of environmental effects on the properties of composites.

20030915 010

DISTRIBUTION STATEMENT A
Approved for Public Release
Distribution Unlimited

14. SUBJECT TERMS

15. NUMBER OF PAGES

16. PRICE CODE

17. SECURITY CLASSIFICATION OF REPORT	18. SECURITY CLASSIFICATION OF THIS PAGE	19. SECURITY CLASSIFICATION OF ABSTRACT	20. LIMITATION OF ABSTRACT
UNCLAS	UNCLAS	UNCLAS	

PRAIRIE VIEW A&M UNIVERSITY FAST CENTER SIXTH YEAR AND FINAL REPORT

By
Dr. Paul O. Biney, Director
Dr. Jianren Zhou, PI
Dr. Laura Carson, PI

GRANT No. F49620-95-1-0512

PRAIRIE VIEW A&M UNIVERSITY FAST CENTER
P.O. BOX 4208
PRAIRIE VIEW, TEXAS 77446
TEL: 936-857-4499

Submitted to

Dr. Charles Y-C. Lee
AFOSR/PKA
4040 Fairfax Drive, Suite 500
Arlington, VA 22203-1613

January, 2001 - May 31, 2002

Subcontractor: UDRI

ACKNOWLEDGEMENT

The success of the Sixth year and the period between January 1, 2002 and May 31, 2002 of the FAST Center was due to the dedication and support received from the University of Dayton Research Institute, the Wright Materials Lab, the Air Force Office of Scientific Research, and experts in the field of high temperature polymers.

On behalf of the FAST Center, I would like to express thanks and appreciation to Dr. Charles Lee, (the Air Force Office of Scientific Research Program Manager for the Center) for his support and advise during the year.

The University of Dayton Research Institute and its personnel have provided expert advice and training to the personnel at the FAST Center, that has made it possible to achieve the successes of the fourth year. In particular, Mr. Brian Rice has been extremely helpful and provided expert advice in setting up the FAST Center Labs, initiation of research topics, helped with graduate student thesis research and advisement, and substantially contributed to the quality of research through their regular participation in the telephone conference calls used as the forum for the FAST Center Technical committee during the year.

Dr. David Curliss from the Wright Materials Lab contributed immensely to the development and implementation of the formulation plans at the Center, and we commend him for his contribution.

Finally, I will like to express my deepest appreciation to the entire PVAMU FAST Center team, Dr. Jianren Zhou, Dr. Yang Zhong, Mr. Kevin Q. Lee, the graduate and undergraduate students, for their dedicated hard work that contributed to making the forth year a success.

TABLE OF CONTENT

LIST OF FIGURES

LIST OF TABLES

1. SUMMARY

The sixth year of the FAST Center at Prairie View A&M University was mainly devoted to the continuation of research in polymer processing and characterization, and mechanical and microstructural characterization, and a study of environmental effects on the properties of composites.

1.1 Research at PVAMU

1.1.1 Vibration Pressure Assisted Processing Method for Improving the Mechanical Properties of IM7/5250-4 Composite Patches Under Field Repair Conditions

A mini vibration press was designed and (1) used under vacuum bag for the patch repair and (2)used for investigating the effects of impacted pressure on the quality and properties of IM7/5250-4 composite. IM7/5250-4 composites panels processed using the mini vibration press with vacuum bag showed higher quality and properties than composites processed by only using vacuum bag. It also showed that the sum of vacuum bag pressure and impacted pressure (14.7 psi $\pm$ 5.23 psi) is much lower than that used on the base line one (over 100 psi), but the mechanical properties are nearly the same. This means that applying the alternating pressure on IM7/5250-4 prepreg panels is more effective than applying the static pressure on the panels in maintaining better resin flow, driving trapped air out, and making composite panels more compact. There is a need for further investigation of the relationship between frequency and properties. The mini vibration press for processing of IM7/5250-4 prepregs can be applied to other materials.

1.1.2 Test method Development and Characterization of Candidate Composites for Cryogenic Tank Application.

Currently the Air Force and NASA have programs in place to develop the next generation of materials for cryogenic applications, however, because of the lack of research in this area there is little in the way of standard screening tests for new materials short of building a small tank and testing it. In addition virtually no research has been conducted to evaluate long term exposure to cryogenic environments for composite materials.

The team lead by the FAST Center at Prairie View A&M University (PVAMU) and University of Dayton Research Institute (UDRI), in cooperation with AFRL\MLBC, are developing laboratory scale test procedures for characterizing the effects of cryogenic cycling on the properties of potential composite materials for cryogenic application. The team began with Cytec's IM7/5250-4.

The results of this research indicate that BMI IM7/5250-4 is a potentially good candidate material for cryogenic propellant tanks and further studies should be conducted in liquid oxygen and liquid hydrogen.

The research conducted at the University of Dayton Research Institute under a subcontract of the FAST Center has focused on developing a fundamental understanding of the formation of microcracks while loading composites at various temperatures and developing a test method to measure the resulting leakage rates of said composites. The results of testing on $[45/-45]_{2s}$ panels of IM7/52504 indicated that the fatigue life increased at -321°F and decreased at 300°F compared with room temperature. Testing results on thermal cycling induced microcracks showed that the stress level at the onset of transverse cracking decreased at –321°F

1.1.3 Ignition Behaviors of Graphite Composites Based on Bismaleimide and Epoxy

The ignition behaviors of different composite under various conditions including heating rate, isothermal temperature, oxygen concentration, sample size, and oxygen diffusion time were characterized. The results indicated that

1. It is carbon fibers that cause composite to ignite and burn. The neat 5250-4 resin does not ignite, it just decomposes oxidatively.
2. There is no obvious effect of sample size on the ignition and combustion temperatures if it is within the range of 2 to5 mg.
3. The higher the heating rate, the faster the ignition and combustion, but the higher the combustion temperature. Very slow heating rate, such as 1°C/min won't cause violent combustion of the composite.
4. High O2 pressure reduces the ignition and combustion temperatures.
5. Keeping the composite powders in high pressure O2 for up to 64 hours did not have any effect on ignition and combustion temperature for both powder and bulky samples.
6. The composite powders will not burn violently when heated up rapidly to certain temperature if the temperature is below 490°C.

1.1.4 Development of Automatic Cryo-High temperature Composite Cycling System

An Auto Cryo-Humid-HT cycling machine has been developed which can be used for long term automatic cycling of advanced composites between any two of the environments including liquid nitrogen temperature, high temperature up to 600 °F, 98% relative humidity at 40 °C, and room temperature. An advanced data acquisition system makes it possible to simulate operational envelopes within the environments listed above. The cycles are (1) thermal cycling of dry composites and (2) hygrothermal cycling of wet composites materials. Prior to the development of this auto cycling machine, the FAST Center developed a procedure for manual cycling. In this procedure, dry panels were thermally cycled (-320°F→74°F →302°F→74°F) one cycle per hour. In addition, saturated panels were hygrothermally cycled (-320°F→ 74° F → 302°F→ 74°F → overnight saturation @ 104°F/98%RH).

1.1.5 Development of a Composite Permeability Measurement System

The barrier properties of candidate cryogenic tank materials are of prime importance as we seek candidate materials for that application. Consequently, the FAST center has spent some time during the extension period to design, build, and test an experimental facility for measuring the permeability of composite materials.

1.1.6 Effects of Thermal Cycling on Permeability of IM7/5250-4 Composite laminates.

The effects of cycling composite panels of IM7/5250-4 between LN2 tempereature and 350oF on the gas transmission rate through the material were studied. The results indicate that even though microcracks developed on the composite surface, the microcracks did not develop in the inner plys, and thus the permeability was not very much dependent on the number of cycles. The helium gas transmission rate from the baseline to those for 1000 cycles were in the range of 25 to 2.6 scc/m^2/day.

1.2 Research at UDRI

The catastrophic failure of the X-33 cryogenic tank has reinforced the need of the composites community to develop predictive test methods for evaluating the performance of advanced composites in cryogenic environments. The principal materials-related cause (as opposed to potential design flaws) of the failure was permeation or leakage of liquid hydrogen gas through microcracks in the composite tank. This year our research has focused on developing a fundamental understanding of the formation of microcracks while loading composites at various temperatures and developing a test method to measure the resulting leakage rates of said composites.

1.3 Industrial Contract Projects

1.3.1 The Wyle Project

A composite material has been identified. Several panels have been fabricated and tested. The mechanical properties are used in finite element analysis. The test and analysis results satisfied the requirement. This work was done at the Future Aerospace Science and Technology (FAST) Center for Lightweight Structural Material and Composite Processing at Prairie View A&M University under a contract from Wyle Life Sciences.

1.3.2 The Raytheon Project

Several Superimide800 (polyimide resin/Astroquartz fibers) panels have been fabricated and tested. All sample sizes/data analysis have been done according to the applicable testing standard. All testing have been performed at three temperatures: Room temperature, 600°F, and 800°F. A final report have been submitted which included all aspects of processing and testing in great detail. This work was done at the Future Aerospace Science and Technology (FAST) Center for Lightweight Structural Material and Composite Processing at Prairie View A&M University under a contract from Raytheon Antenna/Nonmetallics Division, McKinney, TX.

1.4 Infrastructure Additions And Laboratory Development And Maintenance

1.4.1 Design and Construction of Cooling System for the Autoclave

A cooling water recycle system is connected with autoclave cooling system. Before autoclave cooling water directly goes down the sewer. The amount of total water saved for each processing is 14,400 gallons.

1.5 Overall Center Statistics

During the six year funding period of the FAST Center, 40 undergraduate students received financial aid and training, ten graduate students received financial aid and training, seven graduate thesis and M.S. degrees were granted to FAST center graduate students, over 25 papers were presented at technical symposium and conferences, seven first class research labs were developed at a cost of over $800,000, and six high school students participated in summer programs at the center.

2. RESEARCH PROGRAMS

The sections in this chapter describe the research conducted at the FAST Center during the sixth year and the extension period.

2.1 Vibration Pressure Assisted Processing Method for Improving the Mechanical Properties of IM7/5250-4 Composite Patches Under Field Repair Conditions

IM7/5250-4 composites are widely used as structural components for aircraft. These components will be in service for many years. During their service life, they may be exposed to various types of damage conditions. It is important to develop processing techniques for IM7/5250-4 prepregs that reduce the property knockdowns associated with the reduced temperature and pressure during field repair. Usually, if the damage area is smaller than one square foot, on-site or field repair technique will be employed to fix the damage. The on-site or field repair schemes involve applying several layers of prepregs on the damage area, using a heating blanket to cure the prepregs, and at the same time, applying pressure on the prepregs.. The pressure must be applied to the laminae so that there is intimate contact between the fiber layers. The closer the fiber the easier it is to transfer the load. There are several ways to applying pressure.

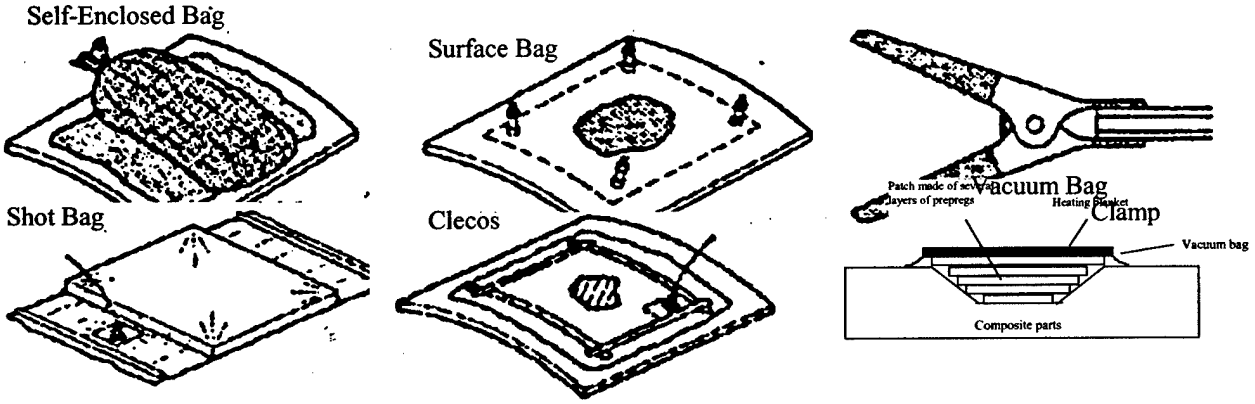

Figure 2.1 Patch Repair methods Used in Field Repair of Composites

Usually, in the case of field repair, the pressure provided by the vacuum bag is 14.7 psi (1 atm), which is much less than that in an autoclave where typical pressures are 100 psi and above. The base line in-plane shear strength of autoclave processed IM7/5250-4 is 90 MPa. Under field repair conditions, the In-plane shear strength is 70 MPa which is 22% lower than that cured in the autoclave. As result of these limitations, mechanical properties of IM7/5250-4 patch are reduced. Therefore, it is necessary to consider how to decrease the property reduction under vacuum bag pressure.

In field repair condition, a proposed mini vibration press can be used to help with resin flow, drive air out and thus reduce voids, making the composite patch more compact and improve its mechanical properties..

The work in this section includes (1) design of a mini vibration press with a controller to control the vibration frequency, and (2) investigation of the effects of the impacted pressure on the quality and properties of IM7/5250-4 composite.

2.1.1 Design of the Mini Vibration Press

The vibration is generated by a motor whose center of mass center 1.27 mm away from the rotation center. The motor itself turns around the rotation center. The design diagram is shown in Figure 2.2. The speed of the motor can be adjusted by using a voltage controller.

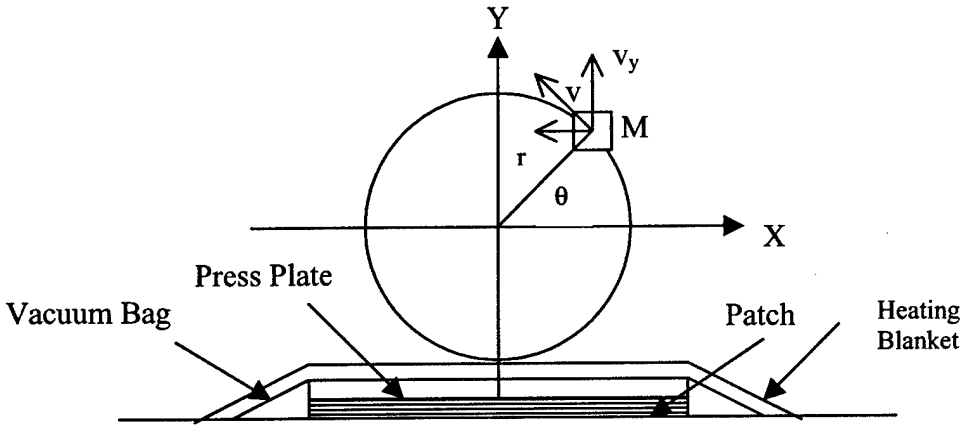

Figure 2.2. Diagram of Mini Vibration Press

2.1.2 Calculation of the impacted force

n is the motor rotation speed
n = 0~13000 rpm

M is the motor mass
M =1.0 kg

r is the distance between mass center and rotation center
r = 0.00127 m

v is the tangential component of the velocity.
$v = 2 \pi r n/60$ m/s

θ is the rotated angle
$\theta = 2 \pi t n/60$ radian

t is the time in sec.

v_y is the Velocity in the Y direction
$v_y = v\cos(\theta) = 2 \pi r n \cos(2 \pi t n/60)$ m/s

a_y is the acceleration in the Y direction

$$a_y = dv_y / dt = -r (2 \pi n/60)^2 \sin(2 \pi t n/60) \text{ m/s}^2$$

$a_{y\,max}$ is the maximum acceleration in the Y direction
This occurs when when $\sin(2 \pi t n/60) = \pm 1$

$$\text{Thus } a_{y\,max} = \pm r (2 \pi n/60)^2$$

$F_{y\,max}$ is the maximum impacted force in Y direction is listed in Table 1

$$F_{y\,max} = M a_{y\,max}$$
$$= \pm M r (2 \pi n/60)^2$$
$$= \pm (0.00127)(1.0)(2 \pi n/60)^2 \text{ N}$$

Table 2.1 The Maximum Impacted Force in Y -direction at Various RPM

RPM	Frequency (Hz)	Impacted Force (N)	Impacted Force (lbf)
1000	16.670	13.920	3.130
2000	33.330	55.640	12.510
3000	50.000	125.220	28.150
4000	66.670	222.630	50.050
5000	83.330	347.800	78.190
6000	100.000	500.870	112.600
7000	116.670	681.780	153.270
8000	133.330	890.390	200.170
9000	150.000	1126.950	253.350
10000	166.670	1391.350	312.790
11000	183.330	1683.410	378.450
12000	200.000	2003.470	450.400
13000	216.670	2351.370	528.610

2.1.3 Determination of the Best Time to Applying Vibration During Processing

The viscosity of resin changes from the beginning of heating to the end of certain isothermal time period as shown in Figure 2.3. The best time to apply vibration is very important. If vibration is applied too early (when the resin is liquid), the vibration will drive the resin out of the prepreg . If vibration is applied too late (when the resin has become solid which means it is at the maximum viscosity), vibration will be of no use in helping resin flow or void reduction. The best timing is when the viscosity is about 60% of the maximum and when the resin is still soft. At this viscosity, the vibration will not drive resin out of the prepreg and the impacted force can still compact the layers closer. The vibration lasts for about 1 hour, and is stopped when the resin viscosity is up to 90% of the maximum.

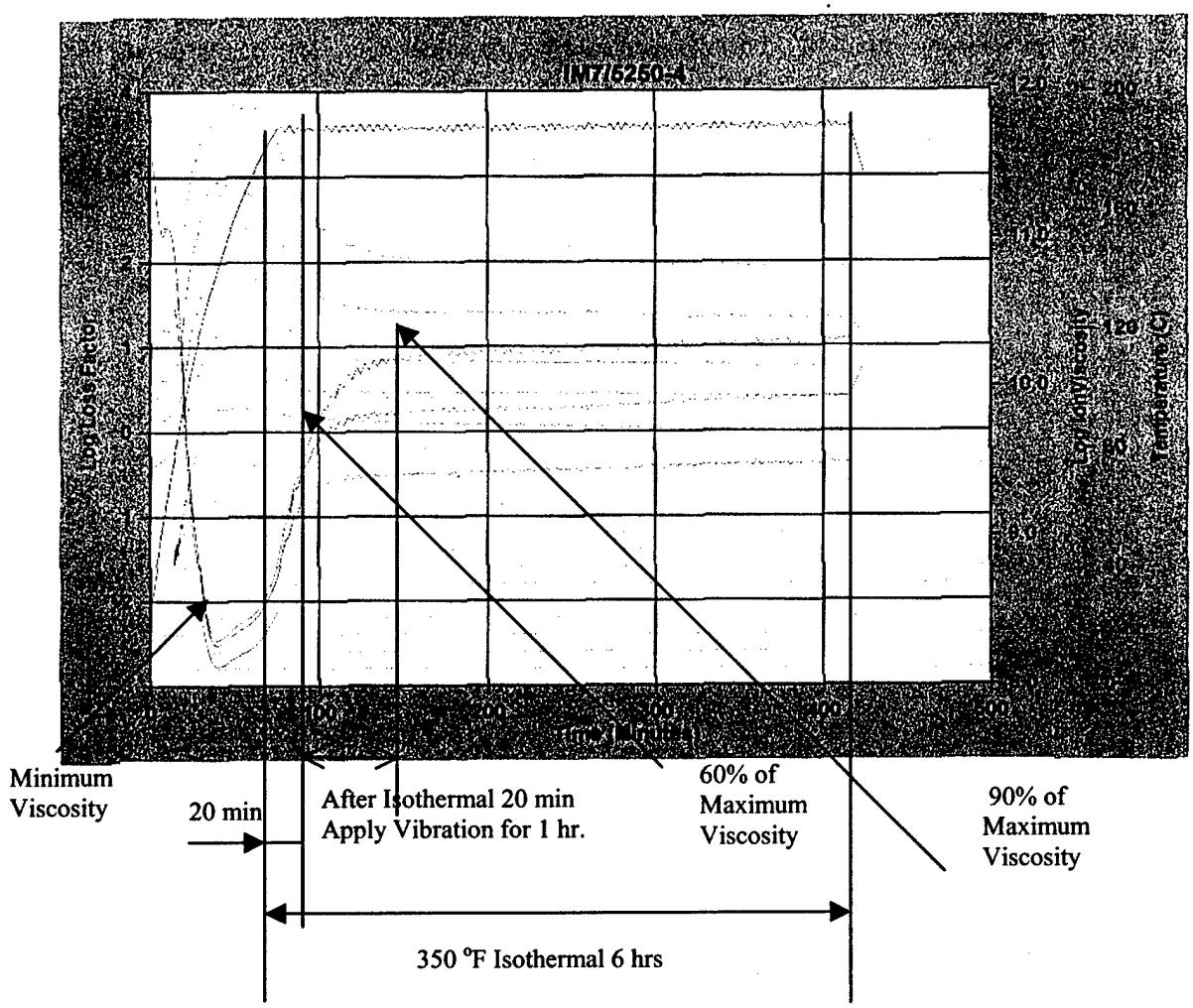

Figure 2.3. The Best Time to Apply Vibration

2.1.4. Experimental Application of the Vibration Pressure Assisted Processing Method

Material

The material used in this study was IM7/5250-4 prepregs from Cytec Fiberite with resin content of 32±2%.

Processing of Composite Panels

Laminates panels of $[\pm 45]_{2s}$ layup and measuring 8.5" x 8.5" (72.25 in^2) were processed using vacuum bag molding and the mini vibration press at 10,900 rpm. The impacted pressure is $\pm$ 5.23 psi (which is impacted force divided by panel area (378.45 lbf/72.25 in^2). The total applied pressure is the vacuum bag pressure plus impacted pressure (14.7 psi $\pm$ 5.23 psi). The curing process used is described under the FRC cure method in Table 2.2.

Characterization and Testing

Ultrasonic scan was used to inspect the quality of the manufactured composite panels. Panel density was measured by liquid displacement method. Dynamic mechanical analysis and in-plan

shear testing were performed to characterize the thermal and mechanical properties of the composites.

Test Matrix

Table 2.2 shows the test matrix used to analyze the effects of various cure processes on the properties of the resulting composites

Table 2.2 Test matrix and Resulting Mechanical Properties

Test No	Cure Method	n (rpm)	Time (hr)	In-Plane Shear Strength (Mpa)	Modulus (Mpa)
0	AC + PC (Base Line)		6 + 6	89.9 ± 6.07	18408 ± 2066
1	FRC		6	71.5 ± 2.3	21197 ± 3000
2	FRC + V	2270	6 + 1v	80 ± 1.22	26378 ± 2742
Need	FRC + V	5300	6 + 1v		
3	FRC + V	10900	6 + 1v	88.5 ± 4.635	29241 ± 4488

AC: Under Autoclave Over 100 psi,
5°F/min ramp-375 °F-6 hr
PC: Free Stand Post Cure 440 °F-6 hr

FRC: Field Repair Conditions
Pressure: 14.7 psi ,under Vacuum Bag
Ramp: 5°F/min to 350 °F
Isothermal hold at 350 °F for 20 minutes
Apply Vibration for 1 hour at 350F
Continue isothermal hold for additional 4 hours 40 minutes

V: Vibration,
Pressure: 14.7 psi ,under Vacuum Bag
Ramp: 5°F/min to 350 °F
Isothermal at 350 °F for 6 hr
Vibration: After isothermal 20min
applying vibration for 1 hr

2.1.5 Results of Property Improvements of IM7/5250-4 Composite Resulting from the Use of the Mini Vibration Press

Panel Density

Panel density can be used as a measure of crosslink degree and void content of composites. Higher density suggests better compaction of the material and lower void content. Therefore, the density of the IM7/5250-4 panels with various processing conditions was measured to compare the effect of the constant pressure and vibration on the degree of compaction of the composites. The results are shown in Figure 2.4. It was found that the density of the panels cured under mini vibration press was the highest and it was about 0.4% higher than that of the panels cured under autoclave. This indicates that panels processed under mini vibration press is more compact, which could mean less voids, than the panels cured by only using vacuum bag.

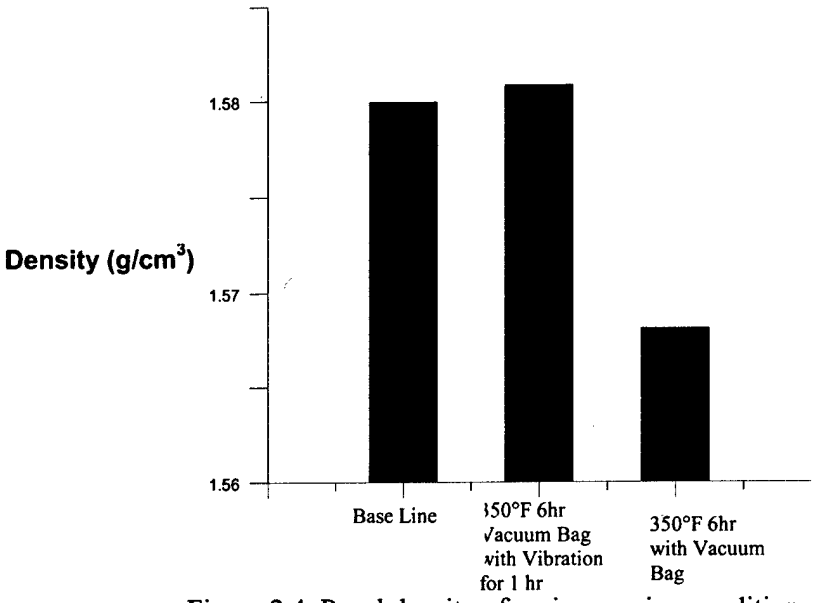

Figure 2.4. Panel density of various curing conditions

Quality of the Composite Panels

C-scan was used to inspect the quality of the composite panels and the results are shown in Figure 2.5. The quality of the panels was quantified by putting a grated transparency on the top of the C-scan graphs (as shown in Figure 2.5), counting the number of the grates according to their color, and calculating the average values based on the percentage of maximum given by the C-scan testing. The quantified panel quality versus cure conditions is shown in Figure 2.6. It was found that the quality of the panels cured with vibration was about 28.5% higher than that of the panels cured with the panels cured by only using vacuum bag.

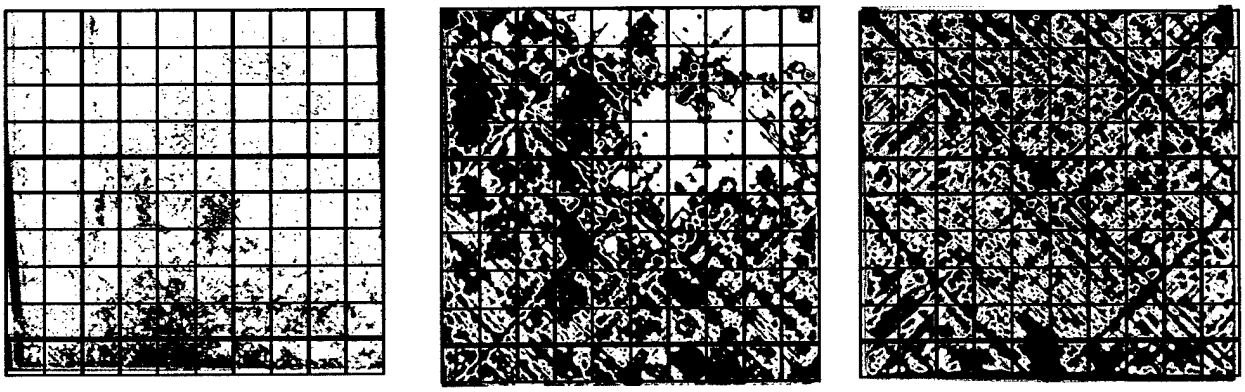

Base Line

350°F 6hr Vacuum Bag with Vibration at 182 Hz for 1 hr

350°F 6hr with Vacuum Bag

Figure 2.5. C-scan Results of Panels with Different Cure Conditions

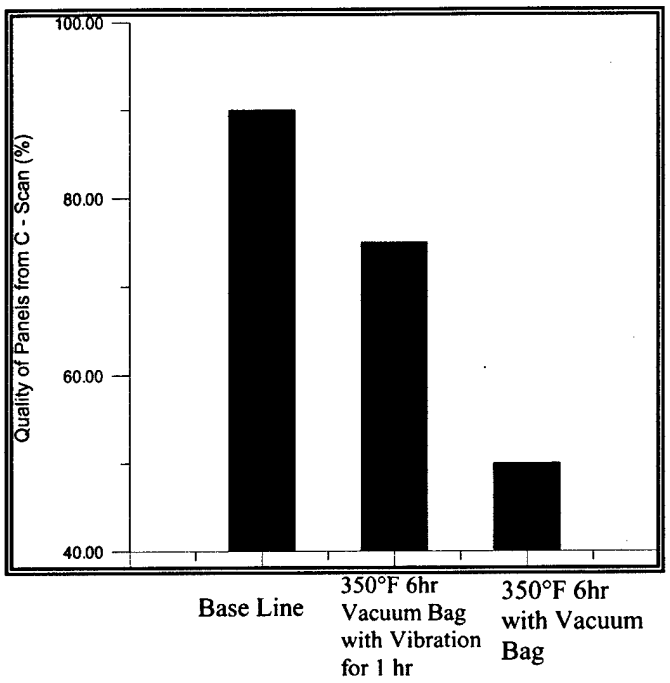

Figure 2.6. Panels Quality Based on Quantified C-scan Result

Mechanical Properties

In-plane shear tests were performed to investigate the effect of constant pressure and vibration on the mechanical properties of the composites. In-plane shear strength versus processing conditions of these panels are shown in Figure 2.7. It can be seen that composites processed using the mini vibration press showed in-plane shear strength that is nearly the same as the base line and 22% higher than the panel cured under vacuum bag.

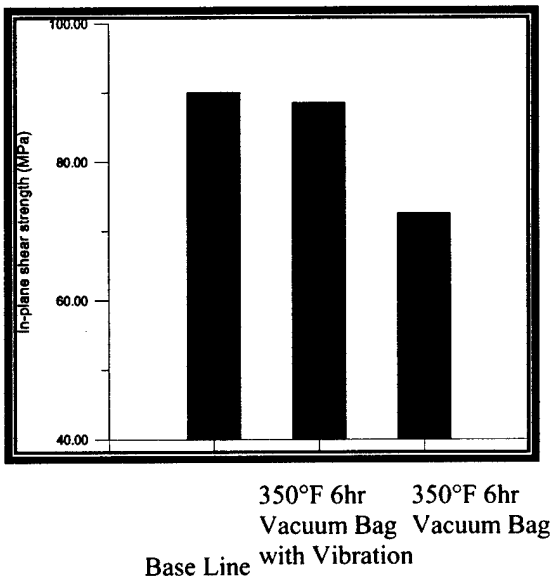

Figure 2.7(a). In-plane shearSstrength versus Processing Conditions

Thermal Properties

DMA was used to characterize the thermal properties of the composites. Glass transition temperature (Tg) based on the tan delta peak temperature in DMA was plotted with respect to processing condition in Figure 2.8. It can be seen that the T_g of the composite processed by using vibration was similar to that of the composite cured at ramp 5°F/min up to 350°F for 6 hours. They were all about 50°C lower than that of the baseline ones which has a high temperature postcure.

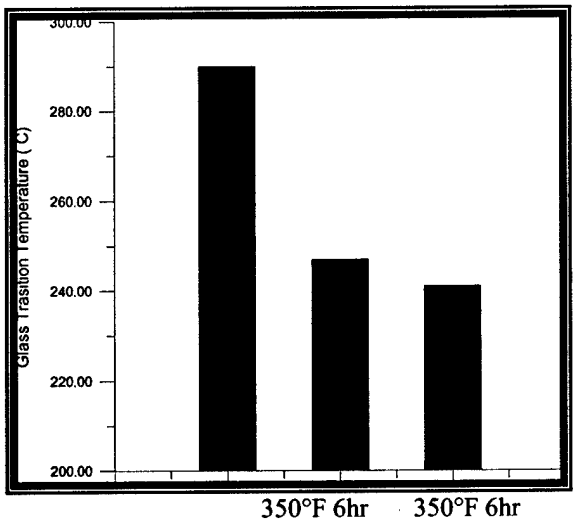

Figure 2.7(b). Tg as a Function of Processing Conditions

Conclusions

IM7/5250-4 composites panels processed using the mini vibration press with vacuum bag showed higher quality and properties than composites processed by only using vacuum bag. It also showed that the sum of vacuum bag pressure and impacted pressure (14.7 psi $\pm$ 5.23 psi) is much lower than that used on the base line one (over 100 psi), but the mechanical properties are nearly the same. This means that applying the alternating pressure on IM7/5250-4 prepreg panels is more effective than applying the static pressure on the panels in maintaining better resin flow, driving trapped air out, and making composite panels more compact. There is a need for further investigation of the relationship between frequency and properties. The mini vibration press for processing of IM7/5250-4 prepregs can be applied to other materials.

2.2 Test method Development and Characterization of Candidate Composites for Cryogenic Tank Application.

This section describes work done at the FAST Center and at UDRI on developing methods and using these methods to characterize candidate composites for cryogenic tank application

2.2.1 Summary of the Previous Work

Lightweight structures are important for reusable space launch vehicles (RLV) because there is a substantial trade-off between structural weight and payload. Planned single stage to orbit RLV's are sometimes referred to as flying fuel tanks because so much of the volume and mass of the vehicles is occupied by cryogenic liquid oxygen (LOX) and liquid hydrogen (LH2) tanks. It is critical that these tanks be made as lightweight as possible, thus there is a strong drive to fabricate them from advanced composite materials. While there is a limited experience base with actual LOX and LH2 tanks developed for programs such as NASP and X-33, there is virtually no understanding of how these tanks may endure hundreds of flight cycles. The extreme anticipated service environment may consist of ambient storage where water is absorbed by the structure, followed by quenching several hundred degrees in liquid oxygen and finally slowly heating to at least 150°C during re-entry. Another important issue is how an unlined composite tank would age in the presence of liquid oxygen. There is real concern that some materials may explode in this oxidizing environment.

Currently the Air Force and NASA have programs in place to develop the next generation of materials for cryogenic applications, however, because of the lack of research in this area there is little in the way of standard screening tests for new materials short of building a small tank and testing it. In addition virtually no research has been conducted to evaluate long term exposure to cryogenic environments for composite materials.

The team lead by the FAST Center at Prairie View A&M University (PVAMU) and University of Dayton Research Institute (UDRI), in cooperation with AFRL\MLBC, are developing laboratory scale test procedures for characterizing the effects of cryogenic cycling on the properties of potential composite materials for cryogenic application. The team began with Cytec's IM7/5250-4.

The principle objective for the first year was to develop and validate laboratory tests, which can be used to screen cryogenic tank materials. The research work conducted in the first year included (1) thermal cycling of dry composites and hygrothermal cycling of wet composites, (2) investigation of the effect of repeated thermal shock and phase change of absorbed water on composite morphology, and (3) non-destructive analysis and mechanical testing of IM7/5250-4 as a candidate composite for cryogenic tank material. The primary composite candidate used for the first year research was BMI based IM7/5250-4. The panels were oriented $[\pm 45°]_{2s}$ and layed up and processed by University of Dayton Research Institute. Two cycling conditions were used. Dry panels were thermally cycled (-320°F $\rightarrow$ 74°F $\rightarrow$ 302°F$\rightarrow$ 74°F), eight cycles per day for seven weeks. Saturated panels were hygrothermally cycled (-320°F$\rightarrow$ 74°F $\rightarrow$ 302°F$\rightarrow$ 74°F$\rightarrow$ overnight saturation at 104°F/98%RH), two cycles per day for eight weeks.

IM7/5250-4 material was selected as the initial material to investigate for potential cryogenic application due to its excellent properties. The new test methods were applied to this material.

The photomicrographs of IM7/5250-4 revealed no signs of microcracking when subjected to repeated thermal shock during thermal and hygrothermal cycling. It was believed that resin erosion occurring in LN2 was the cause for color variations in the c-scans. Even though the c-scans showed signs of decrease in quality as the number of cycle increased, the values remained on the higher end of the scale for both thermal and hygrothermal cycling.

IM7/5250-4 has, in the past, shown mechanical properties to be superior for high-temperature applications. The toughness increased as the number of cycles increased from 0 to 160 cycles during the thermal cycling, because the material showed a trend of failing at higher elongation values and higher shear strength values. This could be attributed to increased cross-linking due to thermal cycling process. After 160 cycles, the composite appears to become brittle because the material failed at very small elongation values and shear stress values. This can be due to possible excessive post-curing effects. After 200 cycles, the shear strength generally increased slightly and the elongation at failure also increased. Initially, the hygrothermally cycled panels decreased in toughness, but as the number of cycles increased the absorbed water increased the ductility and reduced the crosslinks in existence. A mechanism of dehydration resulting in further crosslinking may explain the increase in brittleness and the lower modulus at 40 cycles. After 60 cycles, the strength and toughness increase, but the modulus decreased. Overall, there was no significant variance in the deviations for the shear strength and modulus for both thermal and hygrothermal cycles. In both cycling conditions, the mechanical properties of IM7/5250-4 composite performed well as shown by high strengths and moduli.

The glass transition temperature was measured on the onset of the storage modulus curve. The Tg for the thermal curve showed a very small decrease in Tg until 200 cycles generally post-curing effect tends to increase Tg. However, the slight decrease in Tg indicates some competing effect introduced by the liquid nitrogen that tends to suppress the usual increase in Tg. The high-moisture environment during hygrothermal cycling caused hydrolysis in the BMI resin, which reduced Tg from the baseline. The hydrolysis reaction that occurs at elevated temperatures promotes molecular scission and slightly increases water diffusion. The ductility and toughness increased during hygrothermal cycling. However, because of the plasticizing action, elevated temperature performance was lowered slightly. The baseline glass transition temperature of the dry panel was 13.6°F higher than the baseline for the wet panel. The effect of absorbed moisture was the reason for loss in Tg for hygrothermal cycling. It was obvious that the temperature and humidity affected the Tg of the saturated panels, but did not significantly affect the mechanical properties of the hygrothermally cycled specimen.

The diffusion coefficient was found to be 9.53×10^{-8} $mm^2/s°C$ based on a single-phase Fickian moisture absorption model. The increase moisture absorption can be attributed to the hydrolysis reaction, which involves chain scission thereby increasing moisture diffusion as cycling continued.

The results of this research indicate that BMI IM7/5250-4 is a potentially good candidate material for cryogenic propellant tanks and further studies should be conducted in liquid oxygen and liquid hydrogen.

The research conducted at the University of Dayton Research Institute under a subcontract of the FAST Center has focused on developing a fundamental understanding of the formation of microcracks while loading composites at various temperatures and developing a test method to measure the resulting leakage rates of said composites. The results of testing on $[45/-45]_{2s}$ panels of IM7/52504 indicated that the fatigue life increased at -321°F and decreased at 300°F compared

with room temperature. Testing results on thermal cycling induced microcracks showed that the stress level at the onset of transverse cracking decreased at –321°F.

2.2.2 Microstructural Analysis of Cycled Composites

The overall objective of this research is to develop and validate laboratory tests which may be used to screen candidate cryogenic tank materials and aid in development of life-time prediction models. The FAST Center has been working on investigating the effects of cryogenic/elevated temperature cycling on the morphologies and properties of IM7/5250-4 composites. C-scan results of the samples before and after the cryogenic/elevated temperature cycling showed signal attenuation, especially in moisture saturated samples, indicating that the cycling caused some kind of tiny defects that uniformly distributed across the whole panel. Optical was used to find out whether the cycling had caused microcracks in the composite. The results indicated no microcracks in the panels undergone up to 280 dry cycles and 80 wet cycles.

Then, scanning electron microscopy (SEM) was used to investigate the morphology of the composite. The outmost surface before testing of and the fracture surface after testing were observed. The SEM used was a Joel JSM-6400 and the accelerating voltage used was 15 kV.

The results are shown in Figure 1. When the magnification reached 10,000, spheres about less than half micron were observed on the outmost surface of cycled specimens (Figure 1c and 1e) while no such spheres could be seen for baseline samples (Figure 1a). Comparing the size of the spheres on the surface of thermally cycled specimens (Figure 1c) and hygrothermally cycled specimens (Figure 1e), it can be seen that the spheres in former situation were slightly larger than in the later. Morphology of the fracture surface of the composite showed that hygrothermally cycled specimen had more fragmentation in matrix resin (Figure 1f) than baseline sample (Figure 1b) and thermally cycled samples (Figure 1d).

The SEM results indicated that the defects shown in c-scan images might result from the formation of the micro particles on the surface of the cycled specimens, which may cause less compact of the material. However, the nature of the micro particles and the reason for their formation after temperature cycling need further investigation.

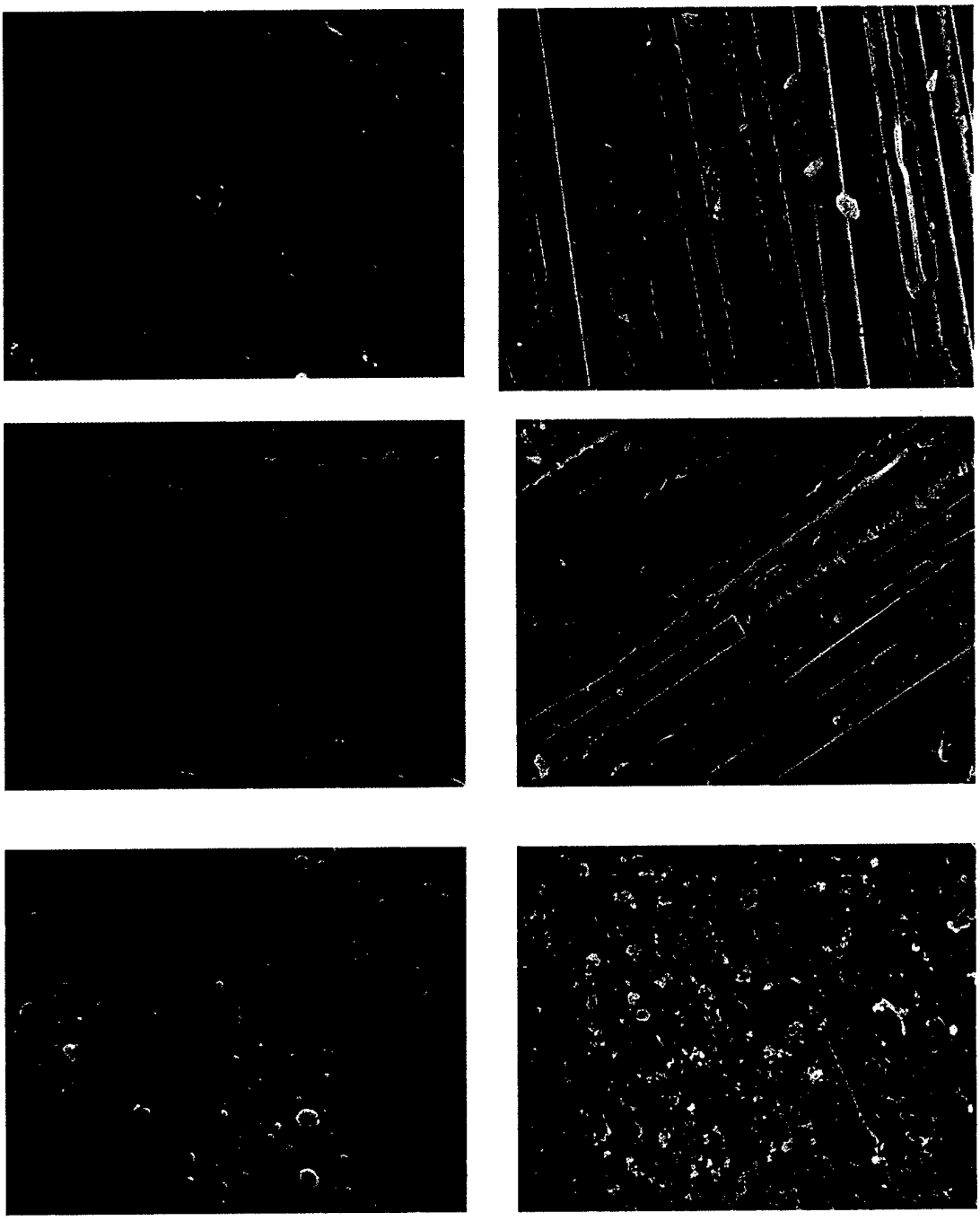

Figure 2.8 SEM photographs of IM7/5250-4 composite. (a) and (b): Outmost surface and fracture surface of baseline sample, respectively; (c) and (d): Outmost surface and fracture surface of sample after 280 dry cycles; (e) and (f) Outmost surface and fracture surface of sample after 80 wet cycles.

2.3 Ignition Behaviors of Graphite Composites Based on Bismaleimide and Epoxy

Graphite composite is a prospective material for cryogenic tank because of its lightweight. The FAST Center is conducting research on screening and characterization of composite materials for cryotank applications. While the research concentrates on studying the effects of cryogenic/elevated temperature cycling on the microstructures, mechanical properties, and permeability of the composite, there is another major concern for the composite cryotank, that is the ignition behavior in oxygen environment. When the reusable launch vehicle is being maintained, foreign objects such as a loose piece of hardware may fall into the cryotank. The kinetic energy of the falling object may create a localized temperature increase. With the oxygen environment around, this sudden temperature increase might cause ignition of the composite. Therefore, it is important to study the ignition and combustion characteristics of candidate composites for cryotanks.

As this project is mainly laboratory scale screening, we tried to avoid working with liquid oxygen but attempted to simulate the actual situation. We used both composite powders and small bulks as testing samples. The samples were heated in an oxygen pressurized DSC cell. The ignition behaviors of different composite under various conditions including heating rate, isothermal temperature, oxygen concentration, sample size, and oxygen diffusion time were characterized.

2.3.1 Experimental Description

Materials: Currently, we are studying the ignition behaviors of several candidate composite materials for cryogenic tank applications, including IM7/5250-4, IM7/977-2, IM7/862, AS4/PEEK, AS4/3501-6, and epoxy-organoclay nano-composites. The composites were ground into fine powders but some IM7/5250-4 composite samples were cut into small bulks to study the sample geometry effects.

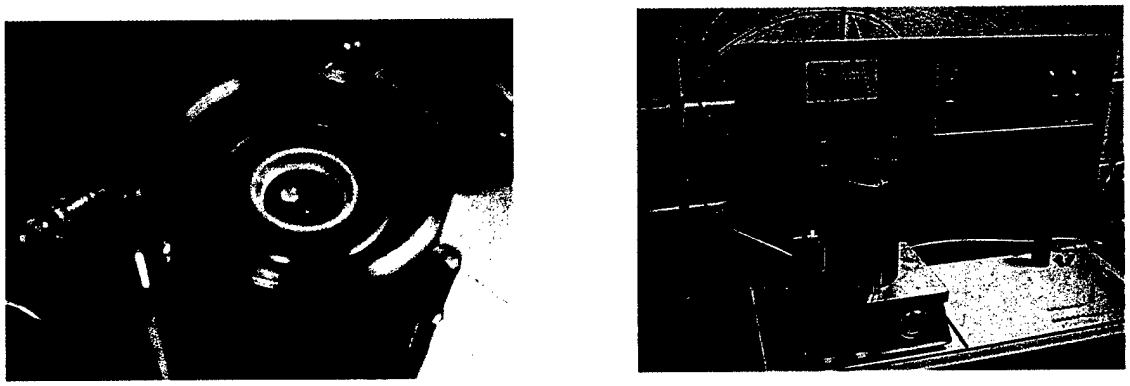

(a) (b)

Figure 2.9 Pressure DSC cell. (a) Sample, (b) Out-look

Testing Procedures: TA Instruments' DSC 2910 with pressure cell and compressed oxygen tank was used in this study as shown in Figure 2.9. First, we tried to close the sample pan as in ordinary DSC tests but found out that composite powders would not ignite because of insufficient contact with oxygen. So, we ran all the tests in open pans to permit good contact between sample and the oxygen environment.

2.3.2 Results and Discussion

This section contains the results of ignition tests for selected materials.

Characteristic DSC Curves of Combustion:

The characteristic DSC curve for combustion of composite powders is a sharp exothermal peak accompanied with a sudden jump of temperature as shown in Figure 2.10. After the tests, the composite samples were found to burn out completely (nothing left in DSC pans). There is also an exothermal slope on DSC curves just before the sharp peak. It was found that if the test was stopped after this exothermal area but just before the heat flow jump, the entire sample was still left in the DSC pan and no changes could be seen visually.

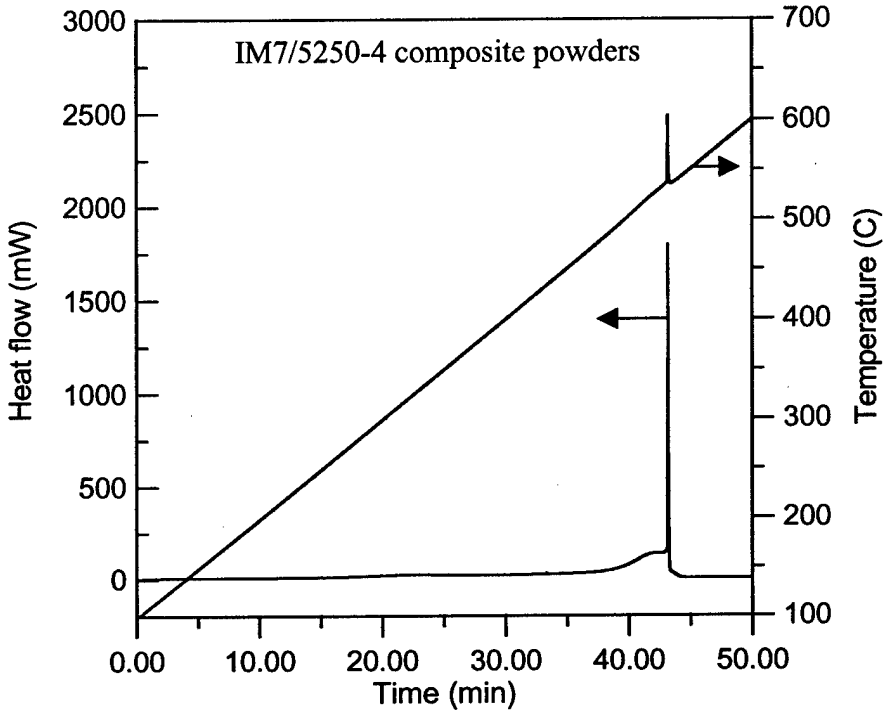

Figure 2.10 DSC curve of IM7/5250-4 composite combustion in oxygen pressurized DSC

Definition of Ignition and Combustion Temperatures

There are several featured temperatures on the DSC curves of the combustion reaction of the composite samples. We defined the starting temperature of the sharp exothermal peak as combustion temperature. The corresponding starting point of the temperature jump was referred as combustion temperature based on temperature curve, as shown in Figure 2.11.

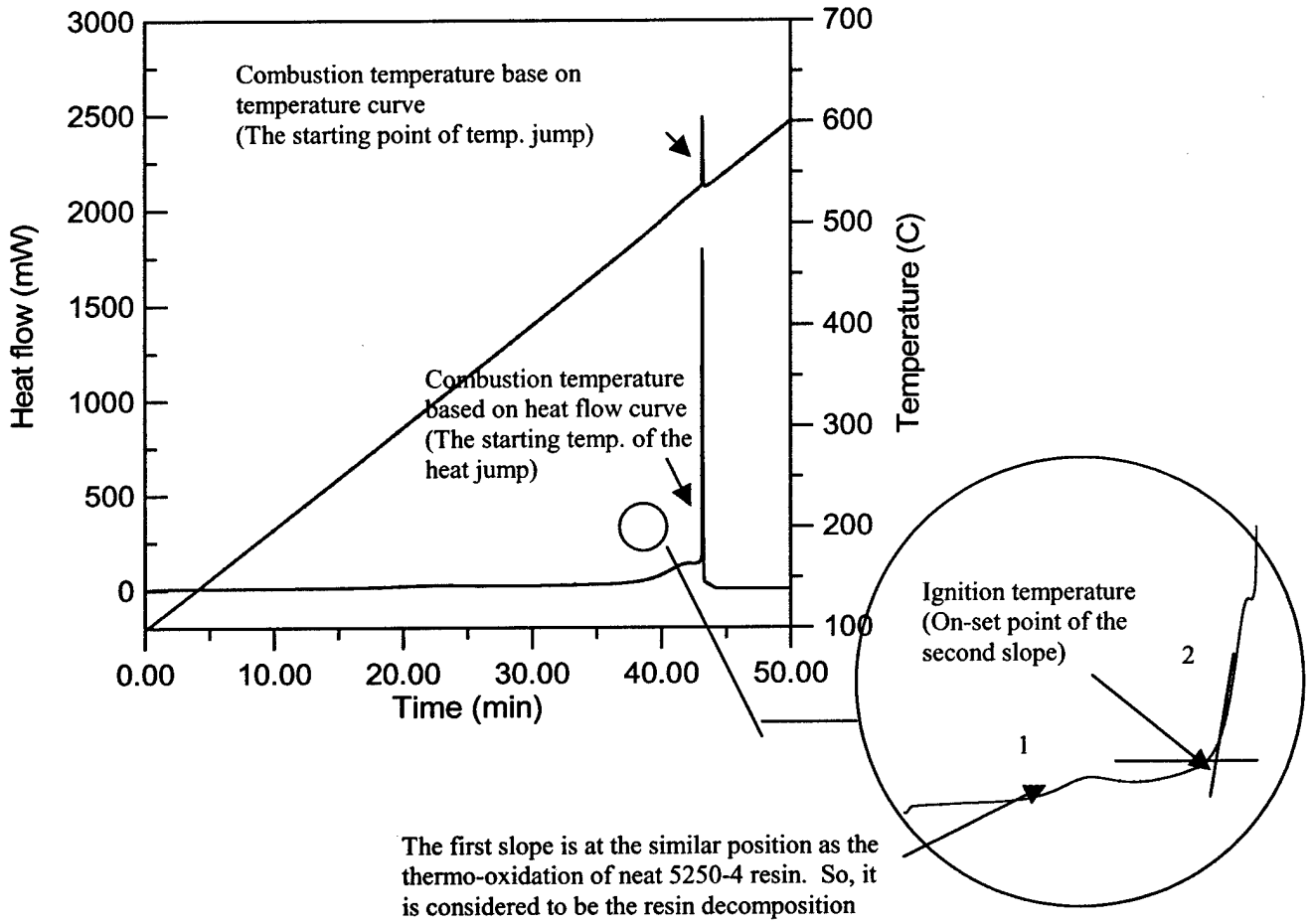

Figure 2.11 Definition of Combustion and Ignition Temperatures

For IM7/5250-4 composite, an enlarged view of the slope area before combustion is shown in Figure 2.11 indicated two slopes, as marked in the bottom circle of Figure 2.11. The starting point and the plateau position of the first slope is very similar to the broad oxidative exotherm of the pure 5250-4 resin. Therefore, the first slope was attributed to the resin oxidative decomposition. The second slope, which is just before the heat flow jump, was considered as the ignition of the sample. The onset of the second slope, as shown in Figure 2.11, on the DSC diagram of the composite was defined as ignition temperature in this report. However, it was found that for composite samples other than IM7/5250-4, the curves before combustion are not as simple as that of IM7/5250-4. Therefore, the ignition temperature can only be defined for IM7/5250-4 system. Thermogrametry and DSC-GC may be needed for a detailed study of the reactions that occurred in this period.

Ignition and Combustion of Pure Resins

Pure epoxy and bismaleimide resins were tested under various heating rates and the results are shown in Figure 2.12. BMI 5250-4 resin showed a lower ignition and combustion temperature than Epoxy 862. Further, the ignition pf the resin is highly dependent on the heating rate. 5250-4 resin only showed a broad oxidative decomposition peak at a heating rate of 10°C/min under an oxygen pressure of 600 psi (Figure 2.12b) while it combusted at 50°C/min.

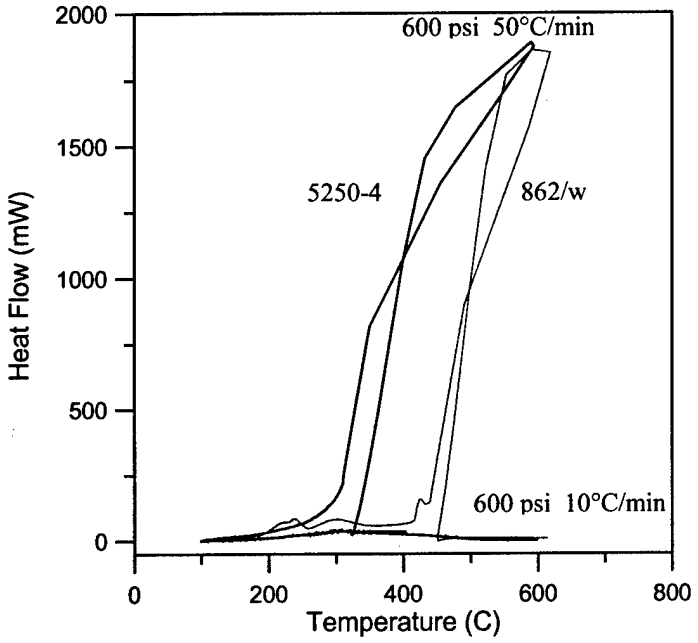

(a) Whole curves

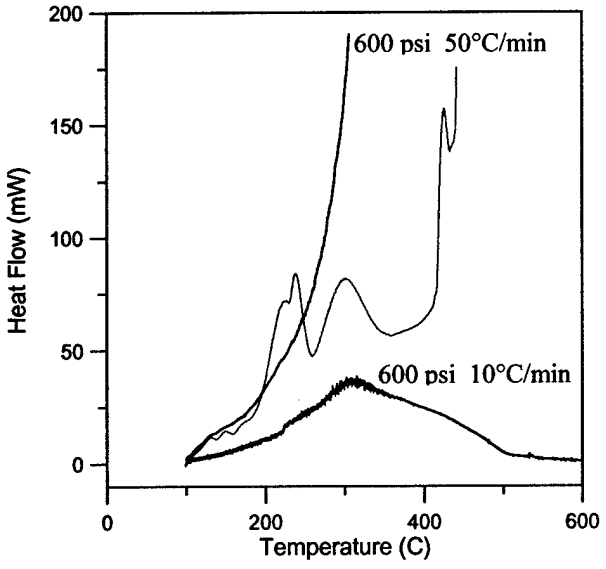

(b)Reduced scale

Figure 2.12 DSC Curves of neat 5250-4 and 862 resins

Ignition and Combustion Behaviors of Various Composites

The combustion temperatures based on temperature jump for various graphite fibers, resins, and composites are listed in Table 2.3. The data showed that the combustion temperature of composite is lower than that of pure fiber, indicating impregnation of resin decreases the combustion temperature of the fiber, but the combustion temperature of composite is much closer to that of the fiber than to the resin. The data also indicated that composite based on PEEK had relatively lower combustion temperature compared with composites based on epoxy and bismaleimide. This could be due to the ether bonds in the backbone of PEEK which are relatively vulnerable to high temperature.

Table 2.3 Combustion temperatures for composites based on various resins (O_2 pressure: 600 psi, Heating rate: 50°C/min)

Materials	Combustion temperature (Starting point of the temperature jump) (°C)
AS4	551.65
AS4/PEEK	447.69
AS4/3501-6	536.78
IM7*	560.06
IM7/977-2	534.54
IM7/862	533.64
IM7/5250-4	541.98
862	441.81
5250-4	311.73

* Tested with O_2 pressure at 450 psi

Effects of Organoclay Content on the Ignition of Epoxy

Organoclays are used to fill epoxy to form nano-composites. These nano-composites are another type of cryo-tank candidate based on the idea that nano organoclay particles filled resin may have less chance to crack at dramatic temperature changes and the nano particles may have a barrier effect for the cryogenic liquid permeating through the material. The ignition behaviors of epoxy containing different organoclays and various percentage of organocly were tested in this study and the results are listed in Table 2.4. The results showed that the addition of organoclay significantly reduced the combustion temperature, especially the addition of sodium montmorillonite which caused more than 200°C drop of the combustion temperature of epoxy. The reason for the drop of combustion temperature is that the organoclays are treated by chemicals containing short hydrocarbon chains. Hydrocarbon chains break into small hydrocarbon molecules when heated up and the small hydrocarbon molecules are very easy to burn in the oxygen environment.

Table 2.4 Combustion temperatures of epoxy containing various organoclays (O_2 pressure: 600 psi, Heating rate: 50°C/min)

Materials	Combustion temperature (°C) (Starting point of the temperature jump)
Pure 862/w	441.81
I30E*	218.37
1%I30E/862/w	402.63
3% I30E/862/w	352.47
6% I30E/862/w	409.66
IM7/6% I30E/862/w	516.26
IM7/862/w	533.64
6%SC8/862/w	232.78

* Under 520 psi O_2

We studied the ignition and combustion behavior of IM7/5250-4 composite under various conditions by the DSC tests. Summary of the DSC results for IM7/5250-4 powders are listed in the appendix of this report. The effects of sample size, heating rate, oxygen pressure, isothermal temperature, and holding time in oxygen on the ignition and combustion behaviors of the composite are discussed below.

Effects of samples size:
Since the ignition and combustion of powders are very sensitive to their pile and amount, DSC tests for the composite powders with different sample amount were run to check the variation of ignition and combustion temperature with sample size. The results are shown in Table 2.5 and also listed in Table 2.9.

Table 2.5 Effects of Sample Amount on the Pressure DSC Results of the Combustion of IM7/5250-4 composite Powders

Conditions	Sample amount	Ignition temperature (°C)	Combustion temperature (°C) (Starting point of the sharp exothermal peak)	Combustion temperature (°C) (Starting point of the temperature jump)
Heating rate: 10°C/min	1.8 mg	483.61	535.68	539.20
	3.4	474.31	535.05	535.80
	4.1	479.55	531.39	534.71
O_2 300 psi	5.3	479.69	534.13	535.80
	8.5	401.56	486.27	511.48
Heating rate: 50°C/min	2.4	435.40	515.54	556.38
	2.6	434.57	514.92	572.84
	3.0	433.80	511.50	570.14
O2 300 psi	3.6	433.84	515.42	566.67
	4.2	431.33	511.50	556.38

The results showed that for the composite powders tested at certain heating rate and oxygen pressure, the sample size did not influence the testing results if it is within the range from 2 to 5 mg. If the sample size is over 8 mg, there is an obvious drop in the ignition and combustion

temperatures. Also, the sudden temperature jump exceeded the limit of the equipment. Consequently, we used sample size between 2 and 5 mg in all the DSC tests for this study.

Effects of oxygen pressure:

The DSC results of the ignition and combustion temperature of IM7/5250-4 composite powders under different oxygen pressures from 20 psi to 600 psi are listed in Table 2.9. Figure 2.13 shows the DSC curves of these tests. The heat release in oxygen under 20 psi was much less than the others, although the samples burned out completely just like the others. This indicates that the composite will ignite but not burn violently when heated up in oxygen with a pressure lower than 20 psi. The ignition temperature and combustion temperature of the composite decreased with increase in oxygen pressure. The ignition and combustion temperatures were plotted against the oxygen pressure as shown in Figure 2.14.

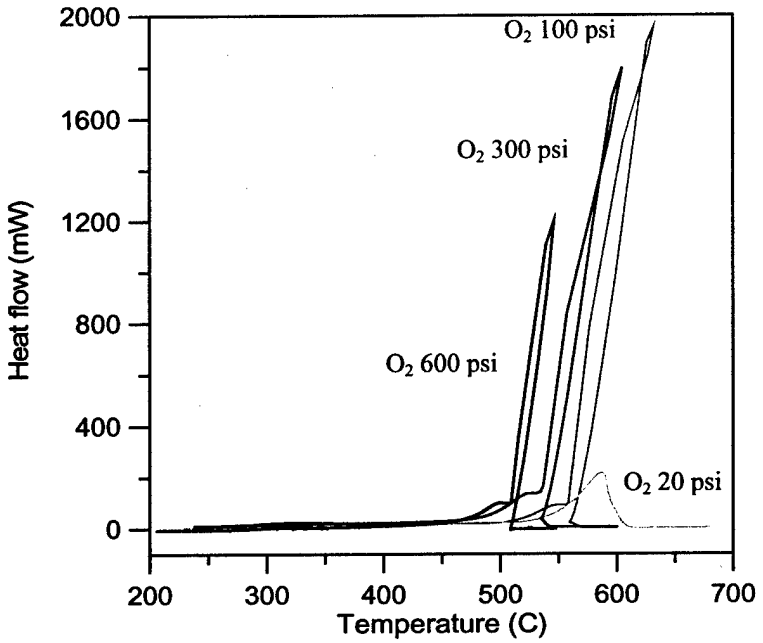

Figure 2.13 DSC curves of IM7/5250-4 powders under various oxygen pressure

Effects of heating rate:

Combustion is a process during which a material reacts violently with oxygen. The reaction temperature is highly dependent on how the material is heated. A series of DSC test were performed to study the variation of heat flow, ignition and combustion temperatures with heating rate. The DSC curves of IM7/5250-4 composite powders under various heating rate are shown in Figure 2.15 and the results of ignition and combustion temperatures are also listed in Table 2.6 and in Table 2.9

Figure 2.15b is an enlarged graph for the heat flows of the composite powder before combustion. It can be seen that with decreasing heating rate, the resin oxidative peak was depressed, which is probably because the oxidative decomposition was so slow under the low heating rate that the DSC could not capture its reaction heat. As mentioned above, thermogrametry and DSC-GC may be needed for further understanding. On the other hand, this phenomenon indicates that the oxidative decomposition of the resin becomes more severe if the composite is heated up at a

faster rate. The DSC curves also showed that the heat flow jump of the sample heated with 1°C/min was much lower than those heated up at higher ramp rate, indicating that the composite will not burn violently under very slow heating rate, although it will decompose completely.

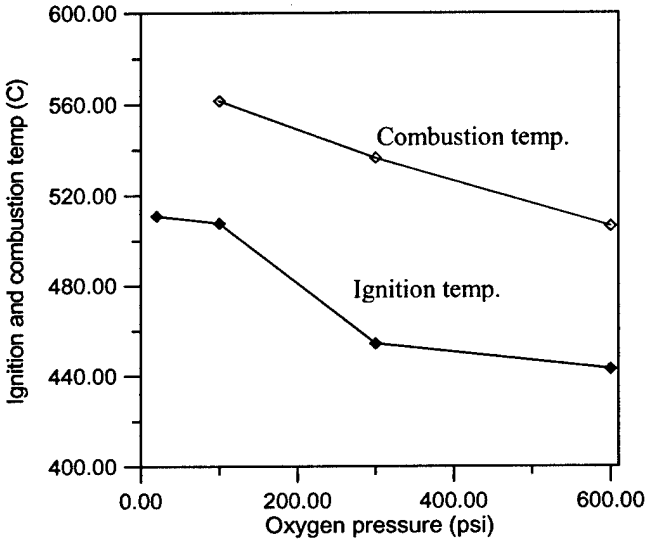

Figure 2.14 Ignition temperature and combustion temperature versus oxygen pressure

Table 2.6 lists the ignition and combustion temperatures of the composite powders under different heating rates. To show a clearer relationship between the ignition and combustion temperatures and the heating rate, the data were also plotted in Figure 2.16.

From the starting point of temperature jump, it was found that with an increasing heating rate, the combustion temperature increased but the time to reach the combustion was shortened. This tendency was more obvious in the lower heating rate range, as can be seen in Figure 2.15. When the heating rate increased from 20°C/min to 50°C/min, the tendency was becoming less obvious. The samples heated at 50°C/min showed a relatively lower ignition temperature and combustion temperature based on exotherm compared with those of the others. This is because the second slope of the sample with 50°C/min heating rate is lower. This means that ignition under 50°C/min occurs earlier but was less violent than that of the samples heating rates lower than this. The difference between combustion temperature and ignition temperature of the sample at 50°C/min heating rate is larger than that of the others, indicating a longer retardant period between ignition and combustion.

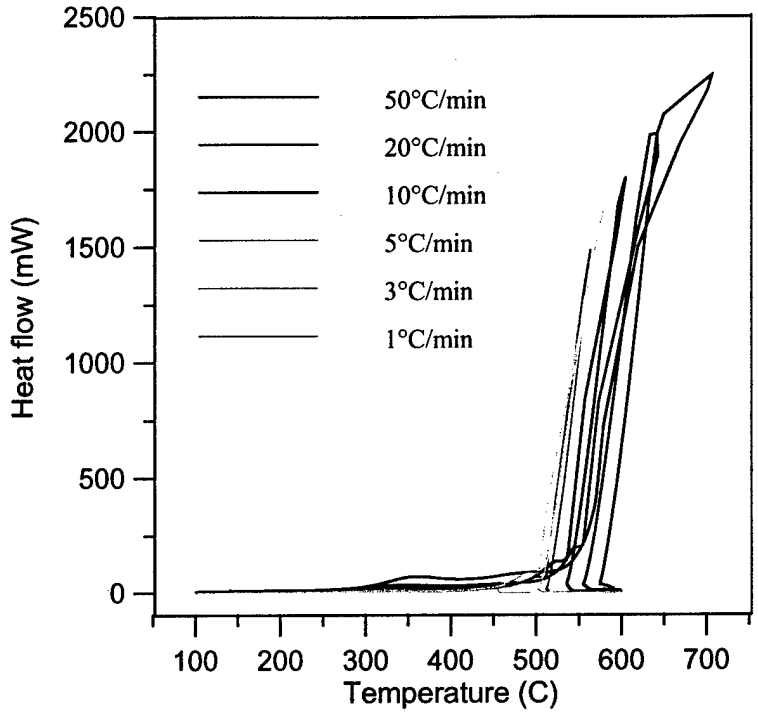

(a) Whole curves

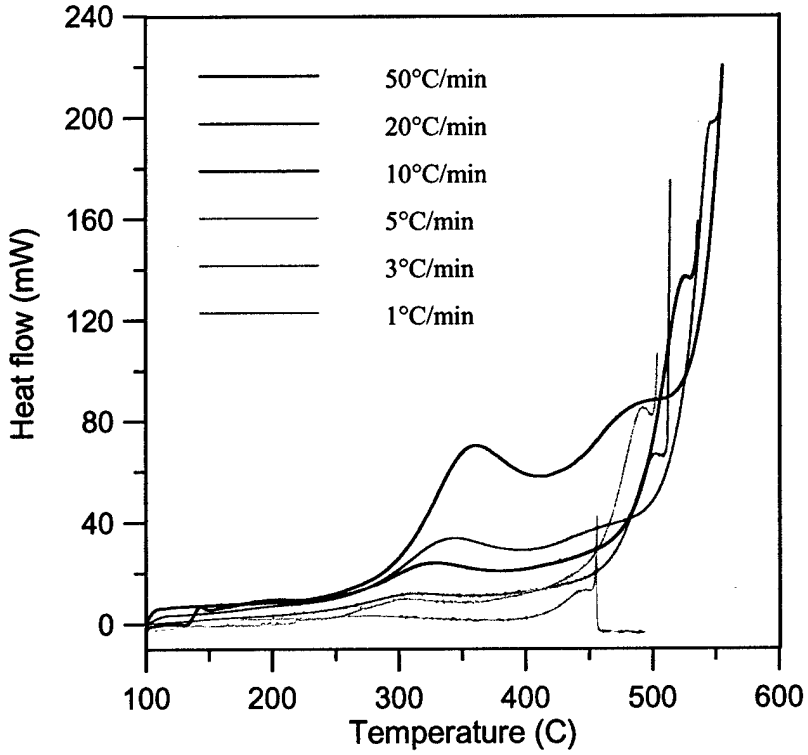

(b) Reduced scale of heat flow before combustion

Figure 2.15 DSC curves for IM7/5250-4 composite powders under different heating rates

Table 2.6 Ignition and combustion temperatures of IM7/5250-4 composite powders under different heating rates

Heating rate	Ignition temperature (°C)	Combustion temperature based on exotherm (°C)	Combustion temperature based on temperature jump (°C)	Time to combustion (min) (From room temperature 25°C to temperature jump)
50°C/min	433.79	513.78	564.48	10.79
20°C/min	503.18	553.35	555.87	26.54
10°C/min	479.29	534.06	536.38	50.91
5°C/min	454.1	509.60	512.86	96.91
3°C/min	440.58	500.29	502.88	158.43
1°C/min	409.57	451.87 (only a small exotherm jump)	(No observed temperature jump)	-

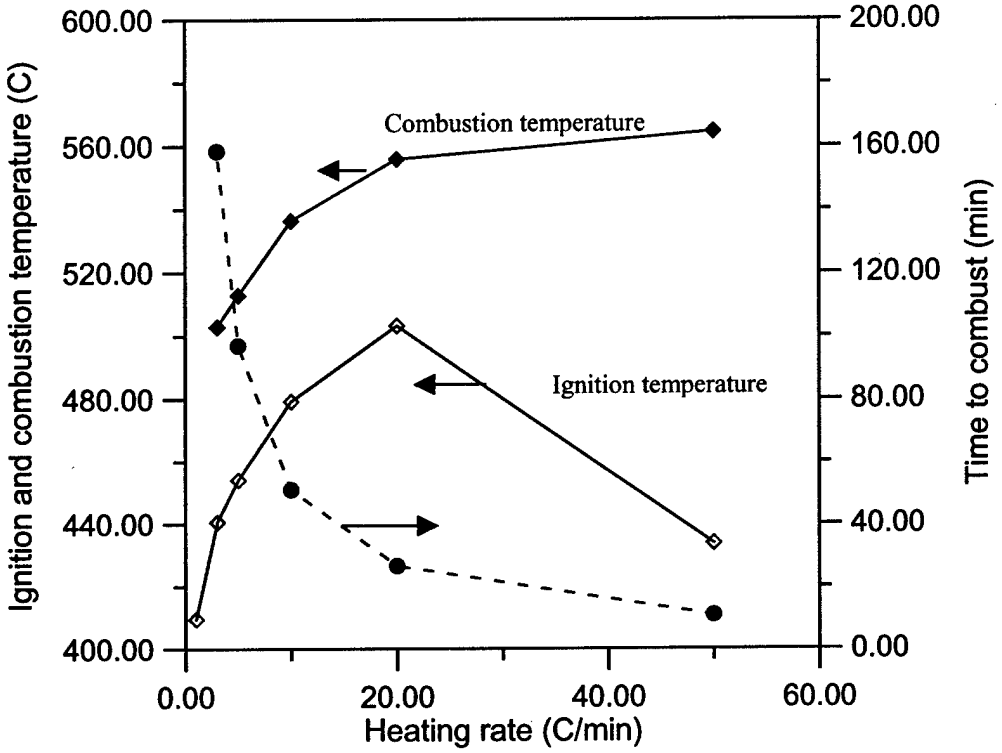

Figure 2.16 Ignition and combustion temperatures as function of heating rate

Isothermal ignition behaviors:

In this research, DSC tests were also run in such a way that the sample was heated at a rapid rate of 50°C/min under 300 psi oxygen pressure to certain temperature and then isothermally held at that temperature. The time period between reaching the isothermal temperature and ignition of the sample (referred to as retardant time) was obtained. This is referred to as measurement of isothermal ignition behaviors of the composite. Figure 2.17 shows the temperature as a function of time in DSC tests with different isothermal holding temperatures. The retardant time at each isothermal temperature were shown in the figure and summarized in the last part of the appendix.

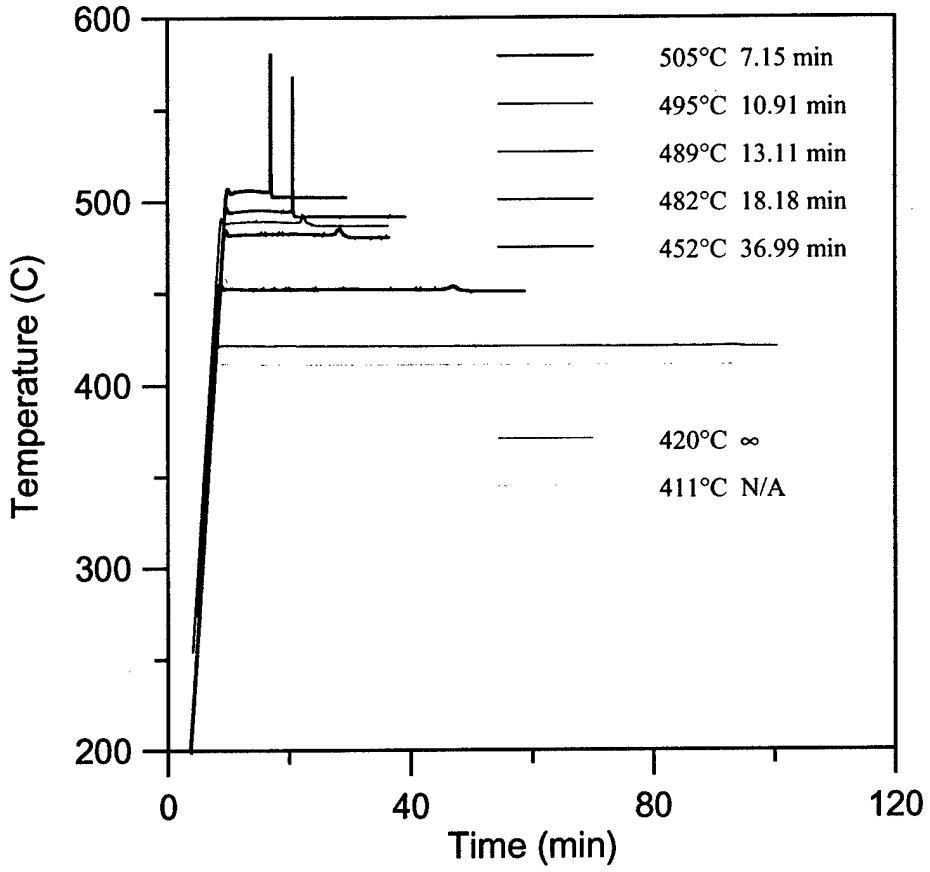

Figure 2.17 Temperature vs time for DSC tests with different isothermal holding temperatures

It was found that with a heating rate of 50°C/min and oxygen pressure of 300 psi, the composite powders showed sudden exotherm and temperature jumps when isothermally held at 505 and 495°C. When the isothermal temperature was decreased to lower than 489°C, the samples only had small exotherm and even smaller temperature increase. When the temperature was lowered to 421°C, there was only a very low exothermal peak left. It is obvious that the retardant time became longer with decreasing isothermal holding temperatures. Finally, when the isothermal holding temperature was lowered to 411°C, the sample did not show any reaction no matter how long it was held at that temperature. The samples were still in the DSC pan after 2 hours holding in oxygen with 300 psi. The results indicated that if the composite powders were rapidly heated to a temperature lower than 490°C, they would not show any violent combustion and if they were heated to a temperature lower than 410°C, they would not burn at all.

Absorption of oxygen:

The actual situation for composite cryogenic tanks might be that the composite absorbs oxygen when it is full of the cryogenic fuel. Although the tank should be empty when being maintained, the absorbed oxygen is still there. It might assist combustion if something causes a sudden temperature increase on the composite tank. Therefore, we performed DSC tests in which the powder samples were kept in high pressure oxygen for certain time period, then heated up to

check whether the ignition and combustion temperatures are different from the ones directly run in the DSC. The holding time periods used in this study were 16 hours and 64 hours. The results are listed in Table 2.7 and also in the appendix. The results showed that the ignition and combustion temperatures did not change with holding time in the high pressure oxygen. It is believed that the amount of DSC samples is too small to uptake sufficient oxygen to influence the combustion.

Table 2.7 Effects of holding time in high pressure oxygen (300 psi and room temperature) on the ignition and combustion temperatures of IM7/5250-4 composite powder

Conditions	Ignition temperature (°C)	Combustion temperature based on temperature jump (°C)
No hold 10°C/min	479.29	536.38
Hold 16 hr then 10°C/min	478.29	541.98
Hold 64 hr then 10°C/min	476.47	537.67
No hold 50°C/min	433.79	564.48
Hold 16 hr then 50°C/min	433.42	561.18
Hold 64 hr then 50°C/min	436.21	566.67

Ignition behaviors of bulky composite:

To make the tests more realistic, small bulky composite samples were also used. The samples were squares about 2 mm wide and the weights about 15 mg. The oxygen pressure used for these bulky composite tests was relatively low, 20 psi, and the heating rate relatively high, 50°C/min. The bulky samples all burned out after the tests. They showed a rectangle peak on their temperature and heat flow curves, as shown in Figure 2.17, instead of sharp peaks of the powder samples. Also, the exotherms were much lower than those of the powder samples. This is due to the fact that bulky samples do not have a good contact with oxygen as powder ones, so that they burn slowly.

The effects of oxygen absorption on the combustion behaviors of the bulky samples were also studied. The procedures were the same as described in the last section for powder samples. The results are listed in Table 2.8 and in the appendix. No significant changes of ignition and combustion temperatures with holding time were found.

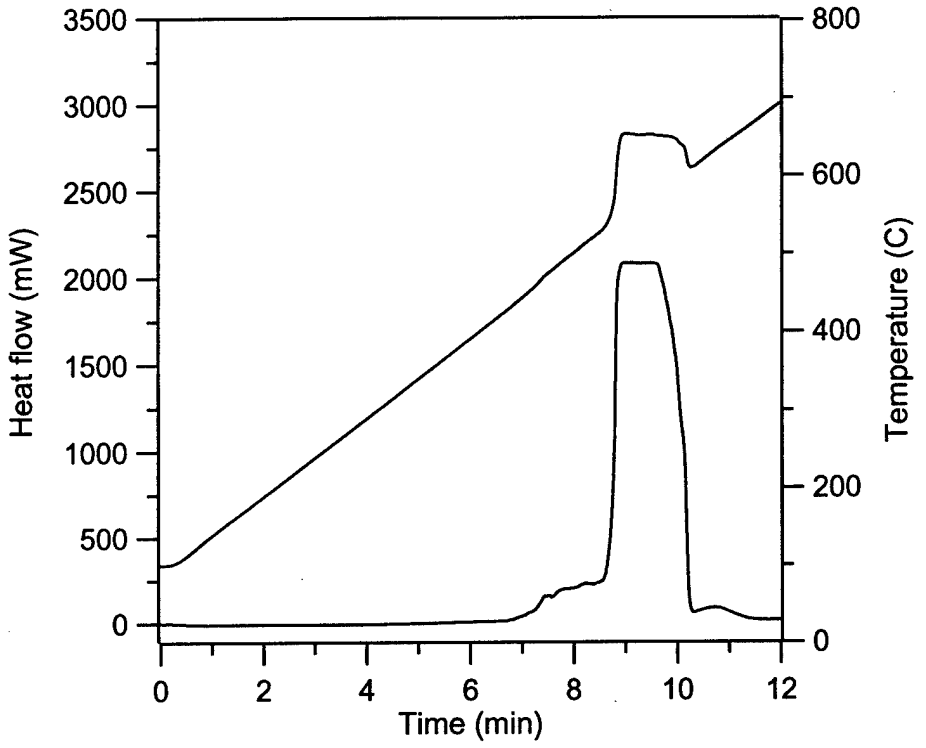

Figure 2.18 DSC curve of IM7/5250-4 Composite Bulk

Table 2.8 Effects of holding time in oxygen on the ignition and combustion temperatures of IM7/5250-4 composite

Conditions (All tests were run in 20 psi O_2)	**Combustion temperature based on exotherm (°C)**	**Combustion temperature based on temperature jump (°C)**
Tested at 50°C/min without prior holding in oxygen	530.69	546.56
Held in 300 psi O2 for 17 hours, then tested at 50°C/min	530.02	542.06
Held in 300 psi O2 for 64 hours, then tested at 50°C/min	525.90	532.39

2.3.3 Preliminary conclusions

7. It is carbon fibers that cause composite to ignite and burn. The neat 5250-4 resin does not ignite, it just decomposes oxidatively.
8. There is no obvious effect of sample size on the ignition and combustion temperatures if it is within the range of 2 to5 mg.
9. The higher the heating rate, the faster the ignition and combustion, but the higher the combustion temperature. Very slow heating rate, such as 1°C/min won't cause violent combustion of the composite.
10. High O2 pressure reduces the ignition and combustion temperatures.
11. Keeping the composite powders in high pressure O2 for up to 64 hours did not have any effect on ignition and combustion temperature for both powder and bulky samples.

12. The composite powders will not burn violently when heated up rapidly to certain temperature if the temperature is below 490°C.

Short-term Plan

Run the DSC tests for more candidate cryo-tank composites, such as composites based on epoxy and nano-composites for the screening purpos

Table 2.9 Summary of IM7/5250-4 Composite Ignition Behaviors in High Pressure DSC

Conditions			Ignition temperature (°C)	Starting temperature (°C) of the sharp exotherm	Starting temperature (°C) of the temperature jump
Materials and Sample shape (10°C/min O2 600 psi)	CF (AS4)		466.58	523.79	535.31
	Resin			A broad peak 100-500°C (Oxidative decomposition)	
	Composite powders		462.87	508.23	508.33
	Composite flakes		430.58	534.24	535.80
Sample size	10°C/min O2 300 psi	1.8 mg	535.68	535.68	539.20
		3.4	535.05	535.05	535.80
		4.1	531.39	531.39	534.71
		5.3	534.13	534.13	535.80
		8.5	486.27 ?	486.27 ?	511.48 ?
	50°C/min O2 300 psi	2.4	515.54	515.54	556.38
		2.6	514.92	514.92	572.84
		3.0	511.50	511.50	570.14
		3.6	515.42	515.42	566.67
		4.2	511.50	511.50	556.38
Heating rate (O2 300 psi)	50°C/min		433.84, 433.80, 435.40, 434.57, 431.33	515.42, 511.50, 515.54, 514.92, 511.50	566.67, 570.14, 556.38, 572.84, 556.38
	20°C/min		505.62, 500.73	552.43, 554.26	554.32, 557.41
	10°C/min		483.61, 474.31, 479.55, 479.69	535.68, 535.05, 531.39, 534.13	539.20, 535.80, 534.71, 535.80
	5°C/min		452.11, 456.08	508.62, 510.57	511.11, 514.61
	3°C/min		440.58	500.29	502.88
	1°C/min		409.57	451.87 (Only a small exotherm jump)	No observed temperature jump
O2 Pressure (10°C/min)	600 psi		437.89, 448.08	508.23, 510.98	508.33, 514.51
	300 psi		483.61, 474.31, 479.55, 479.69	535.68, 535.05, 531.39, 534.13	539.20, 535.80, 534.71, 535.80
	100 psi		508.64, 506.61	555.58, 562.49	558.44, 564.61

	20 psi	508.89, 512.96	582.62	585.19
After hold in 300 psi O2	16 hr then 10°C/min	476.56, 481.01	535.73, 538.77	540.33, 543.62
	64 hr then 10°C/min	477.93, 475.01	534.13, 533.22	539.53, 535.80
	16 hr then 50°C/min	433.18, 432.93, 434.15	510.35, 509.37, 5214.70	558.44, 562.55, 562.55
	64 hr then 50°C/min	434.91, 437.51	512.57, 514.70	558.44, 574.90
Bulky samples (50°C/min 20 psi O2)	No previous hold		529.56, 531.81	538.76, 554.36
	Hold in 300 O2 for 17 hours, then heated		527.73, 532.30	535.36, 548.76
	Hold in 300 O2 for 65 hours, then heated		525.90	532.39

	Features of DSC curves	Retardant time (Time from reaching the temperature to temperature jump starting) (min)
Rapidly heat up (50°C/min) to certain temp., then hold	505°C	Exotherm and temp. jump	7.15 min
	495°C	Exotherm and temp. jump	10.91
	489°C	Small Exotherm and very small temp. jump	13.11
	481°C	Small Exotherm and very small temp. jump	18.18
	451°C	Small Exotherm and very small temp. jump	36.99
	421°C	Small exotherm, No temp. jump	∞
	411°C	No exotherm , no temp. jump. Powders still in the pan after test	

1. All tests were run with open pan;
2. All tested samples were grounded composite powders unless specified in the table;
3. The data with a ? indicate that it is questionable;
4. The samples have burned out in all tests unless specified

2.4 Development of Automatic Cryo-High temperature Composite Cycling System

2.4.1 Introduction

The principal objective of this project was to develop an Auto Cryo-Humid-HT cycling machine, which can be used for long term automatic cycling of advanced composites between any two of the environments including liquid nitrogen temperature, high temperature up to 600 °F, 98% relative humidity at 40 °C, and room temperature. An advanced data acquisition system makes it possible to simulate operational envelopes within the environments listed above. The cycles are (1) thermal cycling of dry composites and (2) hygrothermal cycling of wet composites materials. Prior to the development of this auto cycling machine, the FAST Center developed a procedure for manual cycling. In this procedure, dry panels were thermally cycled (-320°F→74°F →302°F→74°F) one cycle per hour. In addition, saturated panels were hygrothermally cycled (-320°F→74°F →302°F→74°F→overnight saturation @ 104°F/98%RH). The detailed procedure for the manual cycling are described below.

1. Well labeled panels were placed in a stainless steel specimen holder shown in Figure 2.19a. Panels were seperated by dividers coated with Teflon for panel protection.

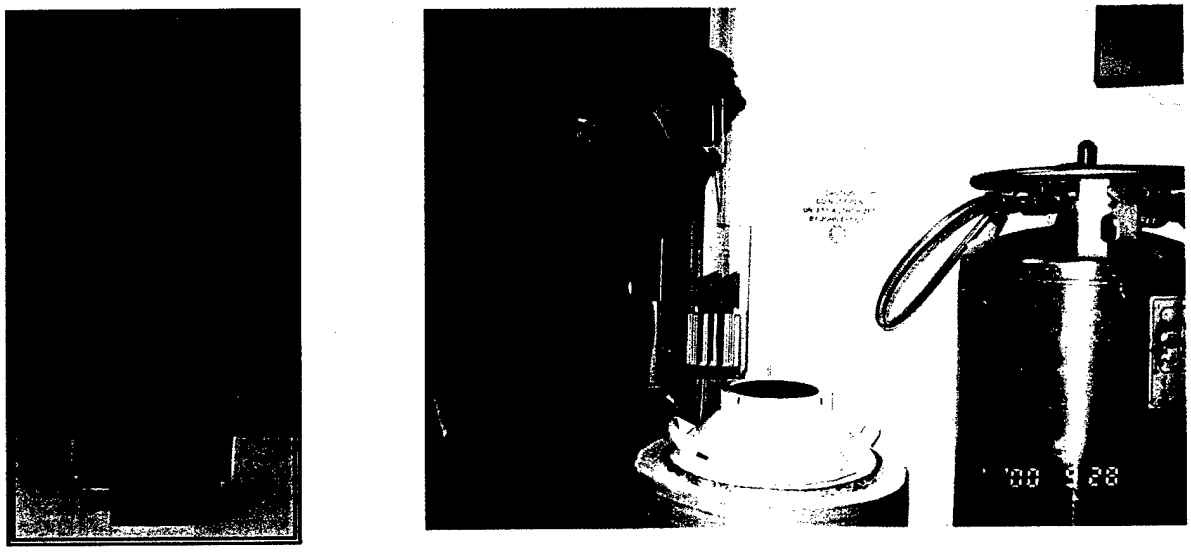

(a) Specimen Holder

b Manual cycling Operation

Figure 2.19 Stainless Steel Carriage With Panels and Manual Cycling Operation

2. Care was taken in the lowering the specimen holder through the neck of the cryo-tank shown in Figure 2.20(a) and submerging them into LN2. Slow rate of descent minimized the splashing effect of LN2.

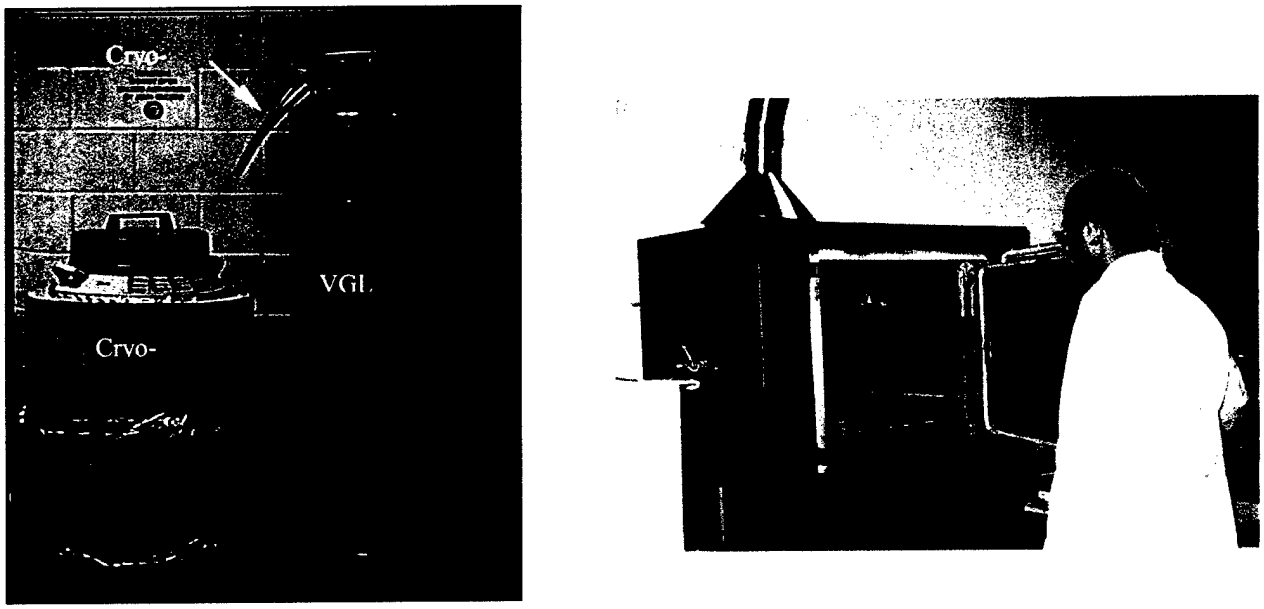

Figure 2.20 Cryo- Storage Tank & VGL

3. Once in LN2, the lid was promptly placed over the cryo-tank. The timer was set to 10 minutes.

4. After 10 minutes the specimen holder was removed from the LN2. Once fully raised over the mouth of the flask, the excess LN2 seeped down the sides for a couple of seconds.

5. The specimen holder was set on the table and the flask was closed and timer set for 20 minutes to allow the specimen to warm to room temperature. Also, at this time the oven is preheated to set temperature 150°C (302°F).

6. After 20 minutes, the oven door was completely open. The specimen holder was slowly placed onto the oven shelves shown in Figure 2.20(b). It was set in the middle of the oven and the door was closed and timer set for 15 minutes.

7. After 15 minutes, the door was open completely and specimen holder was removed from the oven. The oven door was closed and timer set for 15 minutes.

8. The process was repeated starting at step 2 until the number of required cycles were completed.

9. For the wet cycling, the specimen holder was placed into an environmental chamber which is pre-set at 104°F/98%RH.

2.4.2. The Design of Auto Cryo-Humid-HT Cycling Machine

Based on the cycling requirements and procedures, the basic components of the cycling machine shown schematically in Figure 2.21(a) are (1) an automatic door for LN2 flask, (2) a convection oven with an automatic door, (3) the stainless steel specimen holder, (4) frame and motor/pulley transport system, (5) data acquisition and control system.

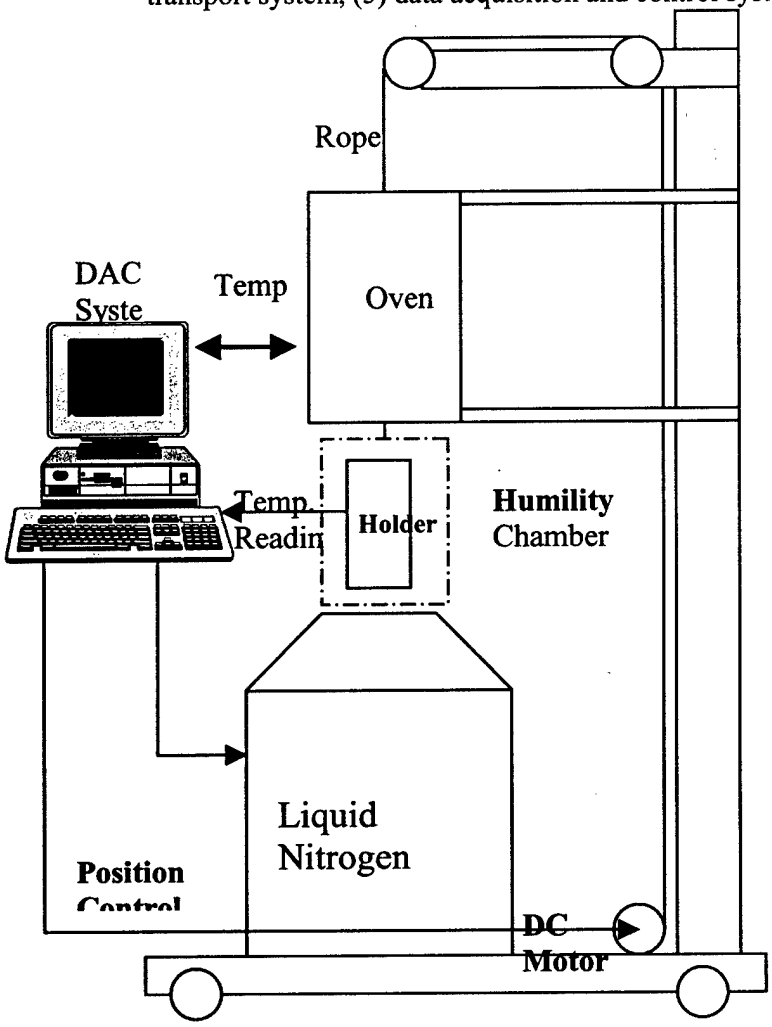

(a) Schematic Diagram

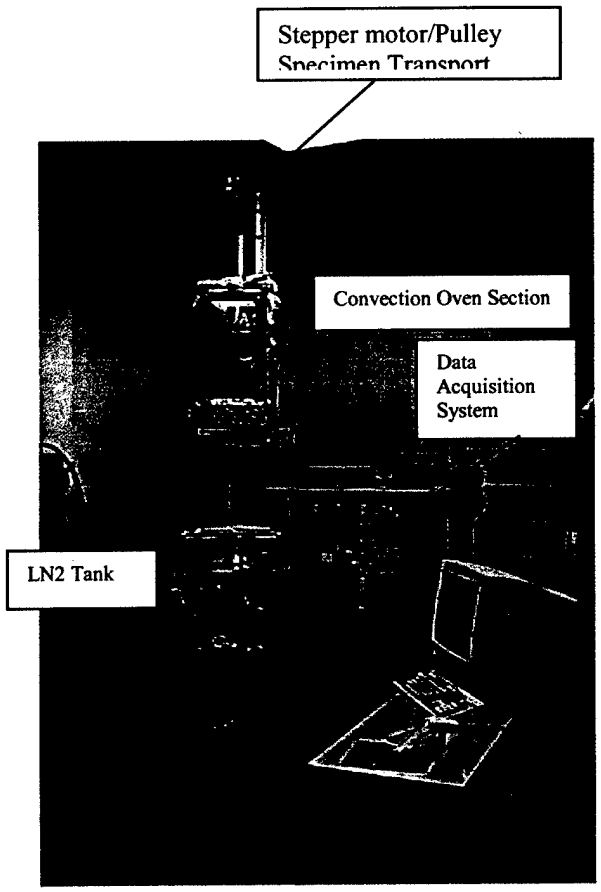

(b) Actual System

Figure 2.21 The Auto Cryo-Humid-High Temperature Cycling System

Cycles:

1. RT → -302 °F → RT → 302 °F RT →
2. 98% RH 440 °F 98% RH

Automatic Door

The flask and convection oven are closed most of the time. The door is opened to allow the specimen holder to enter and exit the cryogenic chamber, air space and the convection oven. The pneumatic door design is shown in Figure 2.22. The opening and closing of the door is controlled by a DAS system.

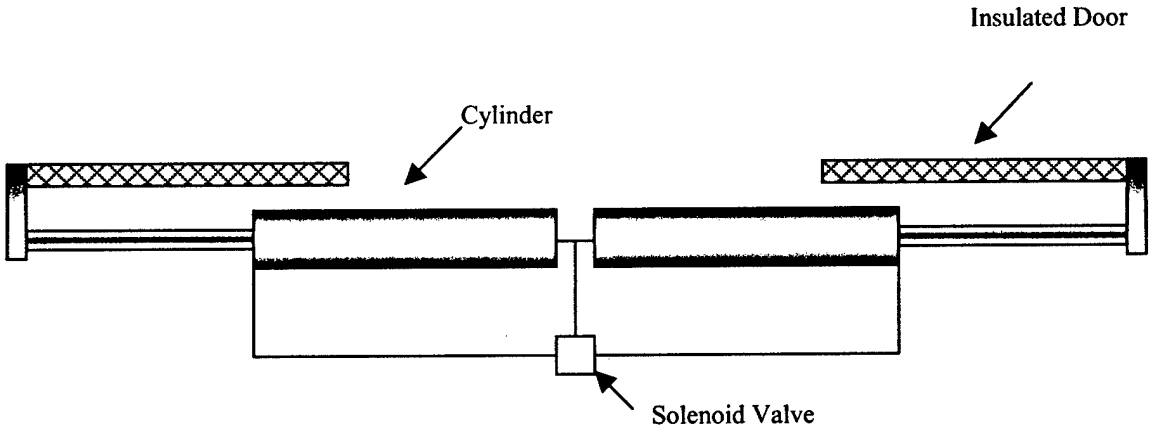

(a) Schematic of Automatic Door System

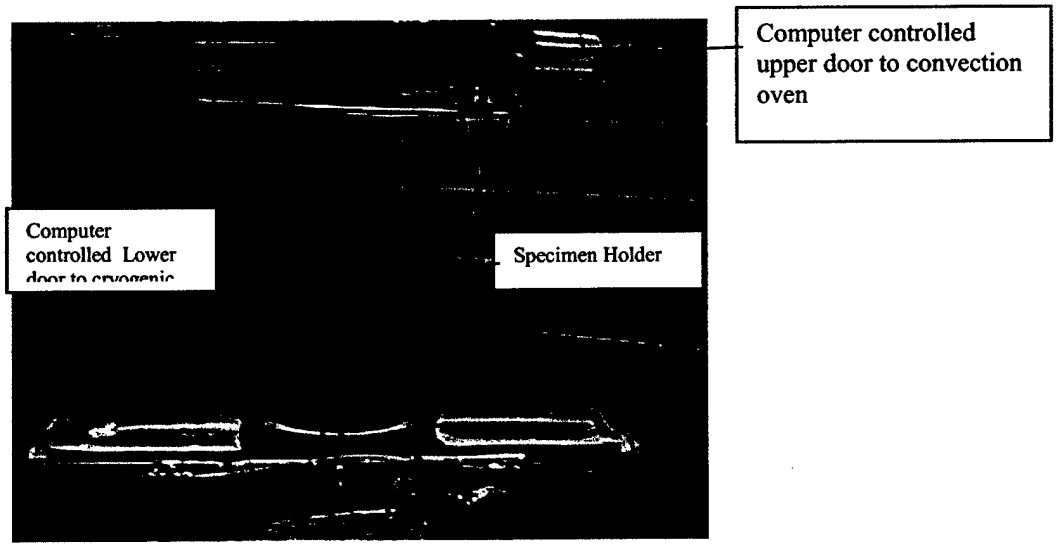

(b) actual Auto-Pneumatic Door System

Figure 2.22 The Auto Cryo-HT Cyclind system showing lower door opened and specimen holder

Motor/Pulley Transport System

The holder is suspended on a steel rope moved by a computer controlled motor/pulley transport system shown in Figure 2.23. The speed and position of the specimen holder are controlled by a DAS system.

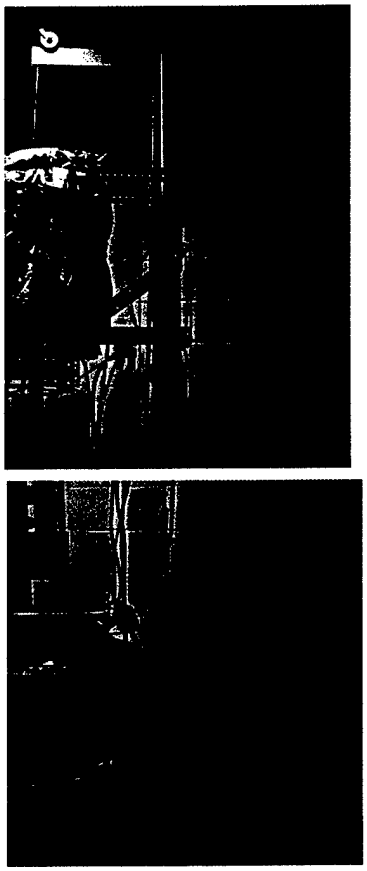

(a) Actual Motor/Pulley Transport System

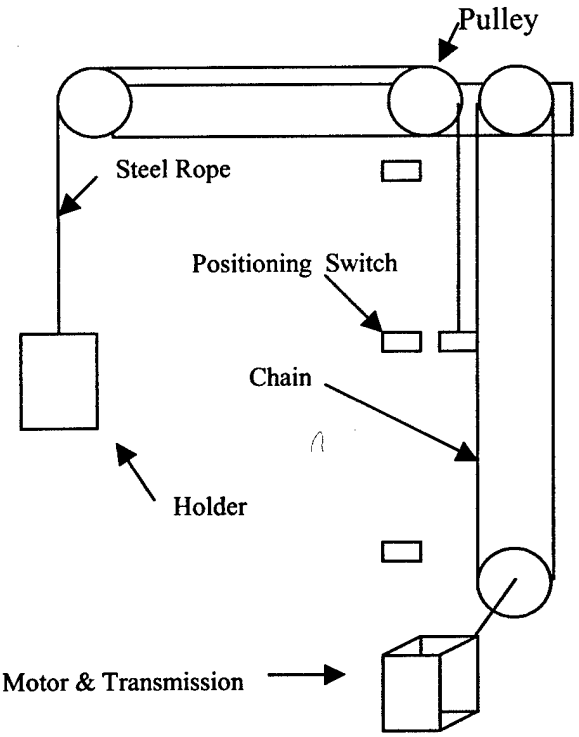

(b) Schematic of Motor/Pulley Transport System

Figure 2.23 Motor/Pulley Transport System

The Design of Convection Oven

The convection oven shown in Figure 2.24 is heated using an electrical heater. The hot air is circulated using a fan and the temperature is controlled by the DAS system

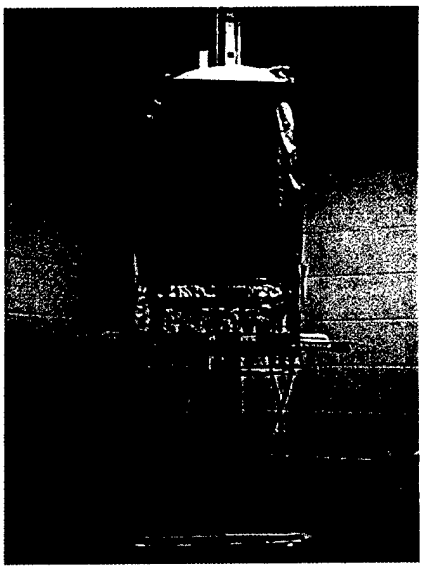

Figure 2.24 Convection Oven

Liquid Nitrogen Flask

The LN2 flask shown in Figure 2.25 is a double walled stainless steel cryogenic flask with vacuum between the walls. It can hold 110 litters of LN2. The tank is further insulated using 1 inch thick fiber glass insulation. The design minimizes LN2 boil off.

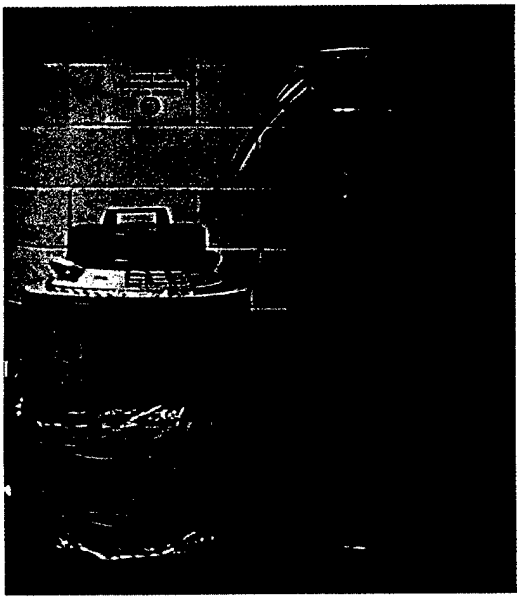

Figure 2.25 The Liquid Nitrogen Flask

Data Acquisition and Control System

A Kethly data acquisition and control system with a relay board is used to control the temperature, the holder position , the pneumatic doors, the heater and the fan in the oven.

Relay Board and Control Panel
Two relay boards and one control panel shown in Figure 2.26 contain most of the hardware used to control the system.

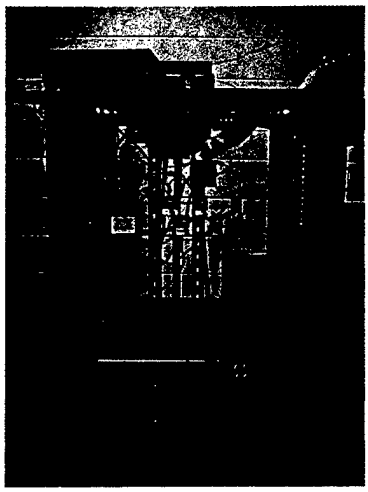

(a) Front Panel of The Control Boards and Frame

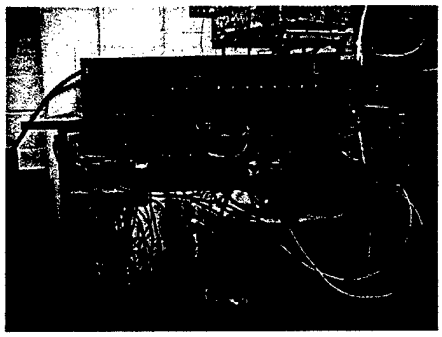

(b) Two Relay Boards

Figure 2.26 Control and Relay Boards

The relay boards are part of the DAS system. There are eight relays (r0 through r7) on the PCM3 board with one connector on each relay as listed in Table 2.10. The devices on the cycling machine need more then one connector on each relay. The secondary relay board with eight relays (R0 through R7) is mounted on the control board. For each relay there are three normally open and three normally close connectors. The coil voltage of the secondary relays is 120 V. The diagram of the relay boards and switches are shown in Figure 2.27

Table 2.10 . List of relay on PCM3 Board

RELAY#	CH	IONAME	DESCRIPTION OF EQUIPMENT ATTACHED
r0	16	FOP	FLASK DOOR OPEN
r1	17	FCL	FLASKDOOR CLOSE
r2	18	HDN	HOLDER MOVE DOWN
r3	19	HUP	HOLDER MOVE UP
r4	20	HCM	HOLDER CONTINUE
r5	21	H&F	HEATER AND FAN ON AND OFF
r6	22	OOP	OVEN DOOR OPEN
r7	23	OCL	OVEN DOOR CLOSE

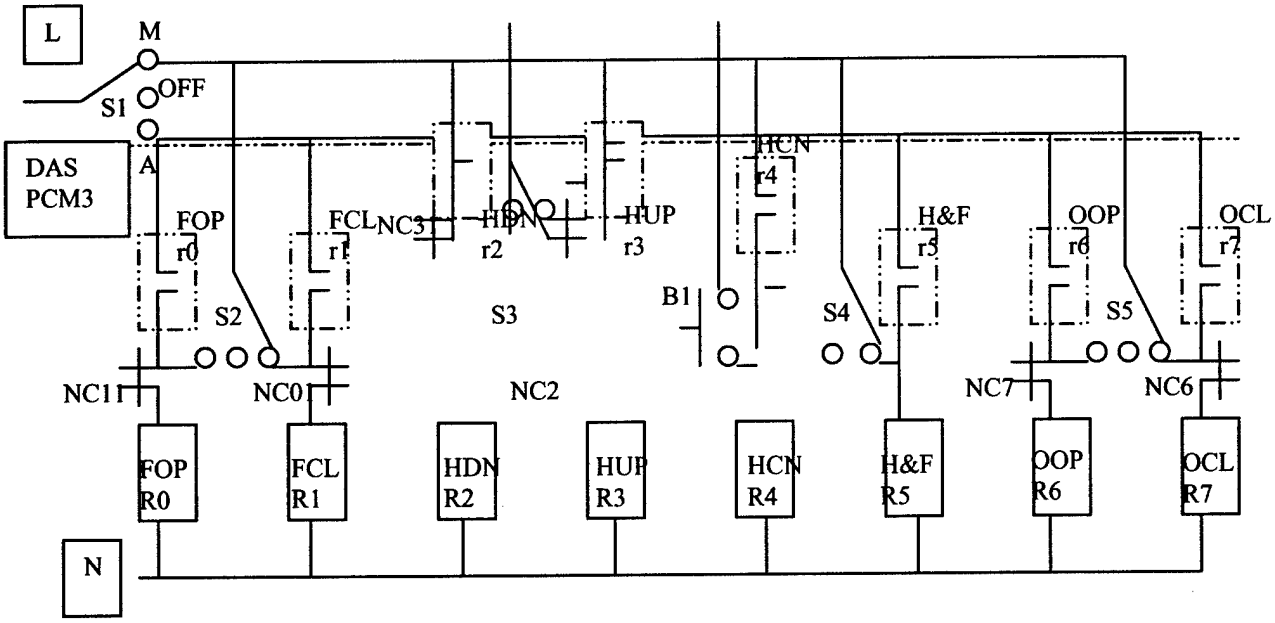

Figure 2.27. The diagram of relay boards and switches.

Description of relay Board

L: Line ~115 V

N: Neutral

S1: M/A and Off selection switch. It is used to select manual, auto control or turning off the system.

M: Manual Control (Switch Control) . when the S1 switch is in the manual control position, the DAS system will read temperature. All the movement, heater and fan are controlled manually by using switches.

S2: Flask Door Open/Close and Off Switch. It is used to control the flask pneumatic door open/close and off. Under auto control, it should be at off position.

S3: Holder UP/Down and Off Switch. It is used to control the rotational direction of the DC motor. Under auto control, it should be at the off position.

S4: Oven Heater and Fan On/Off Switch. It is used to control the oven heater and fan on/off. Under auto control, it should be at the off position.

S5: Oven Door Open/Close Switch. It is used to control the oven pneumatic door open/close and turn off. Under auto control, it should be at the off position.

B1: Holder Continue Moving Button. When the half way position switch (HPS) open, the holder can be stopped at half way. This button is used to restart moving.

A: Auto Control (DAS Control)

HDN/HUP & HCN: Holder Moving Down/UP and Holder Continue Moving
The holder moving down/up and stop/continue at the half way are controlled by relays r2, r3, r4 and R2, R3, R4 respectively. Incase of the the relay R2 and R3 turn on at the same time , they are locked by each other.

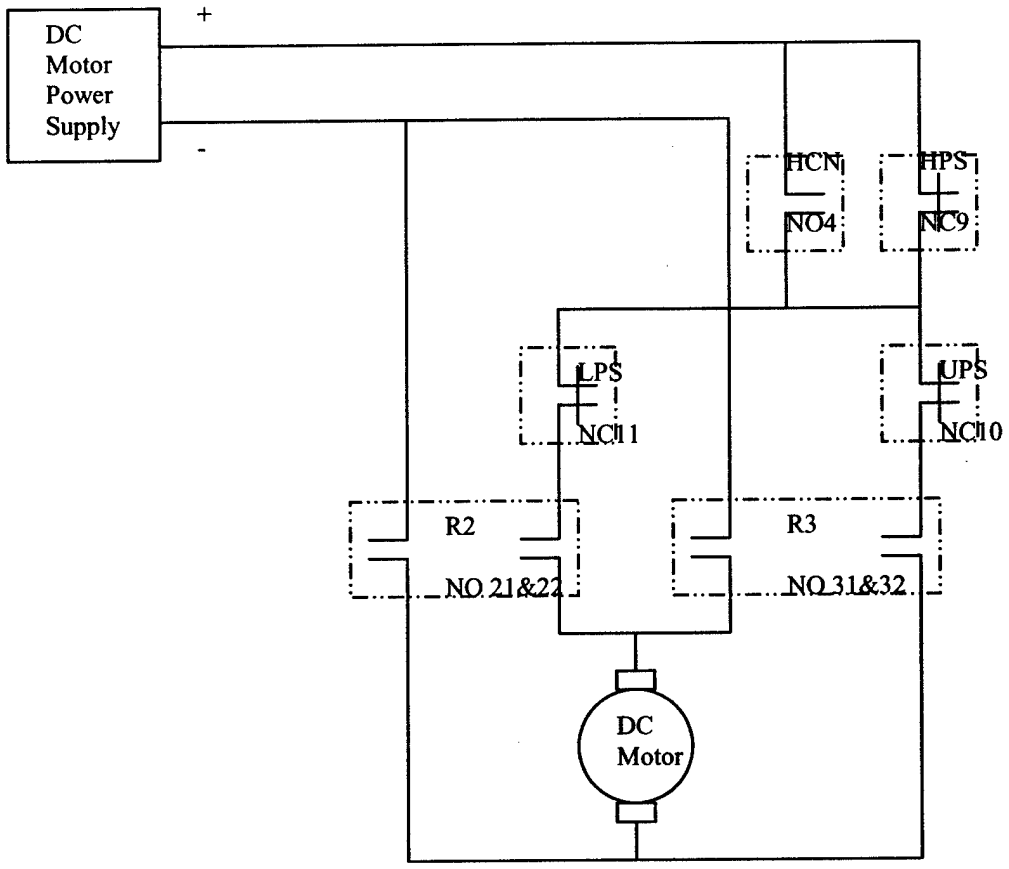

Figure 2.28 Schematic Diagram of Relay Board

LPS: Lower Limit Position Switch.
When the normal open connector 21&22 of relay R2 are connected, the holder moving down When the holder reach the bottom of the flask, the normal close connector NC11 of lower limit switch will open, the holder only can move up.

UPS: Upper Limit Position Switch.
When the normal open connector 31&32 of relay R3 are connected, the holder moving up. When the holder reach the top of the oven, the normal close connector NC10 of upper limit switch will open, the holder only can move down.

HPS: Half Way Position Switch.
When the normal close connector NC9 of HPS opens, the holder will stop moving at the half way. When the holder temperature reachs the room temperature, the normal open connector NO 4 of relay R4 will close and the holder will follow the last move direction.

FOP/FCL: Flask Door Open/Close

The flask door open/close are controlled by relays r0, r1 and R0, R1 respectively. Incase the relay R0 and R1 turn on at the same time , they are locked by each other only alow one on at each time.

H&F: Oven Heater and Fan On/Off

The heater and fan on/off are controlled by relays r5 and R5.

OOP/OCL: Oven Door Open/Close

The oven door open/close are controlled by relays r6, r7 and R6, R7 respectively. Incase the relay R6 and R7 turn on at the same time , they are locked by each other.

2.5 Development of a Composite Permeability Measurement System

The barrier properties of candidate cryogenic tank materials are of prime importance as we seek candidate materials for that application. Consequently, the FAST center has spent some time during the extension period to design, build, and test an experimental facility for measuring the permeability of composite materials

2.5.1 Initial Design of Composite System

The initial system is shown schematically in Figure 2.29

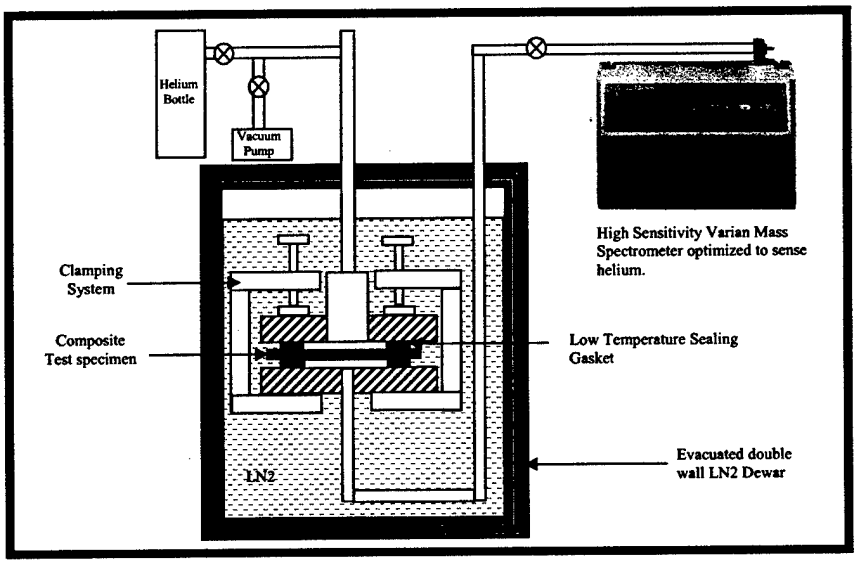

Figure 2.29 Schematic of Initial Composite Permeability Testing System

The system will enable us to have vital understanding of the permeability of composites under several environmental conditions. With this system, we can determine the permeability of composites at cryogenic and high temperatures after undergoing various environmental aging. Permeability tests can be conducted under no load or static loading (Tension) at LN2 temperature, and from RT to 250°C The system consists of a high sensitivity Varian mass spectrometer optimized to sense helium. The composite test specimen is placed between two stainless steel flanges/sealant of various configurations as shown in Figure 2.30. The system is clamped together using a system of clamps.

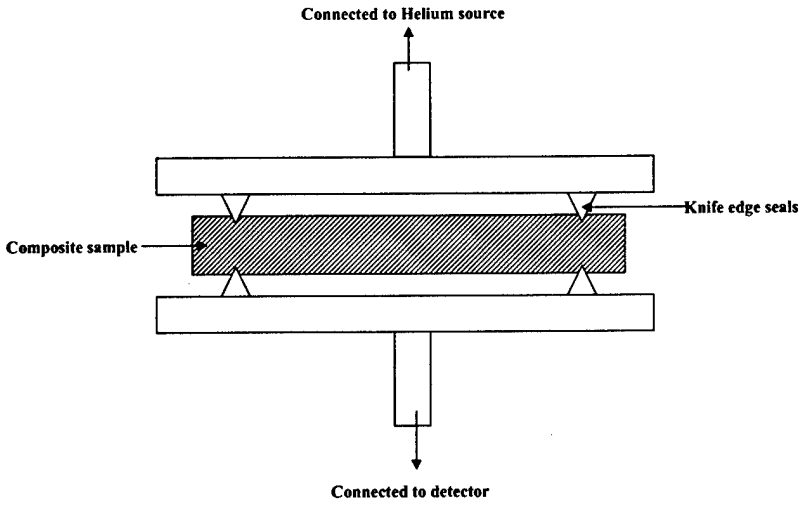

Figure 2.30 Assembly for Testing in LN2 and at High Temperature Without Load

The upper flange is connected to a helium bottle through a stainless steel line. The lower flange is also connected to the Varian mass spectrometer. The entire specimen portion of the system is immersed in a dewar vessel containing liquid nitrogen. The helium enters the top portion of the composite at a regulated pressure of 20 psi. The mass spectrometer side (space in the lower portion of the specimen) is maintained at high vacuum. Any helium or any other gas that permeates the composite enters the mass spectrometer tube. The Varian helium mass spectrometer is capable of detecting helium leaks as small as 2 x 10^{-11} std. cc/s. Figure 2.31 shows the assembly for testing under load.

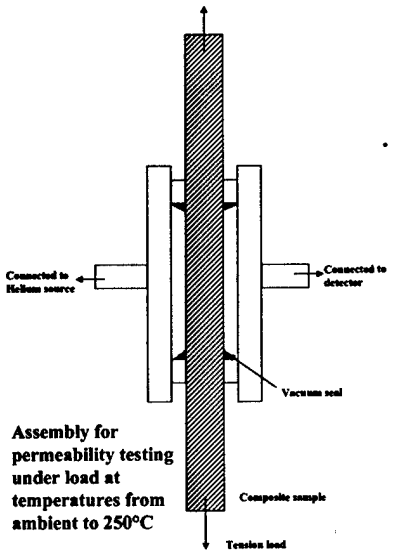

Figure 2.31 Assembly for Measuring Permeability of Loaded Sample

Figure 2.32 shows a picture of the initial system and Figure 2.33 shows a 2" x 2' sample being tested in the completed facility.

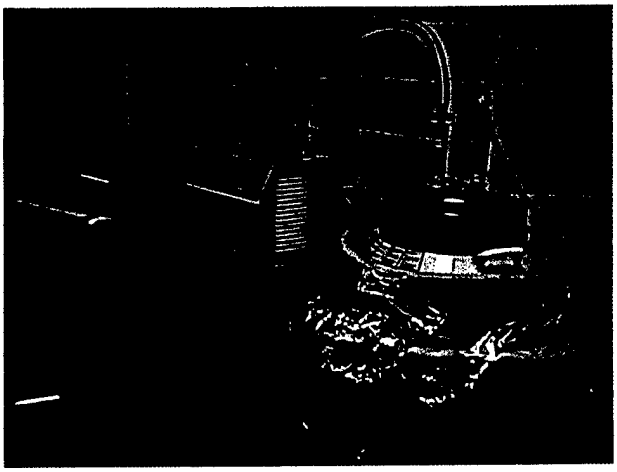

Figure 2.32 Initial Completed Permeability Measurement System

Figure 2.33 A 2" x 2" specimen being tested for permeability at LN2 temperature is shown being removed from the cryogenic tank after testing

The rationale for using helium as the gas for measuring permeability and liquid nitrogen as the cryogenic fluid are:

- In the University environment, safety concern prevents us from testing using hydrogen (gas or liquid), and liquid oxygen, thus the selection of LN2 as the cryogenic fluid.
- The screening tests are designed to be quick and inexpensive and will serve as the first test a cryogenic material should pass before being selected for actual LH2 and LOX test. Thus the LN2 temperature is deemed a reasonable temperature for the screening tests. Obviously if a material fails under this temperature, it will likely fail under LH2 temperature.
- Helium, the lightest inert gas, is monoatomic and has a smaller atomic radius (0.31Angstroms) than the hydrogen atom (0.32Angstroms). Hydrogen, being diatomic, will

have a larger effective molecular diameter than that of helium. It is, therefore, more difficult to contain helium than hydrogen. Thus the use of helium to characterize permeability, is more stringent than using hydrogen, but safer and cheaper.

2.5.2 Initial Test for System

The basic IM7/5250-4 laminate $[\pm 45]_{2S}$ and $[90]_{8T}$ 2x2" were cycled. The number of microcracks and the permeability were measured at 0, 10, 35, 100, and 150 cycles The Microcracks and permeability slightly increased after 100 cycles on [+45]. The microcracks were only visible in the surface layer. There were no microcracks on the $[90]_{8T}$ samples before 150 cycles. Figures 2.34 (a) and (b) show the preliminary results for the effect of cycling on the heliun leakage rate through the material and the effects of the cycling on the microcracks.

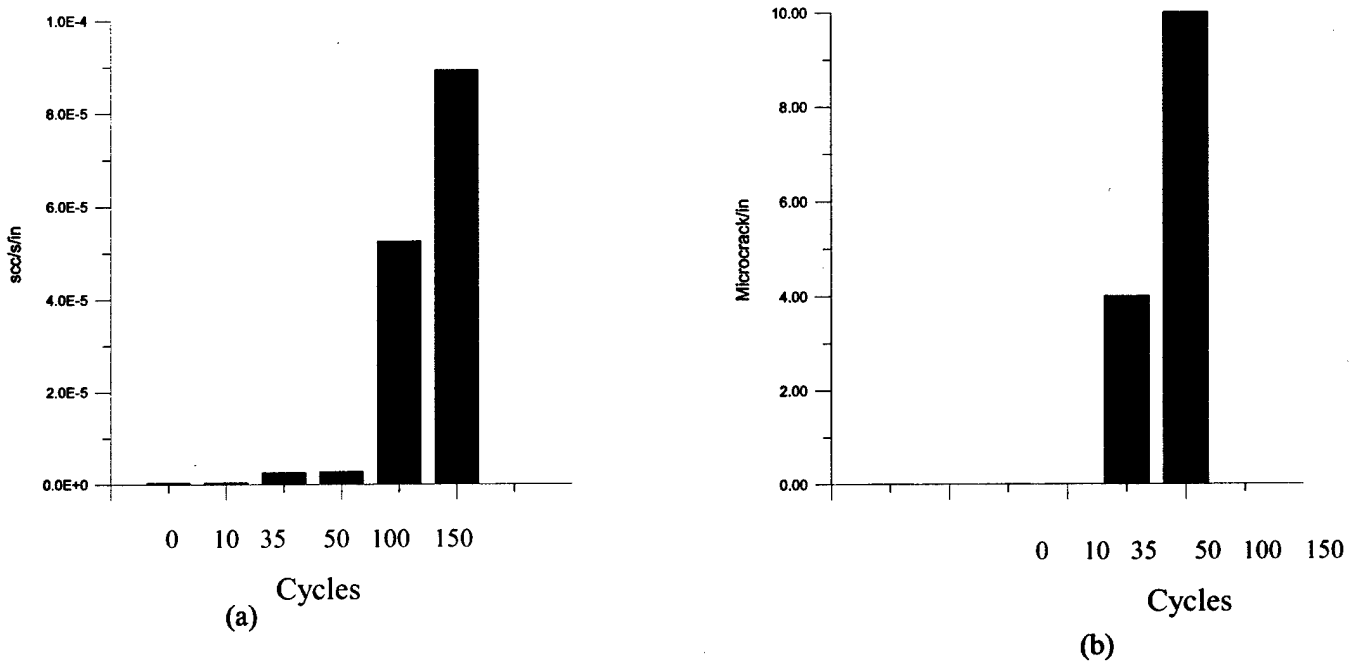

Figure 2.34 Effects of Number of Cycles on the Gas Leakage rate and Number of Microcracks

The permeability of basic laminate $[\pm 45]_{2S}$ 1x6" were also tested under load. The maximum of permeability (3.7e-7) at 75% load is much lower then the permeability (8.9e-5) after150 cycles. The microcracks developed into second layer after 150 cycles

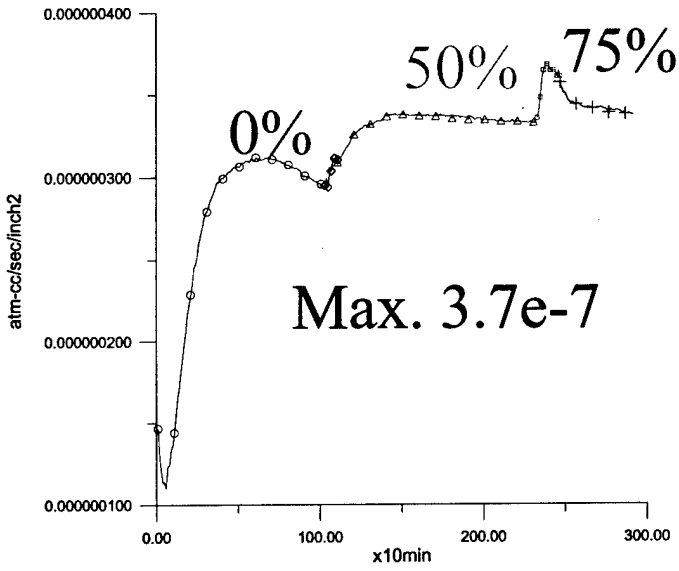

Figure 2.35 Variation of Leakage Rate with time Under Load

From C-scan results, the C-scan is not sensitive to microcrack development.

2.5.3 Modifications to Improve Permeability Measurement System

After the preliminary tests and prior to the use of the system for measuring the permeability of IM7/5250-4 and IM7/977-2 composites, several ideas were proposed to eliminate helium leakage through the specimen holding seals of the system. The four main ideas proposed were:

1. Using slotted viton O-ring as a seal to hold the specimen
2. Using set-up with vacuum external chamber
3. Using vacuum external chamber without pulling Vacuum
4. Using set-up with pressurized external chamber and purge line

To use the viton O-rings proposed in the methods above, it was necessary to design an attachment for cutting circular test samples on our diamond saw as described below.

Cutting Fixture for Making Round Composite Samples for Permeability Test

The diamond saw is designed to cut along a straight line on composite panel. For the purpose of using different helium mass spectrometer fixture, the sample should be cut into round shape of various diameters as shown in Figure 2.36.

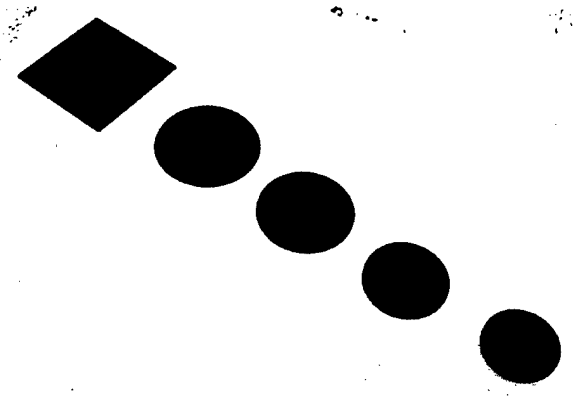

Figure 2.36 Sample Shape and Size

A fixture was been built and attached to the diamond saw. The square sample can be tightly held by a holder and turned. The holder position can be adjusted along the axis and in the radial direction to vary the diameter of the final test specimen. The fixture and round samples cut from it are shown in Figures 2.37 and 2.16 respectively.

Figure 2.37 Round Sample Cutting Fixture

Modification of Viton O-ring Used as Specimen Holder

To rediuce the leakage around o-rings (that act as seals) placed on the top and bottom of the test specimen, the system was modified by cutting a grove in the O-ring and the specimen was inserted in the grove as shown in Figure 2.38. This subassembly was clamped together to the system using the fixtures shown in Figure 2.39. The O-ring containing the sample is sandwiched between the two O-ring holders

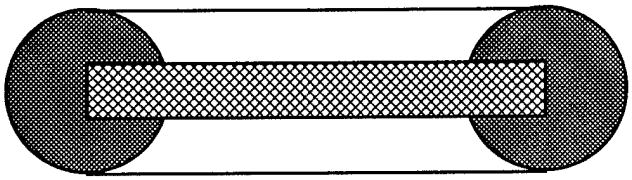

Figure 2.38 Sample Inserted into O-ring

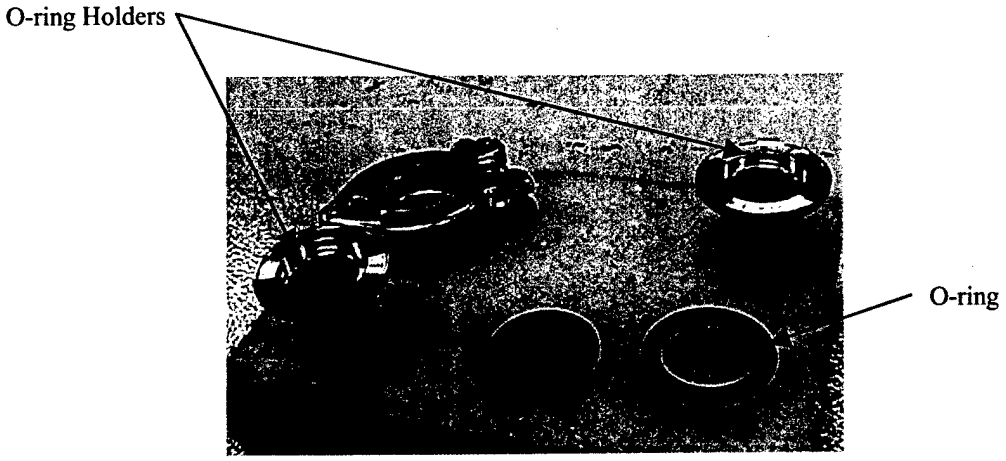

Figure 39 A Set of helium mass spectrometer Fixture

A slot is made in the O-ring to provide better seal when the specimen is inserted in the O-ring as shown in Figure 2.38. Figure 2.40 shows the fixture for making the slot in the O-ring, which was developed at the FAST Center.

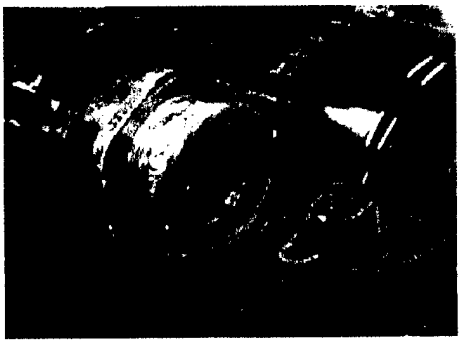

Figure 2.40 Slot Cutting Fixture

CASE 1: Permeability measurment Using Slotted O-ring Fixture
A round sample was inserted into the slotted O-ring and clamped between the two holders as shown in Figure 2.41. Figure 2.42 shows a schematic of the set-up. Helium at 25 psi is introduced at the top. The helium mass spectrometer is connected to the lower section. Under ideal condition helium will permeate through the sample from the 25 psi chamber to the vacuum chamber below the sample with no by-pass leak. However, it may be possible for helium to leak around the viton seal as shown by the by-pass arrows in Figure 2.42.

Experiment are being planned to be conducted to determine if there is any by-pass helium leak with this set-up.

Figure 2.41 Helium Mass Spectrometer Sample Holder

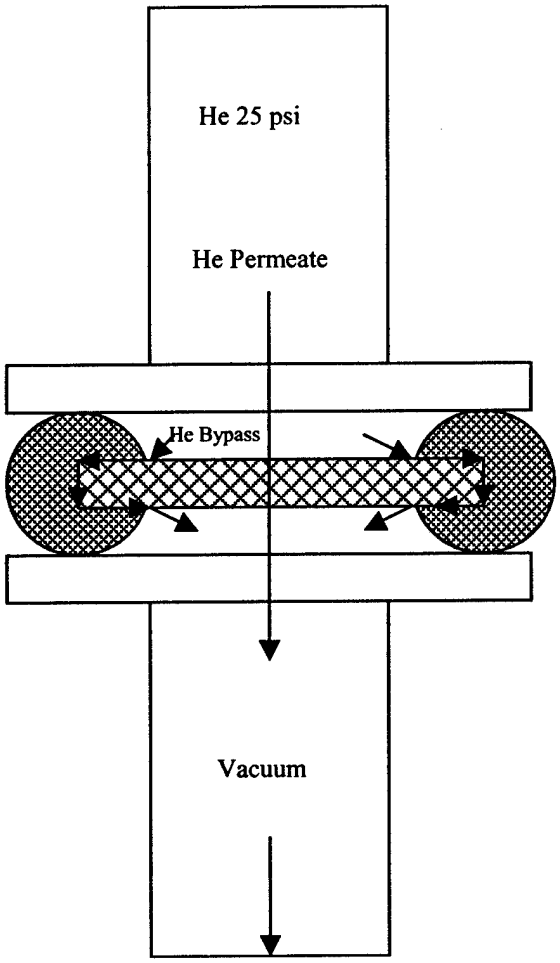

He Detected = He Permeate + He Bypass

Figure 2.42 The Schematic of The Case 1

CASE 2: Permeability Measurement Using Set-up with Vacuum External Chamber
From the schematic of permeability measurement using slotted viton O-ring fixture, the quantity of bypassed helium is part of the detected result even though it is not known. The set-up with vacuum external chamber shown in Figure 2.43 prevents any by-pass helium leak from being detected since it is pulled out by the surrounding vacuum. If there are some micro cracks on the specimen, an amount of helium may be pulled out from the edge. The schematic of the set-up is shown in Figure 2.44.

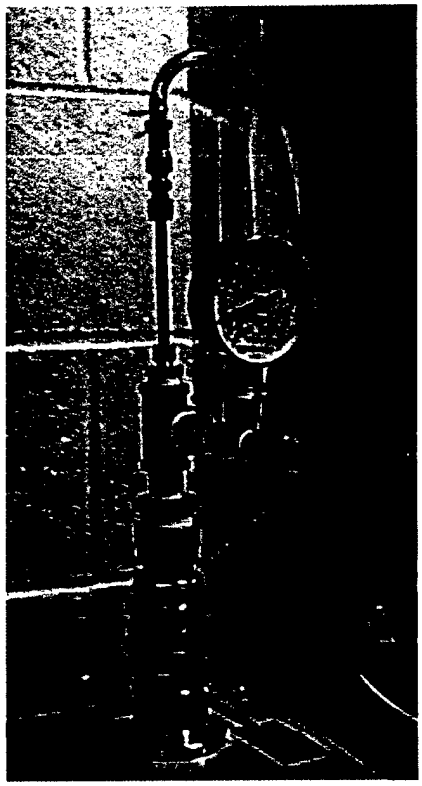

Figure 2.43 Permeability Measurement Using Vacuum External Chamber

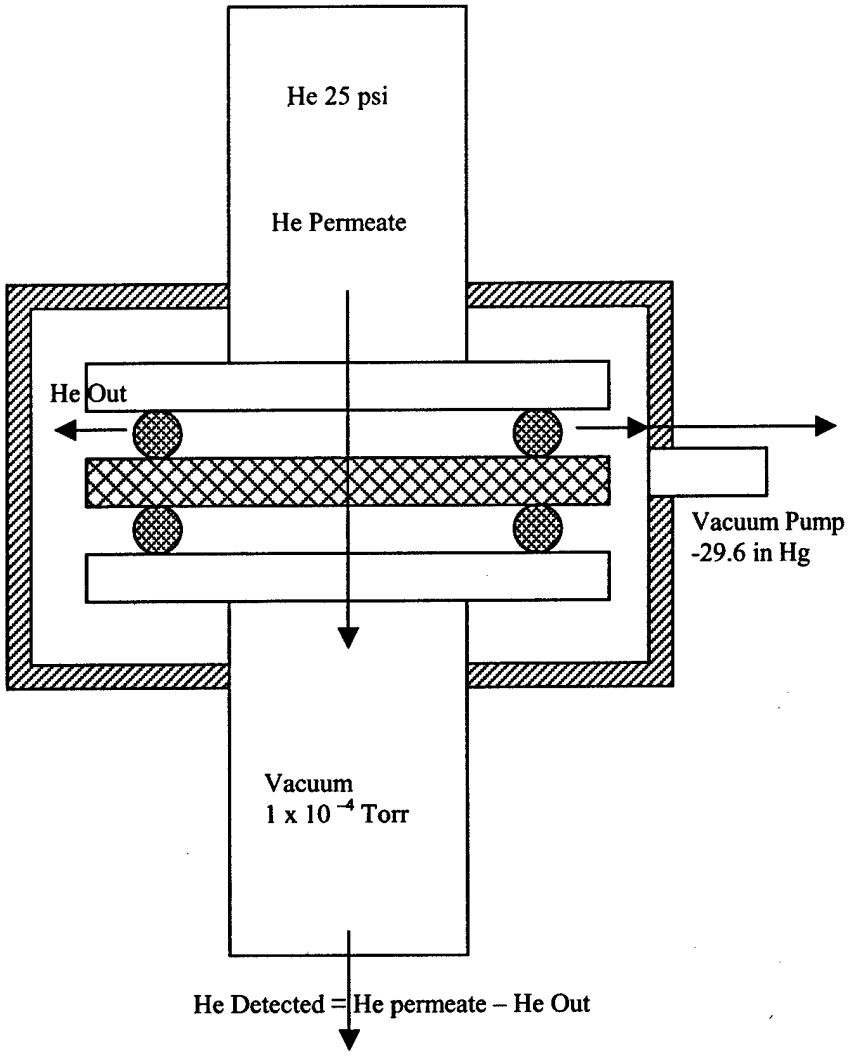

Figure 2.44 The Schematic of Case 2

CASE 3: Permeability Test Using Vacuum External Chamber without Pulling Vacuum
Figure 2.45 shows the schematic of case 3. In this set-up, it is possible for the helium to leak between the upper O-ring and the upper surface of composite panel and come into the mass spectrometer between the lower surface of composite panel and the lower O-ring which cannot be separated from the detected result.

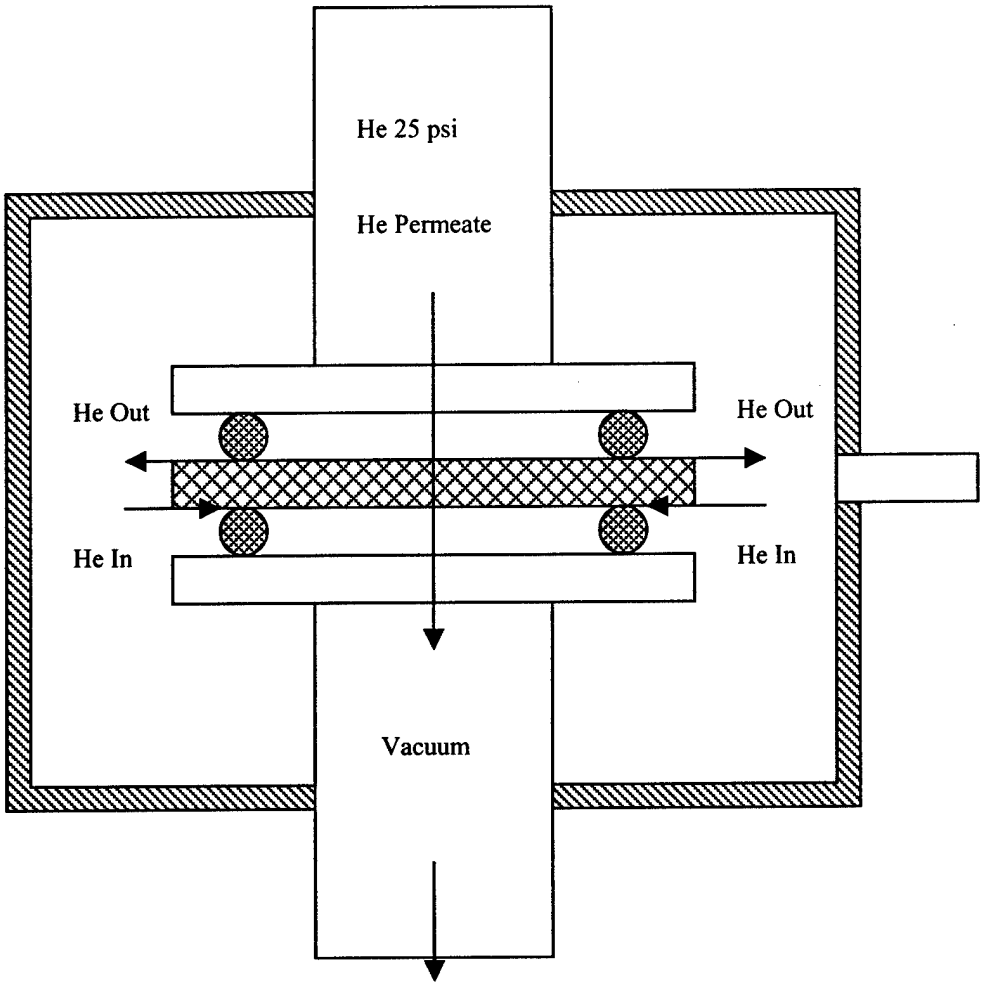

He Detected = He permeate + He In

Figure 2.45 The Schematic of The Case 3

CASE 4: Permeability Measurement Using Set-up with Pressurized External Chamber and Purge Line
From the schematic of permeability measurement using vacuum external chamber fixture (CASE 2), an unknown amount of helium may be pulled out from the edge of specimen. The set-up with pressurized external chamber and purge line shown in Figure 2.46 prevents any helium leak from being detected since it is balanced by the surrounding pressurized argon. Even if some argon come into the helium detector from lower surface of specimen, the helium detector only senses the flow rate of permeated helium. The schematic of the set-up is shown in Figure 2.47.

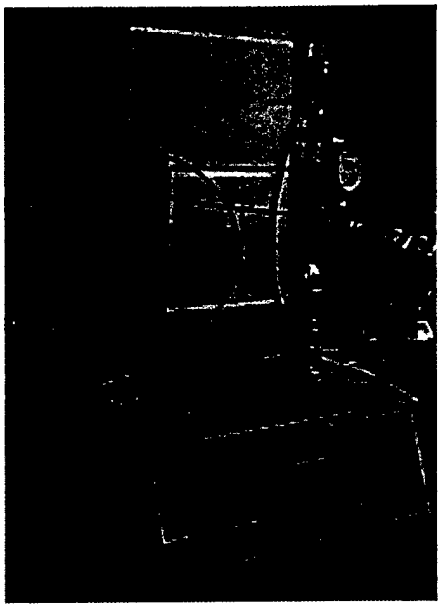

Figure 2.46 Permeability Measurement Using Pressurized External Chamber with Purge Line

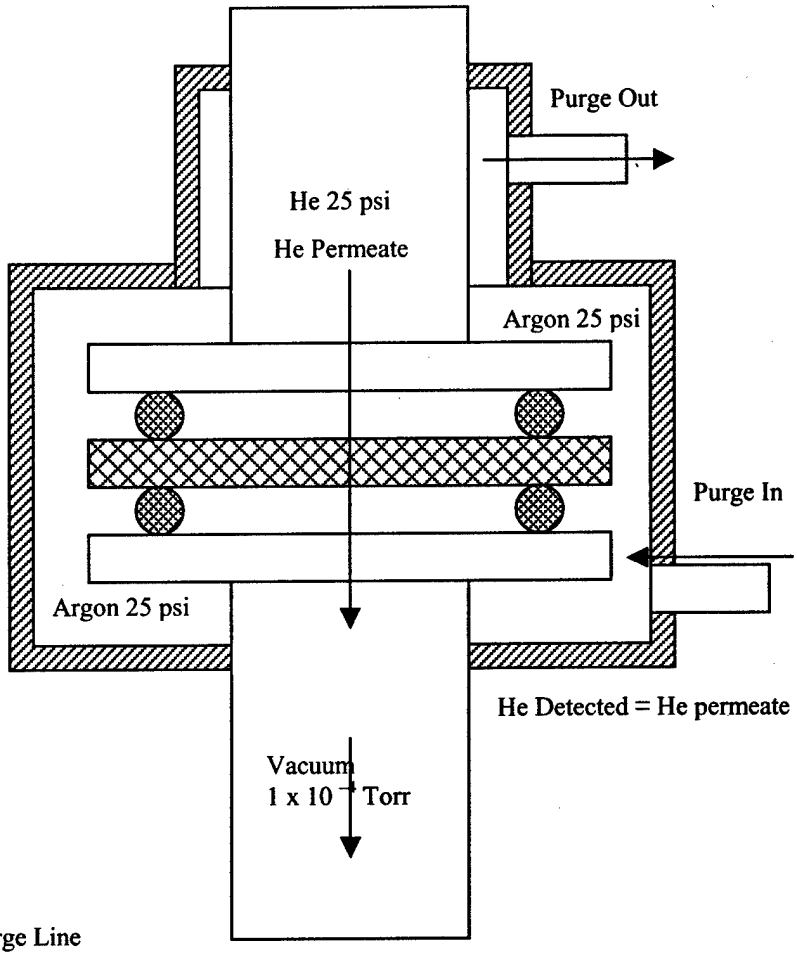

Figure 2.47 The Schematic of Case 4

Testing and Preliminary Investigation on Four Cases

The four method described in Case 1 through 4 have been used to measure the base line permeability of IM7/5250-4 composites using the helium mass spectrometer. The result for using the slotted O-ring (CASE 1) is shown in Figure 2.48 in which the helium permeation rate in cm^3/s is plotted against time at interval of 10 minutes. The stabilized helium permeation rate is 3.70E-07 cc/sec. The test area is 6.13 cm^2. The unit area permeation is **6.03E-8 cc/sec. cm^2**

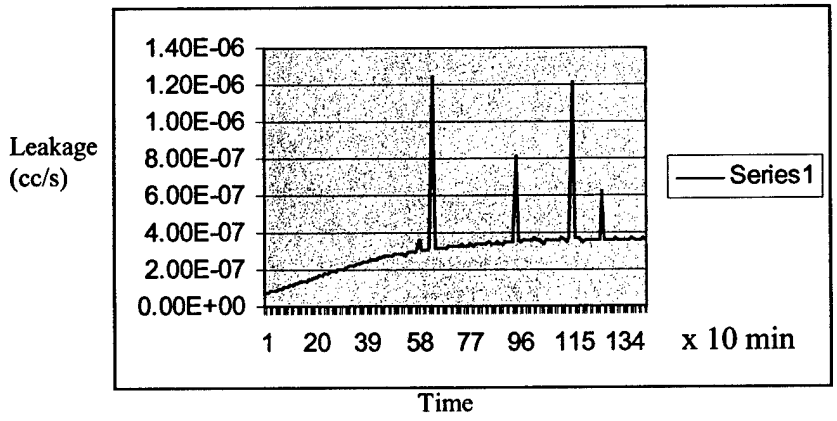

Figure 2.48 Helium Permeation Rate as A Function of Time Using Slotted O-ring Fixture (Case 1)

The result for using the permeability measurement with vacuum external chamber (CASE 2) is shown in Figure 2.49. The stabilized helium permeation rate is 2.40E-07 cc/sec. The test area is 8.82 cm^2 and the unit area permeation is **2.90E-8 cc/sec.cm^2** which is about 51% lower than using slotted O-ring fixture.

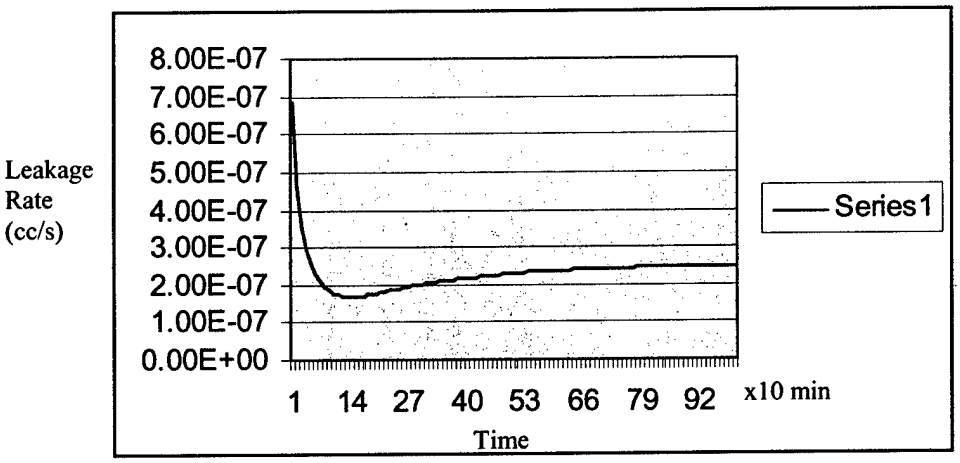

Figure 2.49 Helium Permeation Rate as A Function of Time Using Vacuum External Chamber (Case 2)

The test result for Case 3, in which vacuum was not used in the external chamber is shown in Figure 2.50. The stabilized helium permeation rate is 5.60E-07 cc/sec. The test area is 8.82 cm^2 and the unit area permeation is **6.34E-8 cc/sec.cm^2** which is about 100% more than the result for the Case 2 in which vacuum was pulled in the external chamber.

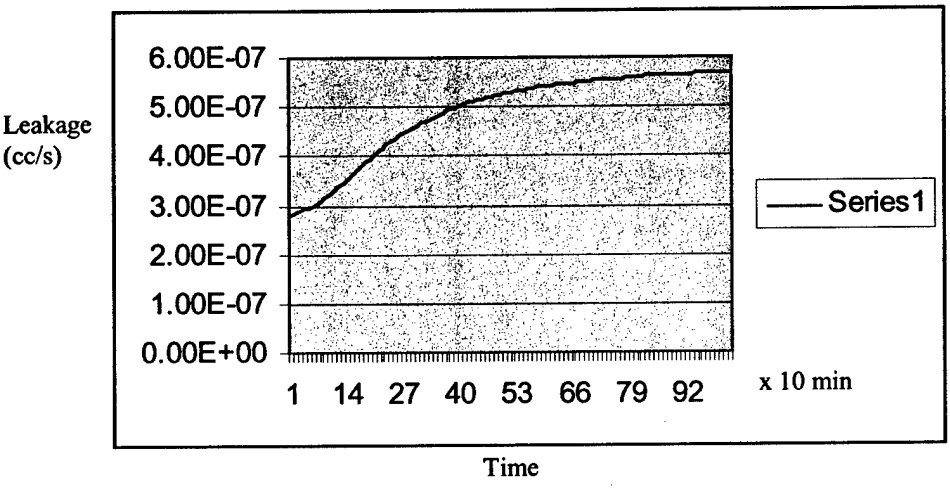

Figure 2.50 Helium Permeation Rate as A Function of Time Using Vacuum External Chamber Without Pulling Vacuum (Case 3)

The test result for Case 4, in which the external chamber is pressurized using argon and purged at 60 ml/sec as shown in Figure 2.51. The stabilized helium permeation rate is 2.15E-07 cc/sec. The test area is 8.82 cm^2 and the unit area permeation is **2.43E-8 cc/sec.cm^2** which is in the same range of the result for the Case 2 in which vacuum was pulled in the external chamber. If there are micro cracks on the surface of specimen, the result will be different.

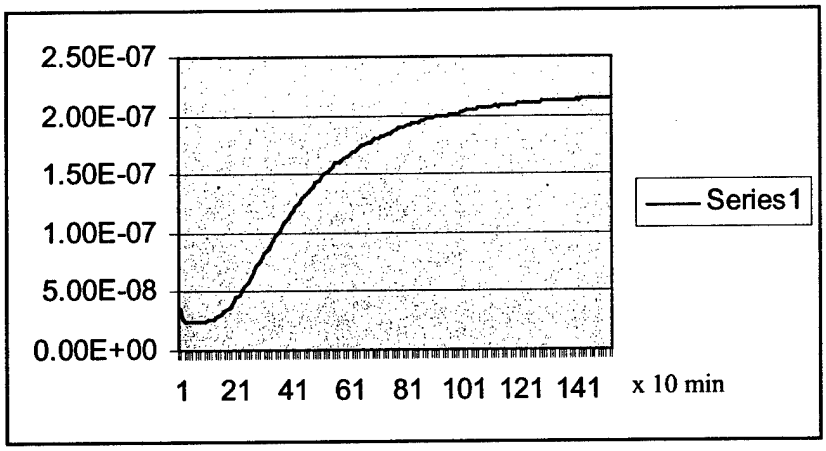

Figure 2.51 Helium Permeation Rate as A Function of Time Using Pressurized External Chamber With Purge at 60 ml/sec (Case 4)

Conclusions

From the schematic of four cases and test result, the permeability measurement using set-up with pressurized external chamber and purge line (Case 4) appears to eliminate any by-pass helium from being measured by the mass spectrometer. The only helium detected is the one that permeates the material, and thus a better characterization of the permeability of the material. It is recommended that this set-up be adopted as a standard procedure for obtaining a quick economical measurement of the permeability of composite material.

2.6 Effects of Thermal Cycling on Microcracking and Permeability of IM7/5250-4 Composite laminates.

This section summarizes the results of work done on studying the effect of cycling IM7/5250-4 composites between –320F and 350F on the permeability of the material to helium gas using the new permeability set-up.

Gas Transmission Rate as a Function of Cycling for IM7/5250-4 Composite

The helium gas transmission rate through the composite is defined as the volume of helium that passes through the material per unit area per unit time. The results from the permeability apparatus is used to compute this quantity.

Result for Baseline Specimen (0 Cycles)

O-ring Diameter = 0.8"= 0.8 x 2.54 =2.03 (cm)
1 sec = 1.157E-5 (day)
Gas Transmission Area

$$A = \frac{\pi D^2}{4} = \frac{(2.03cm)^2}{4} = 3.24\,cm^2 = 3.24x10^{-4}\,m^2$$

The Gas Transmission Rate (GTR) is given by

$$GTR = \frac{Leakage\ Rate}{Gas\ transmission\ Area\ x\ time}$$

$$= \frac{Leakage\ Rate(scc/\sec)}{(3.24x10^{-4}\,m^2)(1.157x10^{-5}\,days/\sec)}$$

$$= Leakage\ Rate(scc/\sec)\ \text{x}\ 2.67\text{x}10^{8}\ \text{secs/day/m}^2$$

Using the data from the gas leakage rate, the GTR curve for the specimen shown in Figure 2.52 was derived.

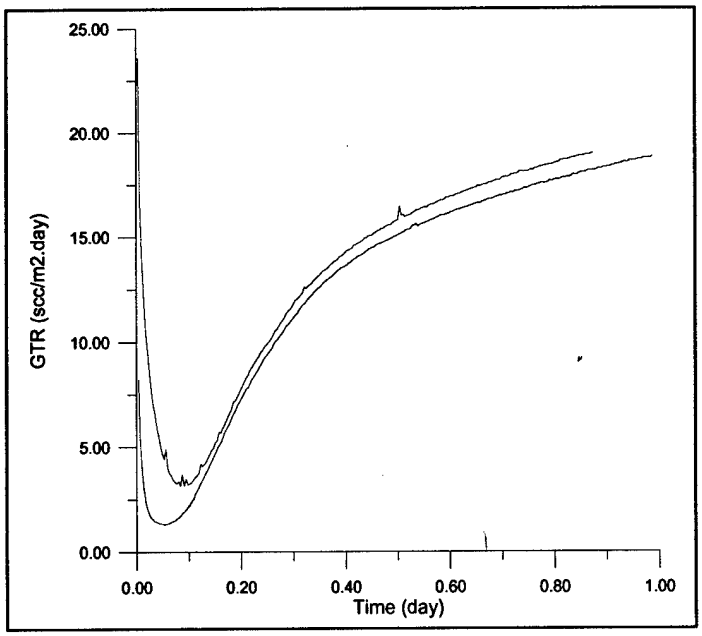

Figure 2.52 IM7/5250-4 GTR@ Base Line

Results for Other Cycles

Tha analysis above was applied to the results of the gas leakage rates for samples that underwent 50, 100, 500, and 1000 cycles to generate the gas transmission rate curves given in Figures 2.53 through Figure 3.56 respectively.

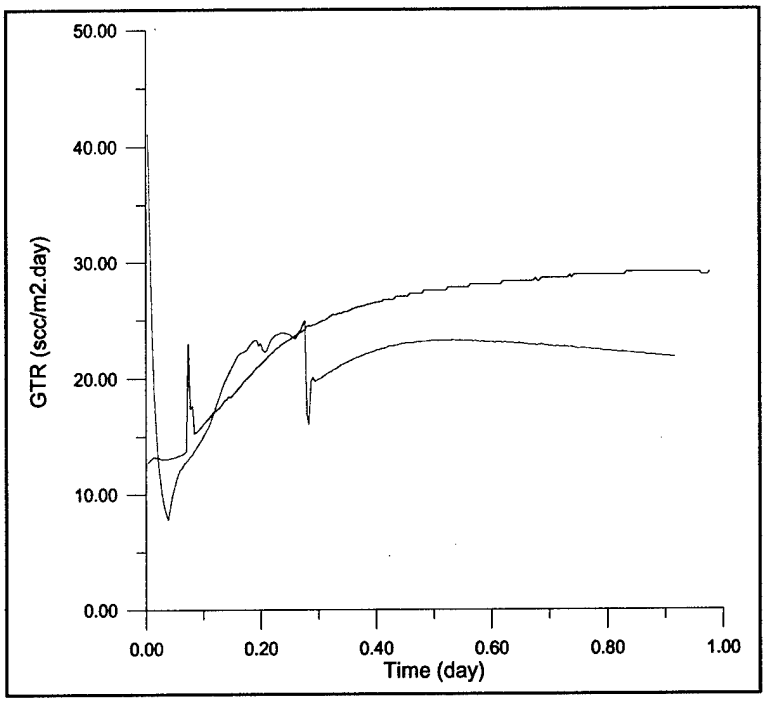

Figure 2.53 IM7/5250-4 GTR@ 50 Cycle

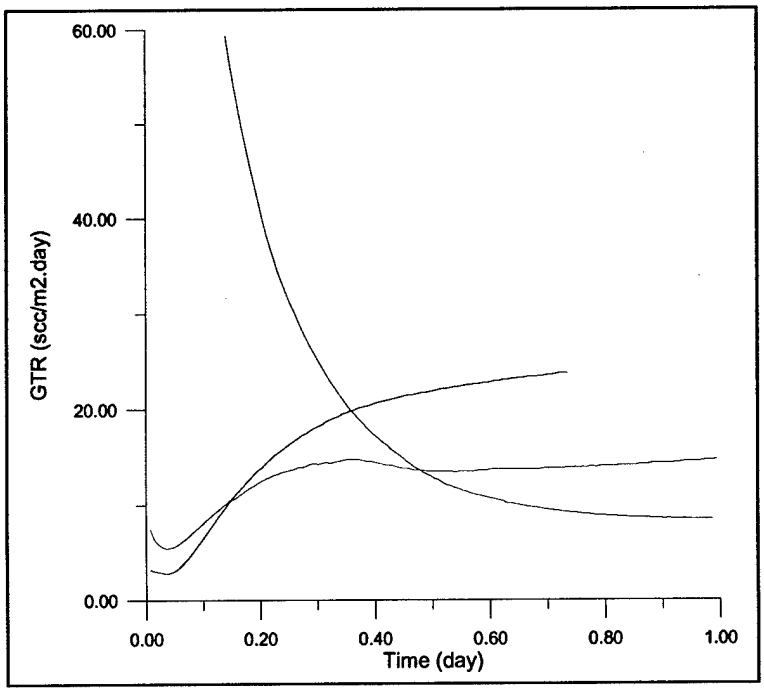

Figure2.54 IM7/5250-4 GTR@100 cycle

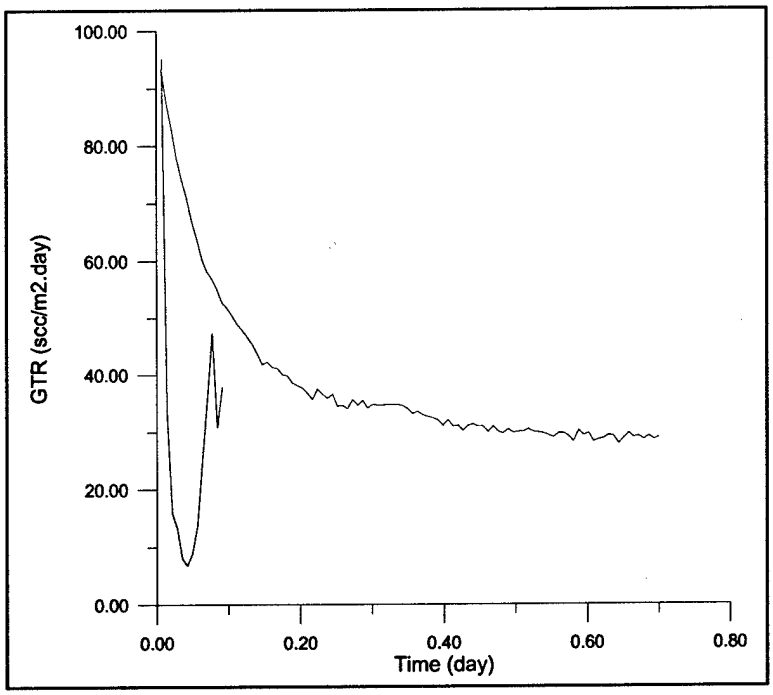

Figure 2.55 IM7/5250-4 GTR@ 500 Cycle

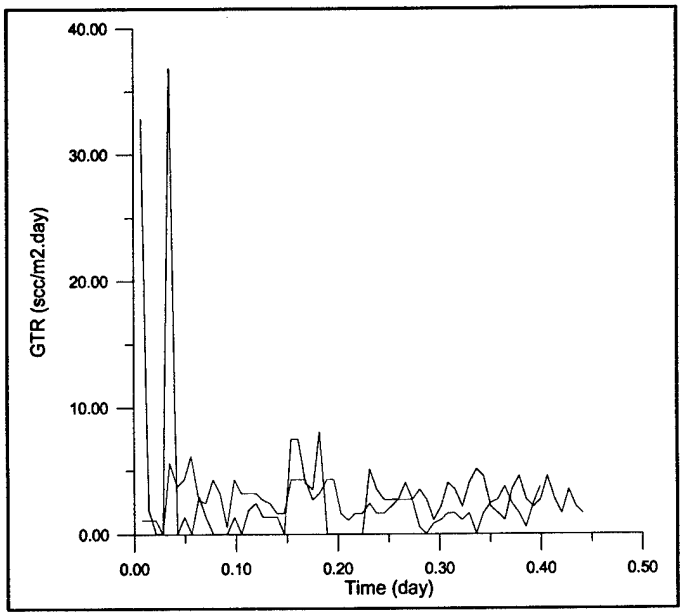

Figure 2.56 IM7/5250-4 GTR@1000 cycle

The steady state GTR using the average of the last 10 steady state GTR values for each sample at a given data point were determined as summarized in Table 2.11 and plotted in Figure 2.57. The results indicate that even though microcracks developed on the composite surface, the microcracks did not develop in the inner plys, and thus the permeability was nat very much dependent on the number of cycles. The gas transmission rate from the baseline to those for 1000 cycles were in the range of 25 to 2.6 scc/m^2/day.

Table 2.11 Average gas Transmission Rate

	Average Gass Transmission Rate (scc/m^2/day)				
	Base Line	50 Cycle	100 Cycle	500 Cycle	1000 cycle
Ave	18.8	25.73031	15.52275	24.8561	2.640333
STD	0.11	5.275779	7.592225	2.999547	0.41955

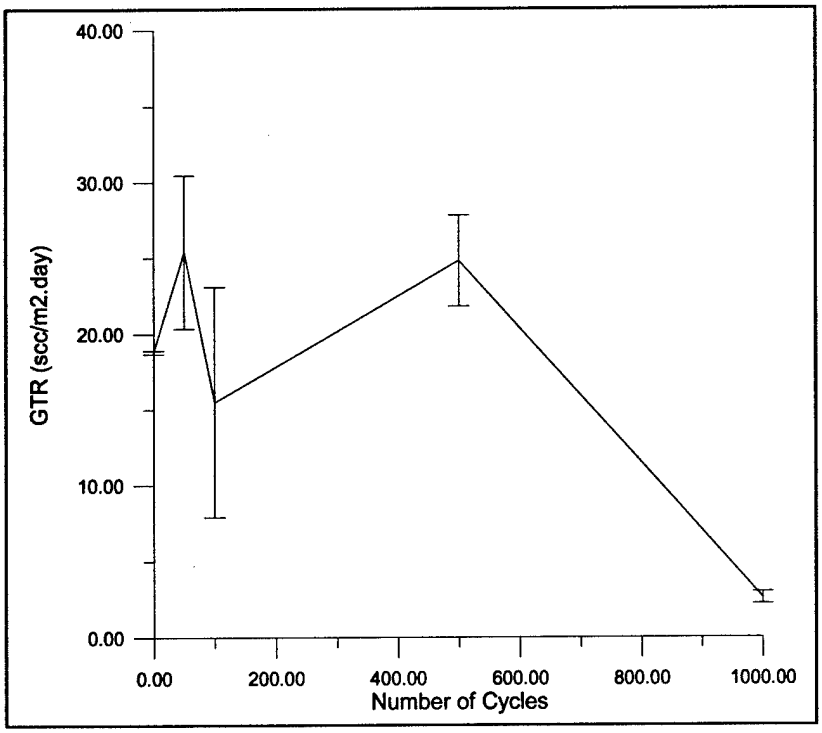

Figure 2.57. The Steady State GTR vs Number of Cycles

3. RESEARCH CONDUCTED IN COLLABORATION WITH THE UNIVERSITY OF DAYTON RESEARCH INSTITUTE

3.1. SUMMARY

The catastrophic failure of the X-33 cryogenic tank has reinforced the need of the composites community to develop predictive test methods for evaluating the performance of advanced composites in cryogenic environments. The principal materials-related cause (as opposed to potential design flaws) of the failure was permeation or leakage of liquid hydrogen gas through microcracks in the composite tank. This year our research has focused on developing a fundamental understanding of the formation of microcracks while loading composites at various temperatures and developing a test method to measure the resulting leakage rates of said composites.

3.2 TEMPERATURE EFFECTS ON FATIGUE LIFE AND MICROCRACK FORMATION

The objectives of this work are to establish test a protocol for evaluation of composite laminates at cryogenic environments, to study the effect of microcracking on the leakage of gases and cryogenic fluids, and to study the effect of thermal environment on the fatigue life of composite laminates. Laminates with a stacking sequence of $[45/-45]_{2s}$ and $[90]_{2s}$ were selected because they show predominant matrix failure, which occurs commonly in all multidirectional laminates. To establish a fast and low-cost method for screening candidate material systems for cryogenic temperatures as low as -452°F, an effort will be made to develop a test protocol to identify the most significant key ply properties before undertaking an expensive full-blown characterization.

Material systems chosen for this study are carbon fiber, IM7 reinforced with toughened BMI, 5250-4 and toughened epoxy 977-3. A total of ten $[45/-45]_{2s}$ panels of IM7/52504 were fabricated for fatigue testing in order to obtain all specimens from the same batch of prepreg. It is noted that the prepreg thickness of this new batch is 0.008", and its fiber content was found to be the same as the thin prepreg. Tension-tension fatigue tests are being conducted to obtain S-N curve relations under three to four constant stress levels corresponding to 85, 75, 65, and 55 percent of the static strength. Three temperatures considered are -321°F, 73°F and 300°F. Five straight-sided specimens under each stress level are fatigued until final failure at a frequency of 10 Hz with a stress ratio of R=0.1. Figure 3.1 shows the S-N curves constructed from tests at four stress levels at the three temperatures. Normalized fatigue stress (with respect to the static strength of the corresponding temperature) is used for comparison purposes. The fatigue life increased at -321°F and decreased at 300°F compared with room temperature.

Two specimens (2" wide) of the $[45/-45]_{2s}$ laminate were fatigued to generate microcracks for gas and fluid leak detection at room temperature and -321°F. Figures 3.2 and 3.3 are the micrographs showing microcracks in the fatigued specimens. Table 3.1 shows the number of cracks per inch in each ply. These samples, expected to represent a worst case, will be evaluated with the gas leakage test (reported in the following section).

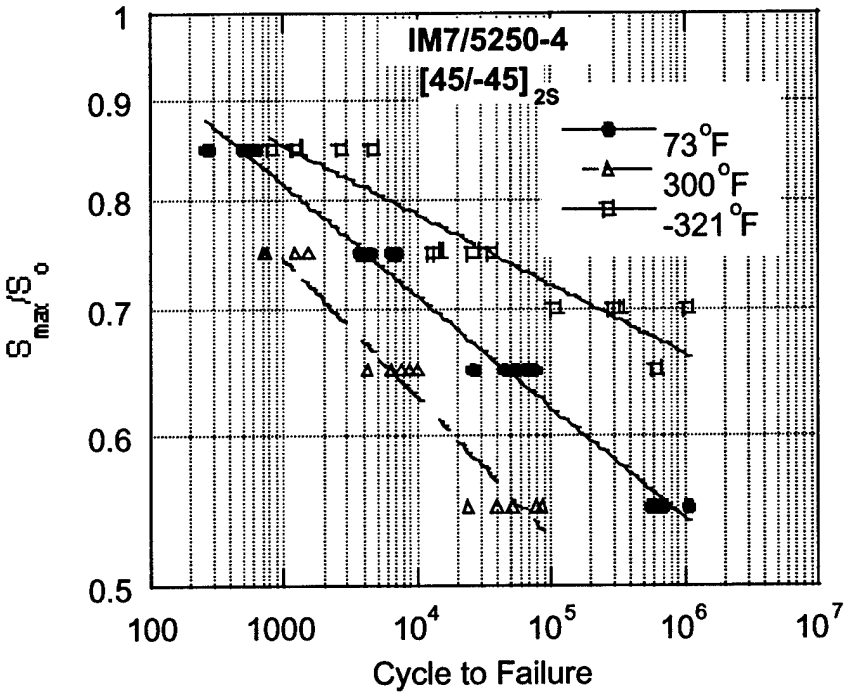

Figure 3.1 S-N curves of $[45/-45]_{2s}$ laminate at -321°F, 73°F and 300°F: S_{max}= maximum fatigue stress and S_o = static strength.

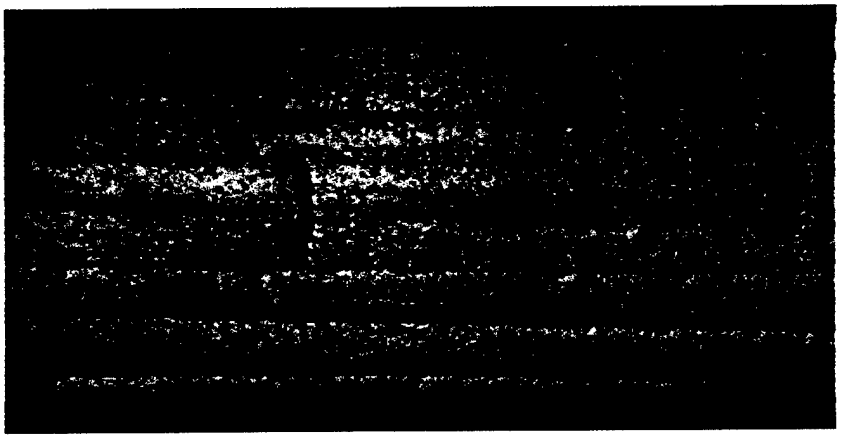

Figure 3.2 Micrograph showing microcracks in a fatigued specimen of the $[45/-45]_{2s}$ laminate after 500 cycles with a maximum fatigue stress of 24 ksi at 73°F.

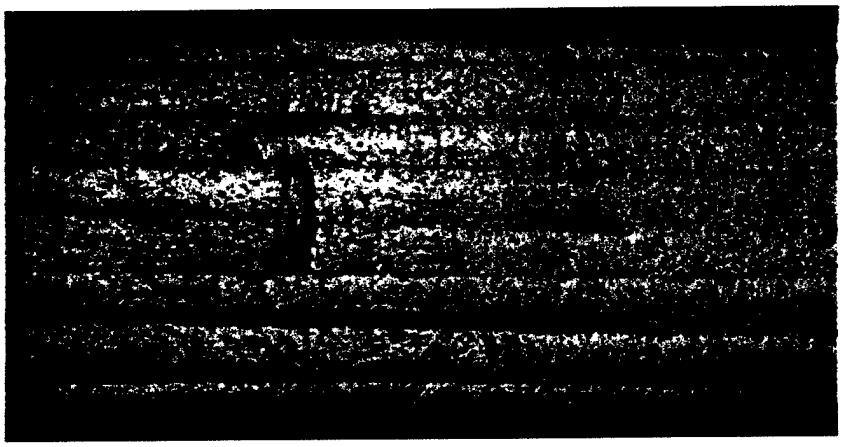

Figure 3.3 Micrograph showing microcracks in a fatigued specimen of the $[45/-45]_{2s}$ laminate after 200 cycles with a maximum fatigue stress of 25 ksi at 73°F.

Table 3.1 Crack Density of Fatigued $[45/-45]_{2s}$ Specimens

ID	S_{max} ksi	Cycle	Number of cracks per inch						
			Ply 1	Ply 2	Ply 3	Plies 4&5	Ply 6	Ply 7	Ply 8
1	24	500	22	41	42	27	38	40	27
2	25	300	34	77	91	55	90	93	35

S_{max} = maximum fatigue stress

3.3 THERMAL CYCLING INDUCED MICROCRACKS

Exposure of composite laminates to cryogenic temperatures can cause ply microcracking due to thermal residual stresses that arise from the anisotropy in the composite ply coefficient of thermal expansion (CTE). Transverse ply cracking often results in a reduction in laminate stiffness and strength and changes in laminate CTE, and provides a pathway for the ingress of moisture or corrosive chemicals; in cryotanks, transverse cracking can cause leakage of the pressurized liquid fuel. The main objective of this work was to understand the mechanical behavior and damage onset in composites at cryogenic temperatures, and to develop a predictive capability for the onset of transverse cracking in composite laminates subjected to isolated or combined thermal and mechanical loads.

Unidirectional and multidirectional laminate panels of IM7/977-3 composite were laid up from the unitape prepreg and cured in an autoclave in accordance with the manufacturer's recommended cure cycle. Cured composite panels were postcured for seven hours at 450°F in an oven. The $[0]_{8T}$, $[90]_{8T}$ and $[\pm 45]_{2S}$ laminates were used to characterize this composite material at cryogenic temperatures and provide the thermomechanical properties required for analytical calculation. The $[0/90_2/0]_T$, $[0_2/90_2]_S$, and $[30/-30/90]_S$ laminates were used to investigate the onset of transverse ply failure in this composite system at 73°F and -321°F. All specimens were 0.5 inch wide with a gage length of six inches. Fiberglass/epoxy end tabs were bonded to the

specimens tested at 73°F; no end tabs were used for specimens tested at -321°F. The edges of the specimens for the ply failure study were first ground with sandpaper and then polished with 5-micron and 1-micron polishing powder to enhance microscopic imaging for crack detection. Prior to testing, all specimen edges were examined under a microscope to determine if specimen cutting and handling induced any damage. No damage was observed in any specimen prior to testing. All specimens were stored in a desiccated cabinet until test.

A special mechanical grip (4,000 lb load capacity) was designed and built for tests at cryogenic temperatures. The clamping face of each grip was coated using a Surfalloy process to enhance the gripping action without damaging the specimen surface by grip force. All specimens were tested on an MTS test machine using a stainless-steel container, designed and built in-house, for tests at liquid nitrogen temperature (-321°F). Specimens mounted on the test machine were cooled to the desired test temperature by immersion in liquid nitrogen in the insulated stainless-steel container and allowed to equilibrate for 20 minutes. They were then loaded in tension at a strain rate of 0.02/min.

Acoustic emission was employed to detect the onset of ply failure in tests. When a sudden acoustic emission event was observed, the specimen was unloaded and examined under a microscope to confirm the presence of transverse cracking. Figures 3.4 and 3.5 show the acoustic emission record for specimens tested at 73°F and -321°F, respectively, indicating the first occurrence of ply failure.

Continuous presence of low level acoustic emission signals in Figure 3.5 exhibited throughout the test as background noise due to the boiling of liquid nitrogen. The large size of the AE signal near the end indicates the onset of ply failure and can be easily distinguishable from the background noise. The onset of ply failure was confirmed using a microscope after unloading. If no ply failure was found under microscopic examination, then the specimen was incrementally loaded to either occurrence of an acoustic emission signal above the background noise level or the prescribed load. This procedure continued until there was a physical presence of ply failure. Figures 3.6 and 3.7 are micrographs of the transverse cracks at 73°F and -321°F.

Unidirectional panels measuring 3" x 3" were prepared to determine the coefficient of thermal expansion (CTE) that is required to calculate the residual stresses. Composite CTEs were measured using strain gages with a 0.25-inch gage length. Ultralow-expansion titanium silicate was used as the reference material for completion of the strain gage bridge circuit. Specimens were cycled between -200°F and 300°F at a rate of 5°F/min, and held isothermally for 15 min after each 40°F increment of temperature in a computer-controlled temperature chamber. Because of low-temperature limitations of the temperature chamber, specimens were immersed in liquid nitrogen (-321°F) and held for 20 min. A software program controlled test parameters as well as continuous acquisition of temperature and strain data during both heating and cooling cycles. The CTE was obtained from a linear fit to the data over the entire test temperature range.

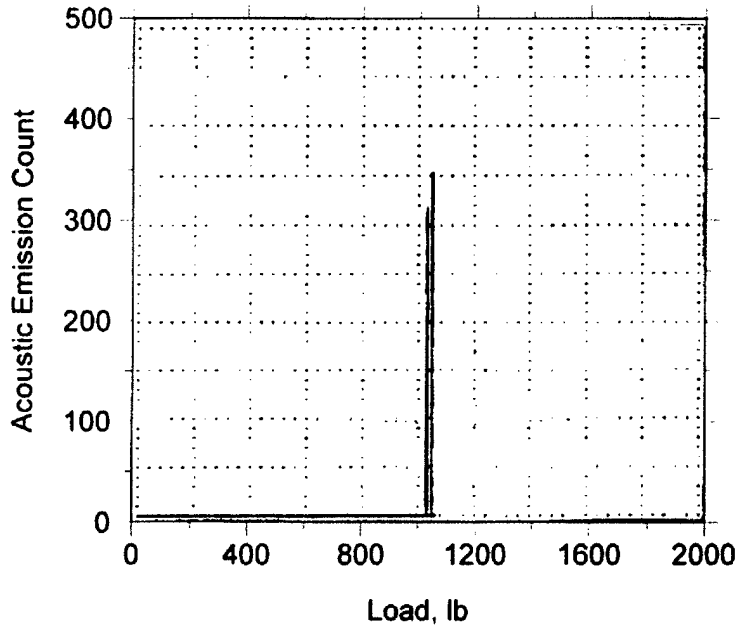

Figure 3.4 Acoustic emission record indicating the onset of ply failure for $[0/90_3/0]_T$ at 73°F.

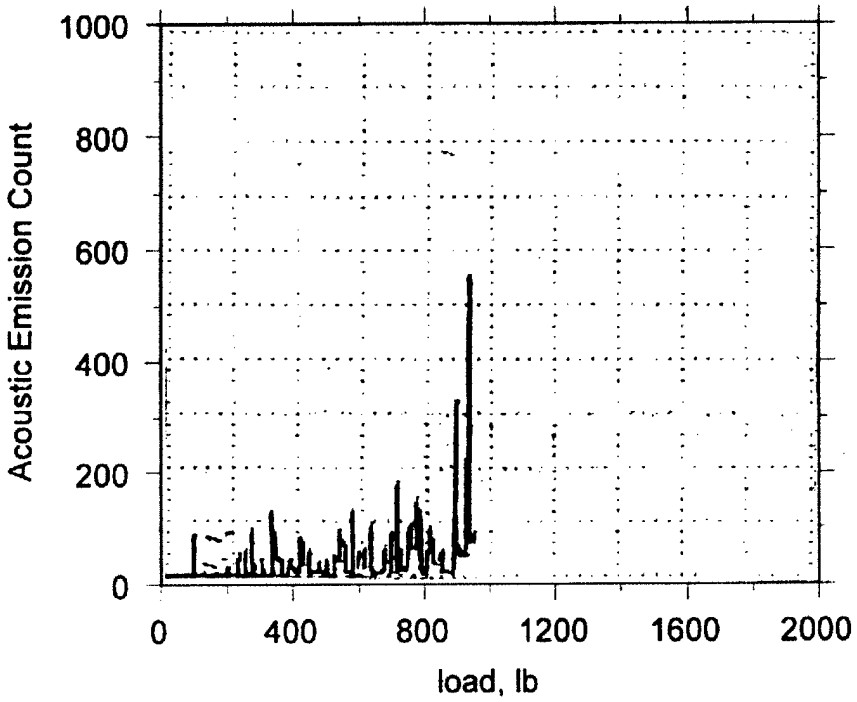

Figure 3.5 Acoustic emission record indicating the onset of ply failure for $[0/90_2/0]_T$ at -321°F.

Figure 3.6 Micrograph showing the onset of ply failure at 73°F for $[0/90_3/0]_T$.

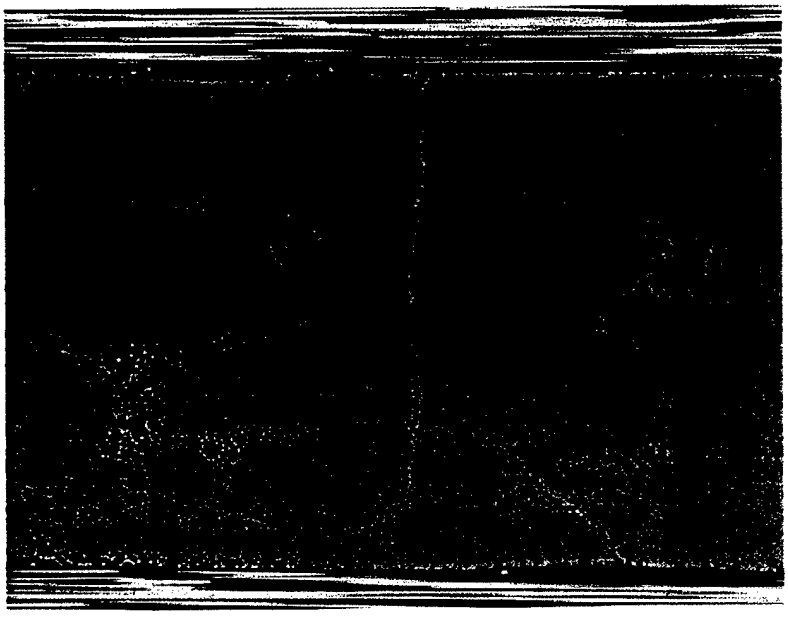

Figure 3.7 Micrograph showing the onset of ply failure at -321°F for $[0/90_3/0]_T$.

Classical laminated plate theory was used to calculate the residual stress resulting from cure. The residual stress σ_i^R in each ply can be written as

$$\sigma_i^R = Q_{ij}A_{jk}^{-1}N_k^T - Q_{ij}e_j^T$$

where

Q_{ij} = reduced stiffnesses at the final temperature of interest
A_{ij} = laminate stiffnesses
N_k^T = stress resultants due to thermal strains
e_j^T = ply thermal strains measured from the stress-free state

Table 3.2 lists the thermomechanical properties determined and used for the calculation of the residual curing stresses.

Table 3.2 Thermoelastic Properties of IM7/977-3 Composite

	Temperature, °F	
	73	**-321**
Longitudinal modulus, Msi	26.1	26.5
Transverse modulus, Msi	1.4	1.9
Shear modulus, Msi	0.88	1.33
Poisson's ratio	0.33	0.33
Longitudinal CTE, α_x, 10^{-6}/°F	0.1	0.1
Transverse CTE, α_y, 10^{-6}/°F	13.0	11.3
Transverse tensile strength, ksi	10.8	14.11
Curing stress-free temperature	325°F	

The stress in the 90° plies of all laminates, $[0/90_2/0]_T$, $[0_2/90_2]_S$, and $[30/-30/90]_S$, at the onset of ply failure, was calculated from the applied stress using classical laminated plate theory for comparison with the transverse strength obtained from tensile tests on $[90]_{8T}$ specimens. The curing residual stress was calculated with the assumption of a stress-free temperature of 325°F (cure temperature 350°F). Table 3.3 shows the 90° ply stresses calculated for all the laminates at the onset of transverse cracking and the measured composite transverse strength. In cross-ply laminates at 73°F, the calculated 90°-ply stress is greater than the transverse strength determined by test using the $[90]_{8T}$ specimens, whereas it is smaller in the $[30/-30/90]_S$ laminates.

The stress level at the onset of transverse cracking decreased at -321°F, mainly due to an increase in the curing residual stresses. The lamination theory, in conjunction with the maximum stress failure criterion, tends to overestimate the onset of the transverse cracking in this laminate.

Table 3.3 Summary of Onset of Ply Failure (FPF)

Laminate	Temperature,°F	Applied Stress at FPF, ksi	Stresses in 90° Ply, ksi			Measured 90° Ply Strength, ksi
			Curing Residual Stress	Mechanical Stress at FPF	Total Stress	
$[0/90_2/0]_T$	73	82.13	4.21	8.46	12.67	10.81
	-321	59.83	10.87	6.16	17.03	14.11
$[0_2/90_2]_S$	73	82.23	4.21	8.45	12.66	10.81
	-321	59.32	10.87	6.10	16.97	14.11
$[30/-30/90]_S$	73	35.56	4.21	4.56	8.77	10.81
	-321	32.43	10.87	4.18	15.05	14.11

3.4 Gas LEAKAGE in Cryogenic Condition

A method for determination of gas leakage under cryogenic conditions of composite materials is under investigation. A schematic of the gas leakage apparatus as run with liquid nitrogen is shown in Figure 3.8. A 1.5-inch-diameter aluminum sample was used to test for gas leakage at ambient and at cryogenic temperatures. The sample was sandwiched between two rubber washers or two indium O-rings, to provide seals against leakage to the environment. To test at cryogenic temperatures, the sample fixture was immersed in liquid nitrogen to a temperature of -160°C. Helium gas was introduced through the inlet at pressures up to 50 psi. The outlet was connected to an inverted graduated cylinder, which was placed in a water bath to measure water level at specific time intervals to determine leakage rates. By tightening down on a spring as the samples cooled, it was expected that the spring would expand – driving the sample together and thus providing a counter force to contraction and sealing the sample fixture.

Rubber washers were first used to construct the sample fixture. No leakage was detected at ambient temperatures and at pressures up to 50 psi. However, leakage occurred at cryogenic temperatures at pressures of 40 psi and higher. The leakage rates were 60 ml/min and 210 ml/min for 40 psi and 50 psi, respectively. Leakage may have occurred due to a large mismatch in CTE between the rubber washer and the aluminum sample.

When an indium O-ring was used rather than rubber at ambient temperature, the leakage rate was one bubble per minute for pressures ranging from 10 psi to 40 psi. At 50 psi the leak rate was 0.05 ml/min. At cryogenic conditions the leakage rates were 0.18 ml/min at 10-psi pressure, 0.4 ml/min at 30 psi to 40 psi, and 0.5 ml/min at 50 psi. It was observed that leakage rates increased a factor of 10 as the temperature was dropped from ambient temperature to cryogenic temperatures.

At this time we have not succeeded in preventing leakage using the aluminum disk. Work is in progress to repeat the leakage test on different sealing materials, including RTV paste and vacuum grease, to prevent leakage. Soon we will evaluate the composite specimen illustrated in Figures 3.2 and 3.3 to determine the scale of leakage we are dealing with. If the leakage rate is high, our current sealing method may be reasonable.

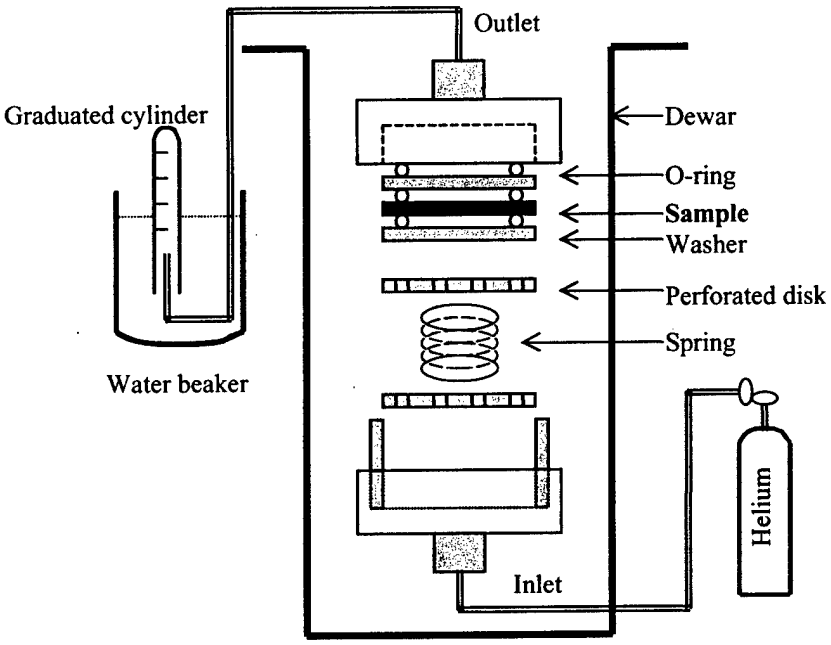

Figure 3.8 Apparatus for measuring gas leakage under cryogenic conditions.

4. INDUSTRIAL CONTRACT PROJECTS

This chapter describes contract work done for Wyle Laboratories Life sciences Laboratory, a major NASA contractor located in Houston and for Raytheon, a major DOD contractor located in Dallas, Texas. The two contract projects were completed on schedule and comprehensive final reports submitted as part of the deliverables.

4.1 The Wyle Project

The work described in this section was done at the Future Aerospace Science and Technology (FAST) Center for Lightweight Structural Material and Composite Processing at Prairie View A&M University under a contract from Wyle Life Sciences.

4.1.1 Statement of Work

The statement of work in connection with this project required the FAST Center to design, fabricate, analyze and test a composite panel, and necessary test coupons, to replace a mid-deck locker aluminum panel (KLSI210564-003) shown in Figure 4.1. In addition a method to eliminate or minimize galvanic activity between the composite panel and the aluminum structure was required while maintaining the aluminum panel dimensions and mechanical properties. Graphite prepreg tape was identified as the required material for the fabrication of the panel. The results to be presented in a report documenting

1 Materials within the graphite tape family detailing mechanical, fabrication and cost attributes for the selection process;
2 The method/system for eliminating or minimizing galvanic interaction;
3 Cost projection for small production runs of the composite panels, including manpower and facility requirements.

The analysis was to include

1 Structural analysis (FEA/FEM) of the aluminum panel to determine tensile, compressive, shear, and bending failure values;
2 Details of design approach and analysis for the composite panel;

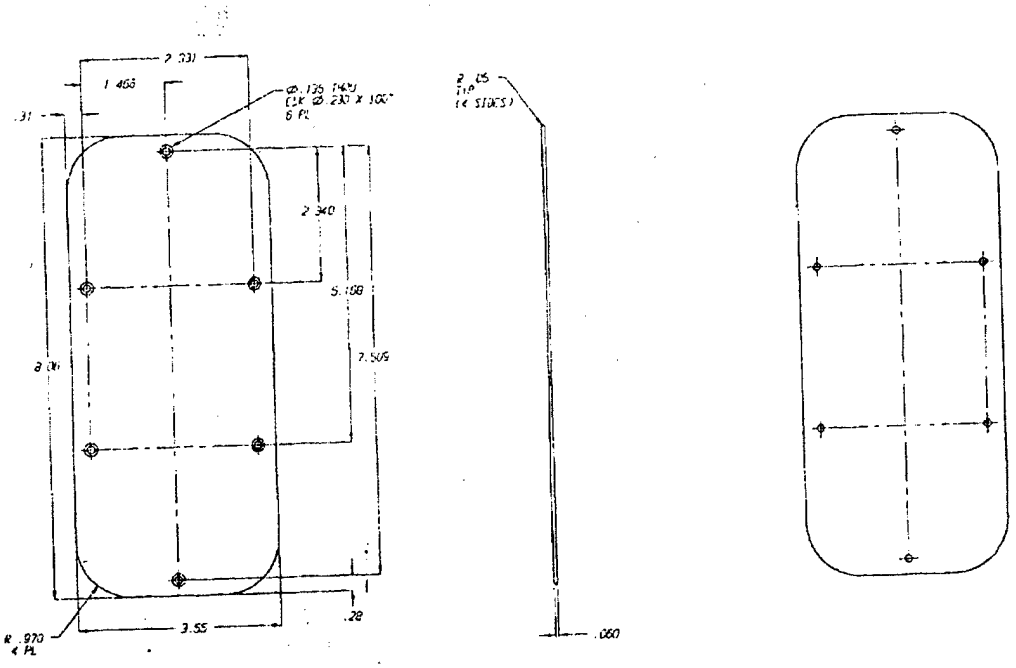

Figure 4.1 The Dimension of Closeout Panel (KLSI210564-003)

3 Analysis of solution for galvanic action between Al locker and composite panel.

The final report was also to include documentation on composite panel fabrication techniques including written and photographic evidences.

The mechanical testing was to include flatwise tensile strength, edgewise compressive strength, and flexural properties per applicable ASTM standard.

4.1.3 Background

Wyle Life Sciences employs shuttle mid-deck locker as carriers for most of its life sciences payloads. These lockers provide payloads with an enclosure, which are being targeted for weight reduction to maximize payload utilization. The locker enclosures utilize up to 8 aluminum panels, which are being identified for replacement.

4.1.4 Objectives

The objective of the project was to design, fabricate, analysis and test a composite panel, and method to eliminate or minimize galvanic activity between the composite panel and the aluminum structure.

4.1.5 Summary of Project results

Composite Material Selection, Fabrication and Testing

Analysis of several fiber and resin systems lead to the selection of IM7/5250 as the composite material for the panels.

Composite panels were processed using compression molding and post-cured using the manufactures recommended cure and post-cure cycles.

Tension tests conducted on samples prepared from the composite in accordance with ASTM D3039 indicated a tensile strength of 131.4 ksi (906.95 MPa) compared to a value of 42 ksi (290 MPa) for aluminum T6061-T6. Flexure tests made in accordance with ASTM D790 indicated a flexural strength of 149.8 ksi (1032 MPa). In addition to these tests, complete panels we tested in tension by pulling on pins through four holes. This test indicated that the composite panels could withstand far larger loads than an aluminum panel.

C-scan images of the composite panels indicated that the process of drilling the six countersink holes did not have any adverse effects on the quality of the composites,

The galvanic electrochemical reaction between the composite and aluminum was measured experimentally. A galvanic corrosion protective coating material, 1C49, was selected for use after reviewing several alternatives. Composite panels were coated with 1C49 and then tested for any galvanic electrochemical reactivity between the coated panel and aluminum, The results indicated that 1C49 provided complete corrosion protection.

4.2 The Raytheon Project

The work described in this section was done at the Future Aerospace Science and Technology (FAST) Center for Lightweight Structural Material and Composite Processing at Prairie View A&M University under a contract from Raytheon Antenna/Nonmetallics Division, McKinney, TX.

4.2.1 Objectives

The objectives of this work are to fabricate and test composite panels made of Superimide800 polyimide resin/Astroquartz fibers.

4.2.2 Scope

The scope of this work includes documentation of all processing parameters as well as mechanical testing of the composite. The purpose of this effort is to provide the customer (Raytheon Antenna/Nonmetallics Division, McKinney, TX) with adequate processing information and basic mechanical properties of this composite system.

4.2.3 Approach

The composite samples should be fabricated to the proper size and orientation as specified in the applicable testing documents. The composite panels must be cured using vacuum bag/autoclave. It is critical that press curing is not used. All processing parameters should be documented in detail. The panels are to be cut as outlined in the applicable testing procedures. Tests to be performed are compression and short beam shear. All sample sizes/data analysis shall be done according to the applicable testing standard. All testing shall be performed at three temperatures: Room temperature, 600°F, and 800°F. A final report shall be submitted which shall include all aspects of processing and testing in great detail.

4.2.4 Summary of Project Results

This section contains a detailed account of autoclave processing and mechanical tests performed on three batches of SuperImide800 composite panels.

The prepregs were purchased from J.D. Lincoln. We believe the resin content was not uniform, since some portions of the prepreg appeared visually to be resin deficient, thus necessitating the application of more resin to those areas before processing.

Six 12"x13" panels with 12 layers of the prepreg were made. Since this was the first time we operated our autoclave at high temperature and pressure, some problems were countered initially. With assistance from the autoclave manufacturer, the problems were fixed, and three panels were successfully cured and postcured according to cure and postcure cycles provided by Goodrich Corporation.

Short beam shear testing was conducted according to ASTM D2344-84 with crosshead speed of 0.05 in/min and span of 0.625 (5 times the thickness). The tests were conducted at room temperature, 600°F, and 800°F. The results indicated that at room temperature, the short beam shear strength were 54MPa, 39MPa, and 36MPa for panels 2, 3, and 4 respectively. At 600°F, the short beam shear strength were 25MPa, 20 MPa, and 20 MPa for panels 2, 3, and 4 respectively. At 800°F, the results were 17MPa, 9MPa, and 10 MPa for panels 2, 3, and 4 respectively.

The compression test results indicated compression strength of 365MPa, 294 MPa, and 395 MPa for panels 2, 3, and 4 respectively at room temperature. At 600°F, the compressive strengths were 252 MPa, 266 MPa, and 264 MPa for panels 2, 3, and 4 respectively. At 800°F, the compressive strengths were 31 MPa, 156 MPa, and 160 MPa for panels 2, 3, and 4 respectively.

The compression modulus at room temperature were 16 GPa, 20 GPa, and 21 GPa respectively for panels 2, 3, and 4 respectively. At 600°F, the compression modulus were 26 GPa, 56 GPa, and 26 GPa for panels 2, 3, and 4 respectively.

The average glass transition temperatures were 360°C, 365°C, and 372°C for panels 2, 3, and 4 respectively.

5. INFRASTRUCTURE ADDITIONS AND LABORATORY DEVELOPMENT AND MAINTENANCE

5.1 Current State of the FAST Center Labs

Currently, the FAST Center has seven well equipped laboratories that are used for research. These are:

1. The composite processing laboratory
2. The thermal analysis laboratory
3. The chemical analysis laboratory
4. The mechanical testing laboratory
5. The environmental exposure laboratory
6. The optical and electronic laboratory and
7. The non-destructive evaluation laboratory

The seven FAST Center laboratories are described in the FAST Center Capabilities brochure attached to this report in Appendix A.

5.2 Additional capabilities Acquired During the period from September 2000 to May 2002

Three major projects were undertaken to increase the research capability at the Center and also to improve the operation of the autoclave. The major research infrastructure addition were the design of the auto-cycling machine and the permeability measurement apparatus described in chapter 2. In addition to these, the FAST Center designed and built a water re-circulator/cooling system for the autoclave described below.

Design and Construction of Cooling System for the Autoclave

Prior to the modification described in this section, the autoclave cooling system uses city water that passes through the cooling coils of the autoclave. After heat removal by the cooling water, the water is discharged toe drain. The flow rate of the cooling water is 30 gal/min and each autoclave processing normally runs for about 8 hours. The total amount of water used for each processing is about 14,400 gallons. Thus this re-circulating system has the potential of saving 14,000 gallons of water per autoclave run. A cooling water recycle system shown in Figure 6.1 was designed and installed. The cooling water is collected in a 300 gallon storage tank. There are two pumps. The first pump is used to cycle the water between the tank and the autoclave. The second pump is used to cycle water between the 300 gallon tank and a 2 ton chiller which is used to cool the water.

The system is designed such that if the water temperature in the 300 gallon tank is over 90 °F, two three way valves are used to switch the autoclave water inlet to city water and the outlet water is then sent directly the drain. When the tank water temperature goes below 90 oF, the three way valves will switch back to have the autoclave cooling water recycled through the 300 gallons tank.

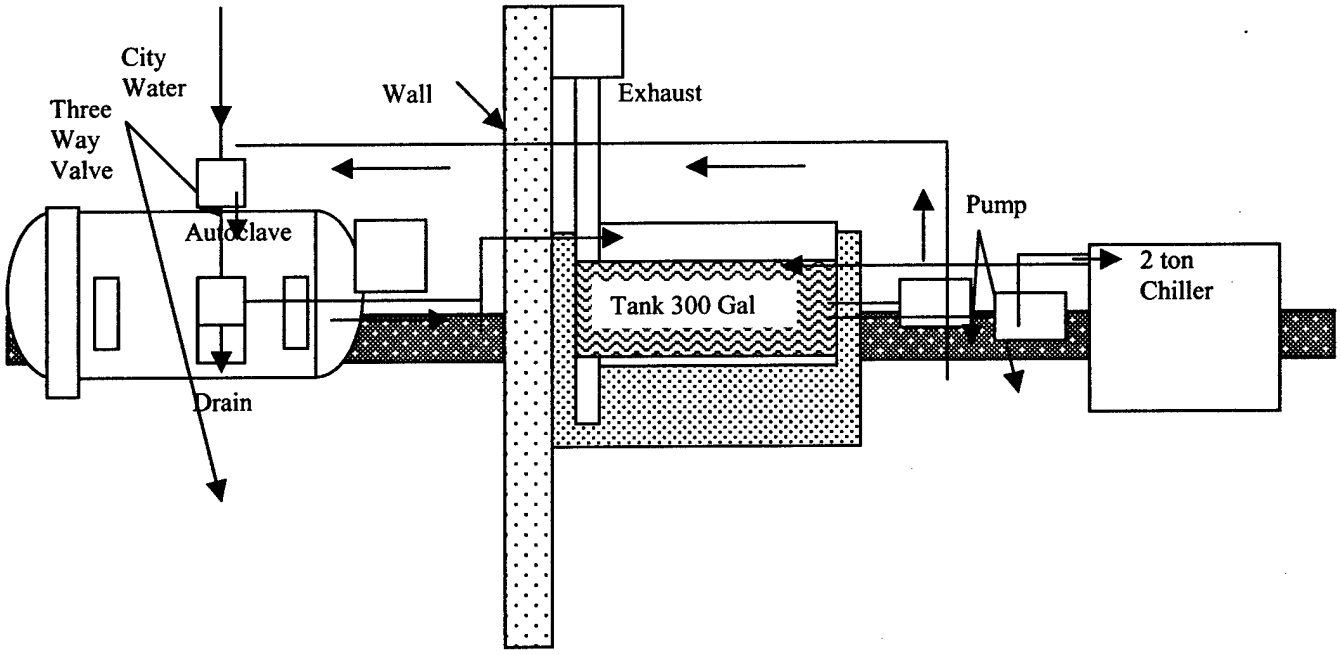

Figure 1. Autoclave Cooling Water Recycle System

6. FAST CENTER OVERALL FINAL SUMMARY REPORT

The funds received from the Air Force office of Scientific Research for the establishment of the FAST center has greatly increased the capabilities for composite materials research at Prairie View A&M University (PVAMU). This chapter summarizes the research highlights, the undergraduate and graduate students trained as a result of this program, the collaboration we have had with industry and other research labs, and the potential for future research afforded by the infrastructure made possible at PVAMU as a result of the establishment of the FAST center.

6.1 Research Summary

6.1.1 First Year Research Summary

In the first year the FAST Center made substantial progress in its research objectives while striving to set-up a state-of-the-art research laboratories during this first year. Six model imide compounds were developed and characterized on the DSC and the TGA. The characterization results showed that these were new imide compounds. These model compounds were used in oxidative and hydrolytic studies to determine the optimum imide compound for synthesis of improved polyimides. In addition, a research effort was initiated to determine the cause of hygrothermal degradation of AFR700B and to develop and/or characterize resin formulations with improved hygrothermal stability. On postulating that possible sites for hydrolytic degradation in AFR700B included the end groups and imide linkages in the backbone, end-group chemistry changes consisting of substitution of the nadic ester with PEPE (4-phenylethynylphthalic ester) were made. Changes in the polymer backbone were made based on the premise that the steric hinderance of the amine would inhibit water transport. This lead to the substitution of pPDA with TMpPDA (tetramethyl-p-phenylene diamine) and MBTA [4,4'-methylenebis(2-trifluoromethyl aniline)]. A third nonfluorinated high temperature polyimide, Superimide 800 was also characterized.

Two FAST Center personnel, Dr. Paul O. Biney (Director) and Dr. J. Zhou (PI) collaborated with McDonnell Douglas Aerospace Division (MDA) and participated in the HBCU Faculty exchange program. Dr. Biney spent three weeks at MDA Research facility in St. Louis and performed durability studies on high temperature IM7/5260 and T650-35/5270 BMI material systems. Dr. Zhou performed laminate bonding stress analysis studies at MDA facility in St. Louis for two weeks. This collaboration was in line with our objective of working closely with the major aerospace companies for future contract in support of our self-supporting objective.

6.1.2 Second Year Research Summary

Formulation

In the formulation area, a total of three nadimides and six phthalimides were selected for study. The goal for the model compound materials was to achieve a minimum level of compound volatility which was assessed to be a minimum melting point of 200°C. However, DSC and TGA analyses determined that each of the seven initial fluorine containing nadimide and phthalimide compounds failed to meet the 200°C melting point and low volatility objectives. A total of four new replacement model phthalimide structures were selected for

study which contain a nitro-substituent along with the fluoro-substituent on the aniline portion of the structure.

The four replacement phthalimides were characterized by FTIR, DSC and TGA. Achievement of the desired imide linkage was confirmed by FTIR. Most importantly, DSC analyses confirmed that we had met our 200°C melting point goal with three of the four new phthalimides. However, pyrolysis of the three fluoro-substituted nadimides at 200°C to 300°C confirmed that these models were still too volatile to be of practical use. We next applied the success achieved with the nitro-substituent in the phthalimide models to nadimides. Two replacement nadimides were synthesized The two new nadimides were characterized by FTIR, DSC and TGA. Achievement of the desired imide structure was confirmed by FTIR analysis. Confirmation that the nadimides possessed the minimum goal of 200°C melting point was obtained by DSC analyses. With the model nadimide and phthalimide model compounds meeting our objective of a minimum melting point of 200°C and apparent low volatiltity, we concluded that the majority of the Formulary Phase I studies objectives were successfully completed in the second year.

Effect of Multiple Post-Cure and aging in Composite Properties. From the experimental results on the effects of multiple post cure on the thermo-mechanical properties of IM7/5250-4, it was found that the shear strength of IM7/BMI 5250-4 composites is stable at room temperature and at 400°F for all samples that underwent multiple post-cure. The experimental results indicated that the shear strength of IM7/BMI 5250-4 composites is stable at room temperature and at elevated test condition of 400°F for all post-cured and aged samples. The sample postcured at 425F for 6 hours had the highest 90 degree tension strength, four points flexural strength, and flexural toughness, but the glass transition temperature was lower than any of the aged samples. The glass transition temperature increased with the higher post-cure temperature and longer accelerated aging time. It increased from 202.5°C to 318.5°C for composites post-cured at 375°F for 6 hours, and for the sample aged for 128 hours at 475°F respectively. The flexure toughness decreased with the longer accelerated aging time. It decreased from the highest value of 4.658 lb/in to the lowest value of 4.160 lb/in. It decreased about 10.7% over aging time of 0 to 128 hours at 475°F. The in-plane shear testing results indicated that the shear strength at 400°F is higher than at room temperature.

Hydrolytic Degradation

Research was conducted on the Influence of hydrolytic degradation on the thermo-mechanical properties of IM7/5250-4 BMI. The result indicated that at constant aging temperature, the glass transition temperature increased with aging time for aged temperature of 350°F. There was not well defined trend in the variation of Tg with aging time for the specimens aged at 300°F and 250°F. We have reviewed our experimental procedures and identified possible causes for the lack of trend in the specimens aged at 300°F and 250°F. The experiments will be redone for these temperatures and the results reanalyzed. The experiments at aging temperature of 400°F were discontinued after 24 hour aging time because, the specimen completely delaminated and became unusable for testing at the aging time of 48 hours. The experiments are still in progress.

Hygrothermal Cycling

Even though the research on the effects of hygrothermal cycling on the mechanical and visco-elastic properties of IM7/5250-4 BMI has not been completed, the data on the two completed cycles indicate that there is a negligible difference between the Tg's for the samples with seven hygrothermal cycling and those with twenty eight hygrothermal cycles.

Research on Superimide 800

Resin flow experiments were done on sixteen Superimide 800 formulations. The results indicated that (1) all sixteen resins did not have flow or consolidate at 450 F, (2) at 550 °F, ten of the sixteen resins had consolidation, with only one that was translucent, and (3) at 650 °F, twelve of the resins experienced consolidation. From the flow experiments, it was possible to determine the optimum cure temperatures for the various resin formulation. The resins that consolidated at 550°F will be cured at 550°F, those that consolidated at 650°F will be cured at 650°F. After the curing cycle is completed, DMA, TOS, and tensile testing will be performed on the samples. Flexural toughness test will also be done on each sample.

Research on the Effect of Processing Techniques on Composite Properties

Research was conducted to determine the effect of processing techniques on the visco-elastic and mechanical properties of polymers. This resulted in the preparation of IM7/5250 composite cured using vacuum bag and heated blanket Dynamic mechanical tests and interlaminar shear tests performed on this composite indicated a Tg of 280.65°C and interlaminar shear strength of $10.9x10^3$ psi. These data are comparable to the data obtained for the autoclave cured panels [1]. The coefficient of diffusion for this composite in the through-the-thickness direction was $1.77x10^{-9}$ in^2/hr. Thermal spike tests performed on this composite indicated that more serious delamination and blistering occur. Furthermore, the delamination and blistering in the quasi-isotropic samples are more serious than those in the unidirectional samples.

AFR-PEPE-N Studies

The hydrolytic stability of three AFR-PEPE-N (where N=2, 4, 8) was determined and compared to AFR700B. The change in the materials dry glass transition temperature, Tg, was plotted versus hours of exposure at 150°C in saturated steam. The results indicated that the AFR-PEPE-2 formulation has a substantially higher initial Tg which is maintained after 96 hours of exposure. For this reason the AFR-PEPE-2 formulation was selected for further studies.

AFR-MBTA-N Studies

Torsional impregnated cloth analysis, TICA and TGA testing were conducted on AFR-MBTA-8 monomeric solution AFR-MBTA-8. The result indicated that polymerization occurs at a higher temperature than AFR700B (180°C vs. 120°C) and further resin advancement occurs shortly after the original melt. A melt flow study conducted by consolidating 2 gram, 1" diameter pellets indicated that this material is very difficult to process because of both its high viscosity and the condensation products generated after consolidation. Despite this processing difficulty a small neat resin plaque was processed for conducting hygrothermal stability tests. Exposure to saturated steam at 150°C for 24, and 96 hours resulted in no reduction of the baseline Tg of 400°C. Further studies of this polymer have been terminated however due to processing difficulties and extreme brittleness.

Moisture Transport and Blistering Study

The initiation and growth of blisters during heating of saturated polyimides was investigated, as well as rates of moisture diffusion at elevated temperatures. The primary emphasis of this work is to improve upon the prediction methodologies currently used for predicting steam pressure-induced delamination.

A more fundamental approach whereby a moisture diffusion model is developed to predict the moisture distribution throughout the material as a function of part thickness and time-temperature

history was proposed. This study was first conducted on neat AFR700B resin. The envelope of safe operation was defined as the maximum actual moisture content in the material (generally located in the midplane) plotted versus the blister initiation temperature. This modeling approach will allow designers to explore parts of varying thickness and multiple thermal cycles, hypothetically, with minimal resources. For the determination of moisture content in the sample, a diffusion model was employed to predict the moisture distribution based on the time-temperature drying cycle a sample went through. There is very good agreement between the model and experimental data.

6.1.3 Third Year Research Summary

6.1.3.1 Formulation

Endcap Replacement Model Compound Research

In the model endcap replacement research, we worked on one of the two nitro-substituted nadimides and their control compound, N-Phenylhimide, that were synthesized and successfully met our 200 °C melting point criteria as described in the 1997 FAST Center report [1]. These nadimides were purified through crystallization and thermally imidized. Pyrolysis was performed on N-phenylnadimide and 2-fluoro-5-nitro-N-phenylnadimide and the insoluble residues extracted and used to initiate preliminary oxidative aging studies The aging results at 300 oC were encouraging and the oxidative studies at this temperature are currently ongoing.

Backbone Replacement Model Compound Research

In the model backbone replacement research, we worked on one (2-Flouro-5-Nitro-N-Phenyl-4,5-dichlorophthalimide) of the three nitro-substituted phthalimides and their control compound, N-phenyl phthalimide, that were synthesized and successfully met our 200 °C melting point criteria as described in the 1997 FAST Center report [1]. These phthalimides were purified through crystallization. They were then thermally and chemically imidized and used to initiate preliminary oxidative studies. The aging results at 300 °C were encouraging and the oxidative studies at this temperature are currently ongoing.

6.1.3.2 Effect of Post-Cure and Thermal Aging on IM7/5250-4 Composite Properties.

Effects of Post-cure IM7/5250-4 Composite

In-plane shear strength showed a conspicuous decrease with increased post-cure temperature. It was a reduction of about 14% and 22% when post-cure temperature was raised from 190°C to 218°C and 246°C, respectively. The secant modulus determined from flexure tests showed an increase with higher postcure temperature . It was increased by about 31.9% when the postcure temperature was increased from 190°C to 246°C. The 90 degree tension strength and modulus, which are dominantly dependent on the tension properties of the matrix and the adhesion of the fiber/matrix interface, are basically unchanged with the variation of postcure temperature and duration. The mode II fracture energy first increased, about 15%, when the post-cure temperature was increased from 190°C to 218°C, then decreased rapidly with a further increase of the temperature to 246°C. The fracture energy of composites postcured at 246°C was about 10% and 22% lower than those postcured at 190°C and 218°C, respectively.

Thermal Aging Effects On The Glass Transition Temperature IM7/5250-4 Composite

It was found that the glass transition temperature (here defined as the peak temperature of Tan δ) of IM7/5250-4 composites increased about 50°C during the first 4 hours holding at 246°C. However, the glass transition temperature did not show significant change after the first 4 hours. It is believed that the large increase of Tg was due to the postcuring effect which led to an increase of the crosslinking degree. The reason for the Tg not changing after the first 4 hours isothermal holding indicated that the crosslinking reactions of the BMI was almost completed during the first 4 hours and the thermo-oxidative effect on Tg was not obvious during the 128 hours duration in this study.

Thermal Aging Effects On The Mechanical Properties IM7/5250-4 Composite

The in-plane shear testing results of IM7/5250-4 composites which were thermally aged at 246°C for a range of aging time from 0 hour to 128 indicated that the in-plane shear strength of the composite with thermal duration of 4 hour was similar to that of the baseline composites. After the first 4 hours isothermal holding, the shear strength dropped about 6% and the drop was believed to be due to thermo-oxidation of the BMI. It also can be seen that the shear modulus did not change with the thermal aging duration. The fracture toughness of the composites thermally aged for 4 hours showed an increase of about 8%. Further addition of thermal aging duration resulted in reduction of the fracture toughness.

Other Research

Hydrolytic Degradation of IM7/5250-4 Composite

For specimen aged hydrolytically at 250°F, 300°F and 350°F each at aging times of 24, 48, 72 and 96 hours, as the exposure time increased at constant aging temperature the Tg value increased. In general the Tg also increased with the increase in aging temperature. This can be due to the further crosslinking in the material, which increases the glass transition temperature.

Hygrothermal Cycling of IM7/5250-4 Composite

The data for this study indicated that the Tg increased up to the fourth week of cycling, followed by a drop in Tg after the fourth week. The Tg at the end of the twelfth week of cycling was below the baseline value. The shear strength dropped slightly from 96.8 MPa for the baseline sample to 92.5 MPa for the specimen cycled for 12 weeks. The shear modulus also dropped slightly from 4.53 GPa for the baseline sample to 3.92 GPa for the sample cycled for 12 weeks.

Research on Superimide 800

Resin flow experiments were done on sixteen Superimide 800 formulations. The results indicated that (1) all sixteen resins did not have flow or consolidate at 450 F, (2) at 550 °F, ten of the sixteen resins had consolidation, with only one that was translucent, and (3) at 650 °F, twelve of the resins experienced consolidation. From the flow experiments, it was possible to determine the optimum cure temperatures for the various resin formulation. The resins that consolidated at 550°F were cured at 550°F, those that consolidated at 650°F were cured at 650°F. A systematic approach based on the use of the TGA and the DMA, and evolved gas characteristics at different temperatures, were used to determine a post-cure cycle that could be used for all of the sixteen formulations. The cycle involved 3 °C/min ramp to 200, 250, 275, 300, 350, 375, 400 °C with 4 hour hold at each temperature except at 400 °C where the hold was for 8 hours. TOS studies on the postcured samples are currently in progress.

Research on Hydrolytic Effects on the Properties of IM7/5250-4 Composites

Thermal properties characterized by the onset decomposition temperature and the maximum decomposition indicated that although the maximum decomposition rate temperatures were similar for composites with and without conditioning, the onset decomposition temperature after hydrolytic exposures did show a conspicuous drop compared with that of the baseline sample. This is believed to be due to the moisture-induced molecular weight drop and crosslink breakage in the composites exposed to moisture and elevated temperature. Interlaminar shear strength of the composites before and after the thermal and accelerated hydrolytic exposures showed that hydrolytic exposure had a significant deteriorating effect on the interlaminar shear properties. The interlaminar shear strength of composite after 48 hour in the hydrolytic environment dropped about 40% while it remained the same in thermal aging process up to about 200 hours and decreased about 16% after 384 hours of thermal aging. The DMA spectra of the hydrolytic samples were quite different from those of the baseline and the thermally aged samples. There was no loss modulus peak for the hydrolytic samples. Instead, their loss modulus exhibited a broad transition region together with an incomplete small peak at temperature above 300°C. In addition, the DMA spectra showed that the storage modulus increased after thermal aging while it decreased after hydrolytic aging, indicating that thermal aging makes the composite become hard while hydrolysis makes the composite soft.

Research on Environmental Durability of Structural Adhesives

Although the 2550 adhesive films became very brittle when they were exposed to 200 °C directly, the shear strength of the bonded system only dropped about 6% after 188 hour exposure at the same condition, and 9% after 432 hr exposure. In addition, the appearance of the adhesives in the bonding system, where the adhesive was sandwiched between the two panels, did not change during the thermal exposure. The failure of the bonded systems was mainly caused by delamination of the composite panels instead of failure of the adhesion. Furthermore, the failure mode of the thermally exposed systems was similar to that without exposure. These phenomena suggests that the adhesive in the bonding systems was much less oxidized because it was sandwiched between composite panels, so that the mechanical properties of the bonding systems were less affected by oxidation.

Effects of Thermal and Hygrothermal Aging Condition on Properties of IM7/BMI5250-4 Composites

In general, comparing the thermally and hygrothermally aged samples at 80 °C, it was seen that the hygrothermally aged samples had a general decrease in shear modulus, a slight increase in shear strength while the thermally aged samples had an increase in both shear modulus and shear strength as the aging time increased. For the samples aged at 180 °C, shear strength decreased for the hygrothermally aged sample while that of the thermally aged sample increased slightly and levelled off after 40 hours of aging. The shear strength decreased with aging time for the hygrothermally aged sample, while it increased slightly for the thermally aged samples. The secant modulus increased for hygrothermal aging at 80°C; nevertheless, for both thermal aging at 180°C and hygrothermal aging at 180°C, the secant modulus of composites shows no significant change with increasing aging time. The glass transition temperature based on loss modulus decreased with longer aging time for samples hygrothermal aged at 80°C while it increased for samples hygrothermally aged at 180 °C.

Blister Initiation and Growth of AFR700B Composites

Moisture diffusion model was begun. Initial blister studies indicated that due to the lower diffusivity of the composite as compared to the neat resin, composites blister more readily than neat resin. For example, a composite sample, 3.48mm thick, heated at 5°C/min blistered at 270°C while a neat resin sample, 3.73mm thick, blistered at a much higher temperature of 330°C.

One difference noted between blister growth in neat resin versus a composite is that the fibers tend to suppress thickness changes, making it more difficult to get a clear blister initiation temperature. This work has shown that even relatively slow heating rates can result in internal damage of composites on the order of 3mm thick and that their use should be limited to applications where parts can be dried prior to thermal excursions above approximately 250°C.

6.1.4 Fourth Year Research Summary

6.1.4.1 Field Repair of Composites

Curing Optimization of IM7/5250-4 Prepregs under Field Repair Conditions

The objective of this research was to improve the thermal and mechanical properties of the composites by optimizing cure parameters under vacuum bag pressure and field temperature limitation. A semi-empirical kinetics equation was developed to describe the curing progress of IM7/5250-4 prepregs in terms of ramp rate and isothermal temperature. Good agreement of the calculated curves with the experimental data was found, indicating that the equation can be used to predict curing reaction progress of IM7/5250-4 prepregs from known isothermal temperature and ramp rate. The research on curing optimization of IM7/5250-4 prepregs under f~eld repair conditions was based on this semi-empirical curing kinetics. The proposed optimum cure cycle is developed by controlling a uniform reaction rate of the prepreg during heating. The reaction rate was controlled by a computer equipped with Labtech Notebook software. Bag molding of IM7/5250-4 composites was conducted with a uniform cure rate of 1%/min together with an isothermal curing at 350°F and below. Density of cured panels, C-scan, and in-plane shear tests were performed to investigate the quality and mechanical properties of the composite. It was found that panels with the cure rate of 1%/min during heating showed higher density (about 1.3%), better panel quality (based on C-scan results), and higher in-plane shear properties (about 11%) than those cured with the manufacturer recommended heating rate of 5°F/min.

Shelf Life Study of IM7/5250-4 Prepregs

This study is to find out (1) whether it is possible to make satisfactory vacuum bag cured patches from aged prepregs and (2) the effects of prepreg storage temperature and time on the quality and properties of the fmal panels. IM7/5250-4 prepregs were put into sealed plastic bags and stored at various temperatures for various time periods. Storage effe,cts on weight loss, curing process, panel quality, and mechanical properties were investigated. The preliminary work in this study led to the conclusion that the quality and mechanical properties of the composite panels made of IM7/5250-4 prepregs stored at room temperature up to 60 days or 1 week at temperature up to 110[1F were acceptable. It is necessary to investigate longer storing duration and higher storing temperatures for IM7/5250-4 prepregs.

6.1.4.2 Environmental Durability Study on Epoxy and Polyimide Structural Adhesives

The objective of this research is to characterize and evaluate the environmental durability of structural adhesives in order to predict their performance under various service environments. The adhesives used for this study were FM300, FM400, and Metlbond2550 film adhesives, in which the former two are epoxy based and the latter is BMI based. IM7/5250-4 composite panels were used as adherents. The adhesive bonding systems were exposed to various temperatures and humidity. Single-lap-shear testing was performed to investigate characterize the mechanical properties of the bonding systems and SEM was used to help to determine the failure mode. It was found that FM300 bonded IM7/5250-4 systems had the highest single-lap shear strength while Metlbond2550 systems had the lowest when no environmental exposures were involved. However, the former was most susceptible to thermal and hygrothermal exposures, especially vulnerable to water, whereas the latter showed the best environmental resistance. When the two high temperature adhesive, FM400 and Metlbond2550, were compared, the latter showed better high temperature performance and more stability to temperature fluctuation. The bonding properties also depend on the lay-up configuration of adherents. It was found that the single-lap shear strength of bonded systems with a unidirectional lay-up in adherents is obvious higher than that of systems with +45 lay-up in adherents.

6.1.4.3 Research on Structure-Property Relationship for Optimizing Superimide™ 800 Polyimide Resin Formulation

The objectives of this research are to determine (1) the effects of molecular weight, stochiometric variation, and p-PDA/(m-PDA+p-PDA) ratio on the processability, thermomechanical properties, and thermo-oxidative stability of Superimide™800 and (2) the optimum formulation and the optimum cure cycle for the optimum formulation among the sixteen different initial formulations. The work involved developing postcure cycle for the 16 different initial formulations of Superimide™ 800 resin and studying the effects of molecular weight, p-PDA ratio, and endgroup order on the processability, thermomechanical properties and thermo-oxidative stability of the resin. Statistical analytical method was used to determine the formulations with best performance. Design of experiment method was used to develop the optimum formulations of SuperImide™800. The dependency of the properties on the structural factors, molecular weight, endgroup order, and p-PDA fraction, were predicted by regression model and measure by experiments. The predicted results and the observed results were not completely consistent. The general expected structure-property dependency was compared with what predicted by the regression model. Linear regression coefficients represented a quantitative degree of dependency of the properties on the structural variables and the values of these coefficients were summarized. In order to select the best formulation for the SuperImideTM800, Table 3.4.4 was made in which the most relevant properties were listed and different shade of colors were filled out for the 16 formulations with the blue represents good performance and the white represents 'bad'. Then, the formulations with most blue ones were selected as the optimum formulations and marked with green. It was found that formulations #5, #7, #8, and #15 had the most shades of color with at least three properties shaded. Among these four formulations, #15 (with molecular weight of 5500, endgroup order of 1.5, and % p-PDA of 0.3) showed the best of the most relevant properties.

6.1.4.4 Processing for Repair of IM7/5250-4

Out-Time Effects on IM7/5250-4

IM7/5250-4 prepregs were stored at 120°F for various time periods, then bag molded at 350°F. The material becomes very boardy at room temperature following the exposure; however, laminates are easily laid up by tacking the corners with a heating iron. Resin bleed during cure has been observed after aging 21 days at 120°F. Essentially, once the material has vitrified at this temperature, it seems to stabilize. The tensile strength of a [~45]3s vacuum bag-cured laminate is about 22 percent lower than the baseline autoclave-cured laminate. The strength and stiffness don't change significantly after 21 days of aging.

Vacuum Bag Cure Cycle Study for IM7/5250-4

The main objective is to determine property knockdowns associated with curing IM7/5250-4 under vacuum bag at 350°F as compared to standard autoclave cure conditions of 100 psi and 440°F. The 300°F test results showed very little reduction in properties. As a result of this initial study, a round-robin test matrix has been initiated which will be used to characterize mechanical performance using a vacuum bag cure with a six-hour hold at 350°F.

6.1.4.5 Fatigue Study of IM7/5250-4

The main objective of this work is to generate an S-N curve and characterize damage progression under fatigue loading of carbon fiber-reinforced bismaleimide composites. The data will be used as a baseline to evaluate the influence of extended hygrothermal aging on the dynamic response of this material.

Tension-tension fatigue tests are currently being conducted'to obtain the S-N curve relations, using five constant stress levels corresponding to 80, 70, 65, 60, and 55 percent of the static strength. Five straight-sided coupons are fatigued at each stress level up to final failure, at a frequency of 10 Hz and with a stress ratio of R=0.1. On completion of the fatigue data analysis,

residual stiffness and strength will be determined for selected fatigue histories. The static strength and fatigue data for the unaged material have been obtained.

6.1.4.6 Environmental Aging Effects on Creep Behavior of AFR700B

Two environmental conditions were used for this study. One batch was exposed to saturated steam in a specially designed pressure vessel for 48 h at 150°C (Condition b, while the second batch was exposed for 48 h at 175°C (Condition II). Both hygrothermal aging conditions cause substantial declines in the dry glass transition temperature, with the decline being greater for the more severe Condition II. Resin fracture toughness, KQ, was determined from compact tension tests, and Young's modulus was determined from the initial linear portion of the stress-strain curve. Aging under Condition I causes no change in the mechanical properties measured at room temperature; aging under Condition II, on the other hand, results in a significant decline in strength and toughness but little change in resin stiffness.

At 23°C the influence of hygrothermal aging under Condition I appears to be negligible, while Condition II produces a significant decrease in creep strain. This trend continues up to a test temperature of 177°C above which specimens aged under both hygrothermal conditions demonstrate a significant increase in creep strain with temperature. At 288°C, for example, the creep strain of a specimen aged under condition II is significantly higher than for an unaged specimen. The experimental results therefore show that the creep response of this resin is

sensitive to hygrothermal degradation, especially at elevated temperatures, to a greater extent than observed for the static mechanical properties. These findings therefore warrant further characterization of the creep response of these material systems before they can be used with confidence in hygrothermal service environments.

6.1.5 Fifth Year Research Summary

6.1.5.1 Research to Improve Quality of Field Repair Composites

Control of Curing Rate of IM7/5250-4 Prepregs under Field Repair Conditions

The objective of this research was to improve the thermal and mechanical properties of the composites by optimizing cure parameters under vacuum bag pressure and field temperature limitation. A semi-empirical kinetics equation was developed to describe the curing progress of IM7/5250-4 prepregs in terms of ramp rate and isothermal temperature. Good agreement of the calculated curves with the experimental data was found, indicating that the equation can be used to predict curing reaction progress of IM7/5250-4 prepregs from known isothermal temperature and ramp rate. The research on curing optimization of IM7/5250-4 prepregs under field repair conditions was based on this semi-empirical curing kinetics. The optimized cycle is based on slowing down the reaction rate during the heating stage which has been found to improve the properties of IM7/5250-4 laminates. The research work included (1) developing a quantitative relationship between cure degree and ramp rate for IM7/5250-4 prepregs, (2) developing a computer controlled curing system to control the cure rate of the prepreg according to the kinetics equations, and (3) investigating the effects of curing rate on the quality and properties of IM7/5250-4 composite. The results showed that IM7/5250-4 panels with uniform cure rate of 0.7%/min and 0.8%/min showed better panel quality (from c-scan results) and higher in-plane shear strength than panels cured at a ramp rate of 5°F/min. However, the glass transition temperature of the formers was similar to that of the latter.

Shelf Life Study of IM7/5250-4 Prepregs

This study is to find out (1) whether it is possible to make satisfactory vacuum bag cured patches from aged prepregs and (2) the effects of prepreg storage temperature and time on the quality and properties of the final panels. IM7/5250-4 prepregs and neat 5250-4 resin were put into sealed plastic bags and stored at various temperatures for various time periods. The out-of-freezer stored prepregs were laid up to make laminates. Ultrasonic detection, mechanical testing, and thermal analysis were performed on the laminates made from the aged prepregs to investigate the effects of storage condition on the laminate quality, mechanical properties, and thermal properties. DSC tests were performed on the neat 5250-4 resin to investigate how much cure proceeded during the storage period. Ultrasonic inspection showed quality degradation in panels made from the aged prepregs. The longer the storage time and the higher the storage temperature, the more delamination that occurred in the laminates. Mechanical testing showed that there was no obvious drop in 90 degree flexure strength after being stored at room temperature for up to 80 days while when the prepregs were stored at 120°F for 40 days, the laminates lost 75% of its flexure strength. It can be concluded that room temperature storage up to 80 days and 90°F storage up to 40 days are acceptable for IM7/5250-4 prepregs while 120°F storage of the prepregs **is not** recommended.

Study of out-of-freezer storage of adhesives

The objective of this study is to investigate the effects of room temperature storage of adhesives on the properties and failure mode of the bonding. With the understanding of the variation of bonding behavior with adhesive storage time, we can evaluate the out-of-freezer storage

limitation of the adhesives. Three commonly used adhesives, FM300, FM400, and Metlbond2550, were used in this study. DSC was used to investigate cure advancement during the out-of-freezer storage of the adhesives and single-lap shear testing was performed to investigate the effects of room temperature storage on the mechanical properties of the aged adhesive bonding systems. The results indicated that FM300 is not suitable for out-of-freezer storage. FM400 has good durability when stored at room temperature for up to half a year. Its drawback is that it becomes too sticky to handle. Metlbond2550 bonding system has about 70% retention of its shear properties when the adhesive was exposed to room temperature for up to half a year. Therefore, Metlbond2550 may be the most acceptable adhesive to be out-of-freezer stored and hence used for field repair.

Development of Test Methodology for Adhesive Bonded Composites

The objective of this work is to develop new testing methods for adhesive bonding composite systems. The new method should have sample geometry that is more similar to the real situation in patch repair of composites than the traditional single or double-lap shear tests. Two types of specimen were made in this study. One t~vpe was prepared by drilling a hole on a composite panel, grinding a 20:1 scarf, applying adhesive and prepregs, then using vacuum bag and heating blanket to cure the patch. This type of coupon was referred to as circular patch panel in this report. The other type of specimen was prepared by grinding one end of a 6x6" panel into a 20: 1 scarf, then applying adhesive film and prepregs, and finally cured in vacuum bag. This type of specimen was referred to as scarf lap joint. The scarf lap joint showed about 70% loss of its parent panel strength and the circular scarf joint showed about 57% strength loss compared to its parent panel. Also, the 20:1 scarf patch repair used in this study led to about 20% recovery of the tension strength compared with the open hole panel.

Development of an Equipment and Process Control for Doubling the Cure Pressure Used in Field Repair of Composites

The Fast Center has developed a method that can be used to increase the vacuum bag pressure from 1 atm to 2 atm in order to improve the repair quality by increasing curing pressure. The assembly designed contains two plates and two layers of plastic bags in which the area of the upper plate is twice that of the lower plate. Vacuum was applied to the inner layer bag matenal at the beginning of the cure, providing 1 atm pressure to the laminate. When the curing reaction reached a certain point, another vacuum was applied to the outer layer. Since the area of the upper plate is twice of that of the lower plate, the assembly provided 2 atms pressure on the laminate. Preliminary conclusions can be drawn from the results obtained to this point. Increasing the cure pressure to 2 atm enhances the strength of the bonding and the patch. This method is expecially suitable for field repair because the method requires a plate with an area twice as much as the patch. The size of patch in field reapir is usually not too large, so that the whole repair assembly has a reasonable dimension. Therefore, this is a method worthy of further development.

6.1.5.2 Hygrothermal Effects on the Fatigue Properties of IM7/5250-4 Composites

This work is a graduate student thesis topic. The work included (1) exposing IM7/5250-4 composites to hygrothermal cycling and accelerated hydrolytic environment, (2) fatigue testing to investigate the effects of hygrothermal conditioning on the fatigue behaviors of the composites. The hygrothermal cycling condition in this study was RT/98%RH ~ 177°C/dry. The hydrolytic exposures were performed in pipe bomb with saturated steam at temperatures of 121°C, 149°C, and 177°C. Fatigue tests of hygrothermally cycled IM7/5250-4 composites showed that the cycle number to failure decreased from about 120,000 for the baseline samples (375°F cured in

autoclaved and 440°F postcured) to about 60,000 for samples that experienced up to 14 weeks of hygrothermal cycling. This indicated that the fatigue life of IM7/5250-4 composites could be reduced by 50% if the composite undergoes several weeks of hygrothermal cycling. Residual stiffness test results showed that the hygrothermal cycling and hydrolytic exposure at 121°C and 149°C did not have significant effects on the residual stiffness of the composite while exposure to 177°C saturated steam caused the residual stiffness of the composite to drop by about 12%.

6.1.5.3 Test Method Development and Characterization of Candidate Composites for Cryogenic Tanks

The overall objective is to develop and validate laboratory tests which may be used to screen candidate cryogenic tank materials and aid in development of life-time prediction models. The research was started using bismaleimides. Key issues which will be addressed include:

· Effect of repeated thermal shock on composite morphology and properties,

· Effect of phase change of absorbed water on composite morphology and properties,

· Effect of launch vibrations at cryogenic temperatures on composite morphology and properties,

· Effect of highly concentrated oxygen on composite chemistry, and measurement of autoignition temperature which may be brought on by kinetic impact, and

· Apply lessons learned from screening tests to aid in the development of new matrix materials which are optimized for cryogenic applications.

Preliminary results showed that there were no microcracks observed in IM7/5250-4 composites after up to 280 temperature cycles between -320°F to 302°F with or without moisture. Also, no significant mechanical property drop occurred after the cycling. This indicates that IM7/5250-4 is a potentially good candidate material for cryogenic propellant tanks.

6.1.5.4 Research Conducted at UDRI

The research conducted at UDRI in the fifth year was to study the effect of thermal environment on the fatigue life of a composite laminate. A series of tension-tension fatigue tests under constant amplitude were conducted at the following temperatures: -321, -200, 75, 200, and 300°F. A baseline S-N relationship was constructed from tests at five stress levels at 75°F. Two fatigue stresses were chosen at each temperature, and their data were compared to the baseline S-N curve to determine temperature effect on the fatigue life. Two stress levels considered were in the range of 55 and 82% of the corresponding static strengths that were determined by averaging more than five specimens at each temperature. Fatigue damage was also assessed at 75, 300, and -321°F by observing stress-strain relation and transverse crack density in the course of fatigue life. To study the thermal aging effect on the fatigue life, some specimens were thermally aged at 300°F for two weeks in a vacuum oven, and static and fatigue tests were then conducted at 75, 300, and -321°F. Preliminary conclusions from this study are (1) The approach employed in this work appears to be useful to understand the effects of environmental degradation on the fatigue life of composite laminates, (2) Classical power law describes fairly well the S-N relation for this laminate under a constant amplitude tension-tension fatigue loading, (3) Fatigue life tends to decrease for all temperatures considered compared with the baseline, whereas fatigue life tends to slightly increase for the thermally aged case, (4) The number of fatigue cycles influences laminate

degradation in terms of loss of stiffness and cracks, (5) Further work is required to substantiate the findings in this work.

6.2 Fast Center Laboratory Development

Over $800,000 of the funds for the FAST Center were invested in the development of permanent infrastructure and equipment used in setting up seven FAST Center Research Laboratories listed in section 5.1. The year by year development of the various labs and the major equipment purchased are described below.

6.2.1 First Year Laboratory Development

In the first year, the University allocated 2,600 ft^2 of dedicated space to the FAST Center in November of 1995, and the process of making the necessary changes in the space to accommodate the needs of the FAST Center was initiated. The major FAST Center Laboratories were planned, and the formulation, thermal analysis, and the mechanical characterization labs were given priority in that order. The fume hood, cabinets, eyewash, and other accessories needed for the formulation (Chemical) lab were ordered, received and installed. The thermal and chemical characterization lab equipment consisting of a thermogravimetric analyzer (TGA), a high resolution differential scanning calorimeter (DSC), and a Fourier transform infrared analyzer (FTIR) were simultaneously ordered. All of the above instruments were received in June 1996 and the FAST Center Thermal Analysis/Chemical Characterization lab was in operation by the middle of June 1996. The major equipment needed for the mechanical characterization lab, an electromechanical Instron unit, was ordered in March 1996 and received in July 1996. The total investment of FAST center funds in equipment and infrastructure in the first year was $182,020 as shown in Table 6.1.

6.2.2 Second Year Lab Development

New equipment including the diamond saw, the HPLC, and a new DMA were received and installed for research use during the year. The compression press was received but not installed. Several other pieces of equipment listed in Table 6.1 were purchased and installed. Engineering estimates were received for the FAST Center infrastructure modification work. The FAST Center developed a proposal for funding the $135,000 cost of the infrastructure modification work. The proposal was submitted to the McDonnell Douglas Foundation. The University provided the seed funds for the detailed engineering design of the FAST Center modification to be completed. The total investment of FAST center funds in equipment and infrastructure in the second year was $195,117 as shown in Table 6.1.

6.2..3 Third Year Lab Development

New equipment including micromet dielectrometer, one additional vacuum oven, and the autoclave were received and installed for research use during the year except for the autoclave which was not installed that year. The platen press, which was received in the 1996-97 year was installed in a rented laboratory space with training on its use provided by Aerospace Services and Controls. The press, controlled by the CPC controller was used in curing composites for research during the third year. Even though engineering estimates were received for the FAST Center infrastructure modification work, no funds were allocated in the third year for that purpose. However, the Director worked closely with Boeing on a proposal submitted to the then McDonnell Douglas Foundation, for funding $104,165 of the cost of the infrastructure modification work. **Boeing responded generously by making a gift of $104,165 to the FAST Center in response to the proposal submitted.** The Check was presented to the FAST Center on August 7, 1998 by Mr. Beauford Daniel of Boeing. An account has been set up

and bids are being prepared to be issued for the construction work needed in the FAST Center lab modification. The total investment of FAST center funds in equipment and infrastructure in the third year was $171,084 as shown in Table 6.1.

INVESTMENTS IN INFRASTRUCTURE AND EQUIPMENT AT THE FAST CENTER

		General Purpose Use	Formulation Laboratory	Processing Laboratory	Thermal & Chemical Char. Lab.	Environ. Simulation Lab	Mechanical Charact. Lab	Optical & Microstructure Char. Lab	Non-Destructive Testing Lab	
FIRST YEAR										
	Pentium PC				$2,168.25					
	Fumehood & Accessories for Chemical laboratory		$18,084.00							
	Magna-IR 560 FTIR System				$31,136.27					
	Pentium PC system				$2,321.25					
	HP Laserjet 5 Printer				$1,233.00					
	Nytech High Temperature Oven					$600.00				
	Handimet Grinder	$1,250.41								
	Air Compressor	$1,398.43								
	Blue-M oven					$1,000.00				
	Electronic balance	$2,560.00								
	100kN Electromechanical Instron Test system						$89,237.96			
	TA Modulated DSC-2910				$17,574.80					
	TA TGA-2050				$15,624.29					
	SUB-TOTAL FOR YEAR 1	$5,208.84	$18,084.00	$0.00	$67,889.61	$1,600.00	$89,237.96	$0.00		
	TOTAL FOR YEAR 1									$182,020.41
SECOND YEAR										
	Compression Platen Press			$31,236.00						
	TA DMA-2980 System				$47,124.80					
	Vacuum Pump			$2,484.79						
	Vacuum Oven	$2,435.99								
	Cold Trap	$2,360.63								
	Diamond Saw					$18,533.80				
	Blue-M Oven system					$8,263.15				
	Refrigerator/Freezer	$2,220.05								
	Freezer	$709.80								
	Laserjet 5P Printer	$867.98								
	Vacuum Oven	$3,616.00								
	Electric balance	$2,146.25								
	Fax machine	$859.16								
	Parr Bomb Vessel					$3,875.28				
	Sensor conditioner for Instron						$1,794.00			
	Flowmeter & sample Press for DSC				$3,374.60					
	Desiccating Cabinet	$1,166.10								
	Waters HPLC System				$32,310.88					
	Environmental Simulation Lab Cabinets					$8,425.00				
	Lexmar Printer	$1,645.63								
	Epson Scanner	$820.00								
			$18,847.59							
	Sub-Totals for Second Year	$18,847.59	$18,847.59	$33,720.79	$82,810.28	$39,097.23	$1,794.00	$0.00	$0.00	
	TOTAL FOR YEAR 2									$195,117.48
THIRD YEAR										
	ASC Autoclave System			$127,397.15						
	Eumetric 100A Dielectrometer			$27,526.30						
	Vacuum Oven	$3,616.00								
	Thermal Analysis Controller for NT OS				$3,518.30					
	Intel PC system	$3,489.00								
	Gateway G6-400 Computer System	$3,559.00								
	Vacuum Pump	$1,979.05								
	Sub-Totals for Third Year	$12,643.05	$0.00	$154,923.45	$3,518.30	$0.00	$0.00	$0.00	$0.00	
	TOTAL FOR YEAR 3									$171,084.80
FOURTH YEAR										
	Pentium 350 PC System	$1,449.00								
	Pentium 350 PC System	$1,195.00								
	Pentium 350 PC System	$1,989.02								
	Blue-M Temperature/Humidity Chamber					$10,158.00				
	HP laserjet 4000SE	$1,149.99								
	Sub-Totals for Fourth Year	$5,783.01	$0.00	$0.00	$0.00	$10,158.00	$0.00	$0.00	$0.00	
	TOTAL FOR YEAR 4									$15,941.01
FIFTH YEAR										
	DSC Cooling System				$6,727.03					
	New Processing Lab Space with Boeing Fund			$104,000.00						
	RTM (Radius) with IDC Funds			$12,000.00						
	LN2 Storage System					$2,225.34				
	IBM 590 PC System	$1,429.21								
	Sub-Totals for Fifth Year	$1,429.21	$0.00	$116,000.00	$6,727.03	$2,225.34	$0.00	$0.00	$0.00	
	TOTAL FOR YEAR 5									$126,381.58
SIXTH YEAR										
	Gateway Select 1000 PC System							$3,430.00		
	C-Scan imaging System								$79,590.00	
	2 Dell 1.8GHz/400MHz PC Systems	$4,096.00								
	Dell Dimension 8200 PC system	$3,333.99								
	LN2 Storage tank (with IDC funds)					$2,225.34				
	Epson projector	$2,982.00								
	High pressure DSC Cell				$9,012.92					
	Varian Leak Detector System					$22,512.70				
	Dell Inspiron 8100 Laptop System	$3,621.00								
	Sub-Totals for Sixth Year	$14,032.99	$0.00	$0.00	$9,012.92	$24,738.04	$0.00	$3,430.00	$79,590.00	
	TOTAL FOR YEAR 6									$130,803.95
	SIX YEAR TOTAL FOR EACH LAB	$57,944.69	$36,931.59	$304,644.24	$169,958.14	$77,818.61	$91,031.96	$3,430.00	$79,590.00	
	TOTAL FOR ALL 6 YEARS									$821,349.23

6.2.4 Fourth Year lab Development

New data acquisition hardware and software were acquired for composite processing and control. A fatigue software was purchased for the Instron electromechanical test stand for low frequency fatigue testing. The servo-hydraulic Instron machine in the Civil Engineering Department was refurbished for use in high frequency fatigue testing. The total investment of FAST center funds in equipment and infrastructure in the third year was $15,941.

6.2.5 Fifth Year lab Development

The Center ordered a state-of-the-art C-Scan instrument enabling the Center to conduct non-destructive testing of composites processed at the Center. An experimental and specimen handling set up for studying composites under cryogenic temperatures was designed. A radius RTM was purchased and installed for RTM processing. The total investment of FAST center funds in equipment and infrastructure in the fourth year was $126,381.

6.2.6 Sixth Year Lab Development

The C-scan was received and installed. A high pressure DSC cell was ordered, received, and installed for use in composite ignition studies. An auto cryogenic to high temperature cycling machine was designed, built and tested for use in testing candidate composite materials for cryogenic tank application.. An experimental set-up for determining the gas transmission rate of helium gast through composite materials that have undergone various environmental conditioning. The total investment of FAST center funds in equipment and infrastructure in the sixth year was $130,803.

6.2.7 Current State of FAST Center Labs

The infrastructure for the FAST Center consists of seven well equipped research laboratories with a total floor space of over 2,590 square feet located on the first floor of the Collins Building at PVAMU and a 900 ft^2 space in the Farm-House Building. Figure 6.1 shows the current floor plans of the FAST center labs.

Table 6.2 FAST Center Rooms and Intended Use

Room	Floor Area (ft^2)	Present Use
104	1,690	Environmental Exposure and Simulation Lab
		Mechanical Testing Laboratory
104A	150	Storage and Office of Research Engineer/Lab Supervisor
104 DR	140	Diamond saw and test specimen preparation room
105	290	Thermal & Chemical Characterization Lab
105A	320	Non-destructive evaluation Laboratory housing the C-scan.
Farm-House	900	Composite processing laboratory housing the autoclave, platen press, micromet electrometer, Radius RTM Injector, and vacuum bag-heated blanket system.
		Chemical Analysis & Formulation Laboratory
TOTAL	3,490	

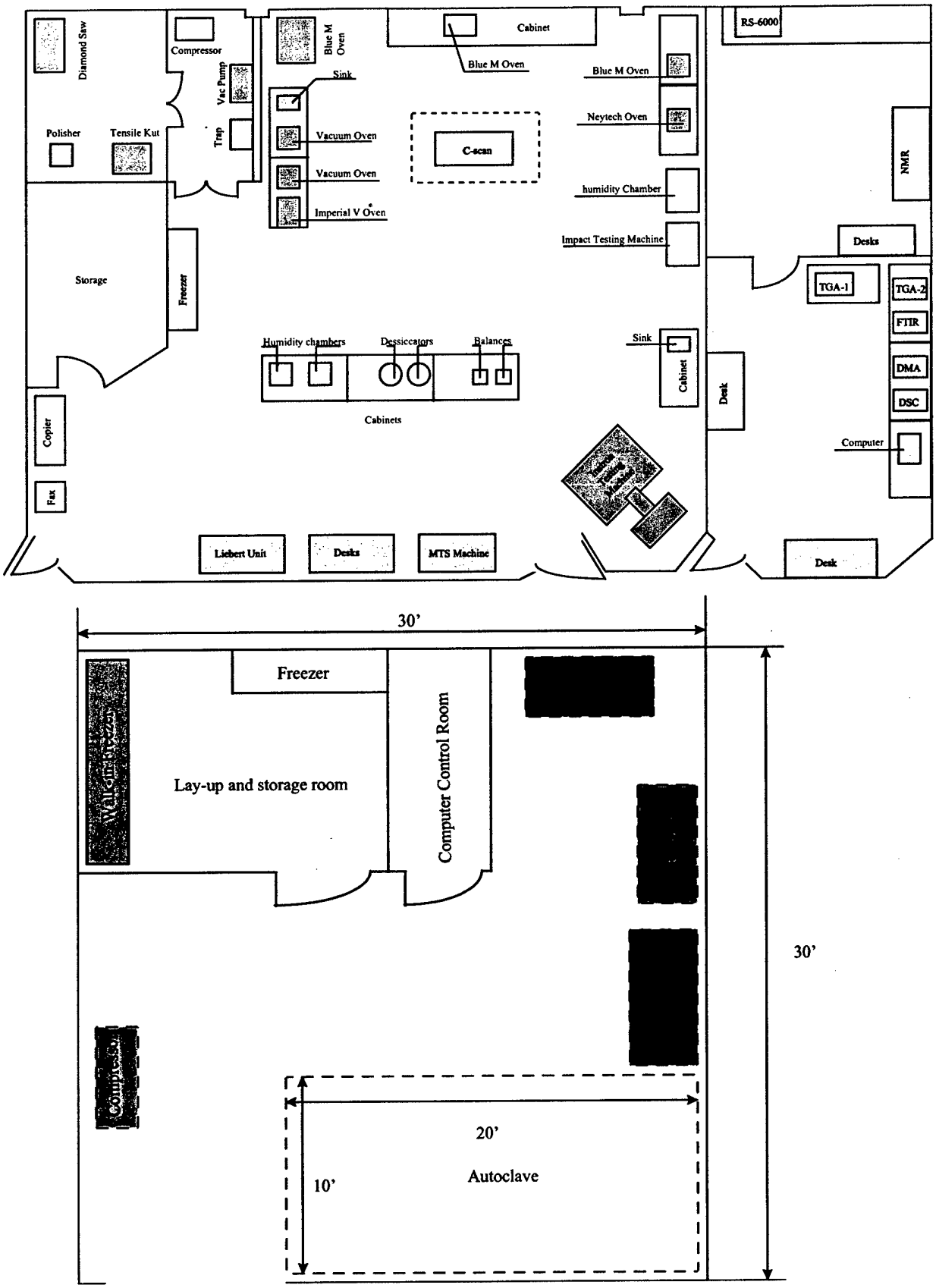

Figure 6.1Current Layout Plan for Major Equipment at FAST Center

6.3 Student Participation & Training

6.3.1 Student Participation in First Year

In the first year six undergraduate listed in Table 6.3 and four graduate students listed in Table 6.4 received financial support and research exposure. Two high school students listed in Table 6.5 were accepted into the summer intern program, and had rich exposure to research in the formulation and characterization of model compounds.

Table 6.3 Undergraduate Students' Participation in FAST center Activities in First Year

Name	Classification	Activities Involved In
Tamar Holley	ME Senior	Facility Development Planning, Literature search on Autoclave BMI Processing
Marcus Piper	ME Senior	Processing laboratory Development Planning Literature search on polymer processing using platen press
Sonja Fields	ME Junior	Technology Transfer Planning Web Home page Development Literature search on out-of Autoclave BMI Processing
Atieno Obala	ME Junior	Mechanical Characterization Laboratory Planning, Preparation of donated equipment for installation Literature search on Mechanical testing of polymer composites
Tonica Pool	ME Junior	Thermal Analysis Laboratory Development Planning Literature search on thermal analysis of polymers & composites.
Stanley Armstrong	Chemistry Junior	Formulation Lab Development Planning Literature search on thermal analysis of polymers.

Table 6.4 Graduate Students' Participation in FAST Center Research in First Year

Name	Major	Area of Research	Thesis Title
Candi Hudson	Mech. Engr.	Processing	Environmental Effects on High Temperature Polymers
Yu He	Mech. Engr	Mech. Characterization	Failure Analysis of Polymer Composite
Patrick Wilson	Mech. Engr	Thermal characterization	Long-term Oxidative and Hydrolytic Stability of High Temperature BMIs
Charles William	Chemistry	Formulation	Synthesis and Characterization of Model Imide Compounds

6.3.2 Student Participation in Second Year

In addition to the six students who participated in the activities of the FAST Center during its first year, three more undergraduate students participated in the activities in connection with the FAST Center laboratory development and research this year . The objective for including undergraduate students in the activities of the FAST Center is to arouse the students' interest in the materials area early in their careers, expose them to research methodology, and encourage them to pursue

advanced degrees in the materials or other engineering disciplines. Table 6.5 provides the names of the undergraduate students, and the activities they were involved in.

Table 6.5 Undergraduate Students' Participation in FAST Center Activities in Second Year

Name	Classification	Activities Involved
Missy Profit	ME Senior	Mechanical Characterization of composites
Nikalenko Joseph	ME Senior	Vacuum bagging and heater blanket processing of epoxy and BMIs
Ambrose Brooks	Chemistry	Development of model compounds
Tamar Holley	ME Senior	Facility Development Planning, Literature search on Autoclave BMI Processing
Marcus Piper	ME Senior	Processing laboratory Development Planning Literature search on polymer processing using platen press
Sonja Fields	ME Junior	Technology Transfer Planning Web Home page Development Literature search on out-of Autoclave BMI Processing
Atieno Obala	ME Junior	Mechanical Characterization Laboratory Planning, Preparation of donated equipment for installation Literature search on Mechanical testing of polymer composites.
Tonica Pool	ME Junior	Thermal Analysis Laboratory Development Planning Literature search on thermal analysis of polymers & composites.
Stanley Armstrong	Chemistry Junior	Formulation Lab Development Planning, Literature search on thermal analysis of polymers.

High School Student Involvement (NASA Sharp Plus Program)
During the Summer 1997, five high school students (top student selected nationally by NASA Sharp Plus Program) participated in FAST Center research work for eight weeks. Table 6.6 shows the names and titles of their final reports and presentations.

Table 6.6 Names and Research Titles for NASA SHARP PLUS Students

Name of NASA SHARP PLUS Student	Project Title
Giselli Ruth Alvarez,	Mechanical behavior and microstructural characterization of fiber reinforced composites and super plastic aluminum alloys
Tracy Crawley	Mechanical testing and scanning electron microscopy analysis of fiber-reinforced composites and super plastic aluminum alloys
Roberto Young	The effects of hydrolytic degradation on BMI 5250-4
Roscoe Casey	Hygrothermal study of IM7-5250-4 composite
Giselli Alverez	Mechanical properties of superplastic aluminum Alloy

6.3.3 Student Participation in Third Year

Eight undergraduate students participated in the activities in connection with the FAST Center laboratory development and research in the third year. The objectives for including undergraduate students in the activities of the FAST Center are:

(1) to arouse the students' interest in the materials area early in their careers,
(2) expose them to research methodology, and
(3) encourage them to pursue advanced degrees in the materials or other engineering disciplines.

Table 6.7 provides the names of the undergraduate students, and the activities they were involved in.

Table 6.7 Undergraduate Students' Participation in FAST Center Activities in Third Year

Name	Classification	Activities Involved
Missy Profit	ME Senior	Mechanical Characterization of composites (graduated)
Nikalenko Joseph	ME Senior	Vacuum bagging and heater blanket processing of epoxy and BMIs (graduated)
Ambrose Brooks	Chemistry	Development of model compounds (Now a graduate student)
Sean Slade	ME Senior	Processing
Brian Spalding	ME Senior	Microstructural Characterization
Rettina Bourda	Chemistry Junior	Model compound synthesis
James McClinton	ME Senior	Thermal Analysis
Larry Truss	ME Junior	Thermal and Chemical analysis

6.3.4 Undergraduate Student Participation in the Fourth Year

Six undergraduate students were involved in Center's research work as undergraduate student research assistants. The names of these undergraduate students, along with their research activities, are listed in Table 6.2.1

Table 6.8 Participation of Undergraduate Students in FAST Center in 1998-1999

Name	Classification	Research Work
Alicia Hamilton	ME junior	Optimization of curing parameters of IM7/5250-4 prepregs for field repair applications
Joshua Moro	ME junior	Optimization of curing parameters of IM7/5250-4 prepregs for field repair applications
Sean Slade	ME senior	Investigation of Shrinkage and Deformation of IM7/5250-4 laminate during postcure
Ted Mercer	ME senior	Investigation of Shrinkage and Deformation of IM7/5250-4 laminate during postcure
Chris Spears	ME junior	Study of shelf life of IM7/5050-4 prepregs
Cicely Boone	ME senior	Study of shelf life of IM7/5050-4 prepregs

Sergio Mayberg and Torren Watson worked as undergraduate research assistants from Fall 2001 to Fall 2002.

6.3.5 Graduate Student participation in Fourth through the Sixth Years

During 1998 - 1999 fiscal year, there were six graduate students working as graduate research assistants at the FAST Center, as listed in Table 6.1.1. Two of them, John Will and Rong Fan, completed and defended their MS thesis based on their research work in the Center in December 1998. Other four graduate students, Philips Morris, La Toya Morrison, John Escoto, and Min Liu, joined the Center in January 1999. Philips Morris, a graduate with BS from Prairie View A&M University in 1995, came back to the school after working in petroleum industry for four years to pursue higher degree.

Table 6.8 Graduate Research Assistants in FAST Center during 1998-1999

Name	Current Status	Major	Expected Graduation Date
John Will	Earned MS degree in Dec., 1998; Working in GM in MI	Mechanical Eng.	(Graduated in Dec. 1998)
Rong Fan	Earned MS degree in Dec., 1998; Working in a consulting firm in CA	Mechanical Eng.	(Graduated in Dec. 1998)
Philips Morris	The second semester	Mechanical Eng.	Graduated 2002
La Toya Morrison	The second semester	Mechanical Eng.	Graduated 2001
John Escoto	The second semester	Mechanical Eng.	Graduated 2001
Min Liu	The second semester	Mechanical Eng.	Transferred

Min Liu transferred to another university in the fifth year, and Philips morris, La Toya Morrison, and John Escoto continued with their research in the fifth year.

6.4 Addition and Modification of New Courses as a Result of FAST Center Program

6.4.1. Undergraduate Courses Modified or Added

The Department of Mechanical Engineering at Prairie View A&M university, offered an advanced Material course for undergraduate students in Spring semester, 1996. In addition, the Mechanical Engineering Department restructured some of the materials related undergraduate courses to include polymer composite topics. The following actions were taken:

1. MCEG 3033 Manufacturing Processes

The content of this course was revised to include PMC material processing techniques. A laboratory, requiring controlled use of some polymer processing equipment at the FAST Center lab, including cure ovens, autoclave, heated platen, and other out-of-autoclave processing methods will now be required in the course.

2. MCEG 4193 Engineering Materials
This course was revised to include composite mechanics. Even though no lab was required in this course, a term paper is required.

3. MCEG 4143 Introduction to Composites
This course was developed for approval in the 1996-97 academic year.

These three courses provided the necessary background, at the undergraduate level for the students who persued to pursue the MS degree in the materials area.

6.4.2 Graduate Courses Developed and Introduced into Curriculum as a Result of FAST program

MCEG 5253 Advanced Engineering Materials
This new graduate course was offered in spring 1997. Fourteen (14) students were enrolled in the course. Each student in the class performed four mini-projects in FAST Center material laboratory. This course covers quantitative relationships between microstructure and mechanical properties, dislocation theory, elasticity, plasticity, fracture, fatigue and creep.

MCEG 5263 Polymers and Composite
This is the second of the three courses planned. It was submitted to the Texas Higher Education Coordinating Board for approval in January 1997. The course covers formation, structure, properties, characterization, and application of polymers and composites. The course has a laboratory component that uses the facilities at the FAST Center labs..

MCEG 5273 Analytical and Experimental Mechanics of Composite Materials
This course was developed for submission to the Texas Higher Education Coordinating Board for approval in January 1998. The course covers mechanical and thermal behavior of composites, laminate mechanics, micromechanics, failure criteria, and experimental methodology. A la will be an integral component of this course.

Training of FAST Center Personnel
In December of 1996 all the personnel at the FAST Center received three days of intensive training by UDRI personnel at the FAST Center Laboratory in the processing and characterization of composites and their constituents. The training emphasized a hands-on approach to working with composites while imparting the fundamental principles of these anisotropic materials.

GNEG 5193 Advance Materials Science
During Spring and Summer semesters of 1998, a graduate course, GNEG 5193 Advance Materials Science, was revised to include in polymeric composites. This is a 3 semester hours course that covers qualitative and quantitative relationships between microstrucure and mechanical properties; studies of dislocation theory; elasticity; plasticity; brittle and ductile fracture; fatigue and creep; design criteria and statistical aspects of failure. Besides dealing with metallic materials and ceramics, this course will put more weight on polymeric composites. Several lab experiments will be arranged for the course, which will be performed in the FAST Center and cover topics in polymeric composite. The course will be offered in Fall semester 1998 and be taught by FAST Center personnel, Dr. J. Zhou

7. CONCLUSION

The funds received from the Air Force Office of Scientific Research for the establishment of the FAST center has been greatly beneficial to the University. It has lead to modifications in the mechanical Engineering program through addition and modification of courses to increase the teaching of materials related courses in the department.

Students have greatly benefited from the FAST center program through provision of financial assistance, and practical hands-on training for students using the state-of-the-art research equipment and instrumentation. Students who worked and trained at the center were in high demand by aerospace industries when they graduated.

Faculty also derived great benefits from the Center. Several faculty members used the facilities at the center for research and teaching that they could otherwise have not been able to do.

Over $800,000 of the FAST center funds were invested in equipment and infrastructure used in developing the seven first class research labs at the center. These labs will continue to be beneficial to the University even after the funding period for the center.

The research conducted at the center has advanced the knowledge of processing and the effects of environmental and service conditions on composite materials.

students, faculty greatly increased the capabilities for composite materials research at Prairie View A&M University (PVAMU), has This chapter summarizes the research highlights, the undergraduate and graduate students trained as a result of this program, the collaboration we have had with industry and other research labs, and the potential for future research afforded by the infrastructure made possible at PVAMU as a result of the establishment of the FAST center.

Table 7.1 summarizes the important statistics resulting from the FAST Center

Number of Undergraduate Students Trained	40
Number of Graduate Students Trained	10
Number of Graduate MS Degrees received from FAST Research	7
Number of related papers presented at Technical Symposiun & Conference Proceedings	32
Number of Journal Papers published	4
Research Labs Developed	7
Total FAST center Funds Invested in Equipment/Infrastructure	Over $800,000
Number of High school students in summer FAST program	6

On behalf of Prairie view A&M university, the Mechanical Engineering Department, the center director wishes to express its gratitude for the investment made by the AFOSR in establishing the FAST center at PVAMU. The facilities will continue to enhance student education for years to come.

8. PUBLICATIONS

1. Thermal effects on the Properties of Eposy and polyimide Adhesives Bonded Graphite.Bismaleimide Composites, Journal of Advanced materials, Vol. 35, No. 2, april 2003.
2. "Study of thermal and hygrothermal behaviors of glass fiber/vinyl ester composite", Fiber Reinforced Plastics and Composites, 18(17), pp. 1619-1629, 1999.
3. "Curing optimization of IM7/5250-4 prepregs under field repair conditions", 20th High Temple Workshop, San Diego, CA, January 24-27, 2000.
4. "Thermal and hygrothermal aging effects on the properties of IM7/BMI composites", 7th Annual International Conference on Composites Engineering, Denver, Colorado, July 2-8, 2000, pp. 915-916.
5. "Physical and mechanical characterizations of glass/vinyl ester composite under hygrothermal cycling", submitted to Fiber Reinforced Plastics and Composites, 2000
6. "Effect of hygrothermal cycling on properties of glass/vinyl ester composite", 12th International Conference on Composite Materials, Paris, France, July 5-9, 1999, paper 626.
7. "Short-term aging effects on thermal and mechanical properties if IM7/5250-4 composites", 44th International SAMPE Symposium & Exhibition, Vol. 44, 741, 1999
8. "Hygrothermal effects on the thermal and mechanical properties of IM7/5250-4 Composites", 44th International SAMPE Symposium & Exhibition, Vol. 44, 734, 1999.
9. "Post-curing effects on physical and mechanical properties of IM7/5250-4 composites", 30th International SAMPE Technical Conference, Vol. 30, 226, 1998.
10. "Neutron and proton damage on shielding materials for space exploration", National Alliance of NASA University Research Center-Student Conference, Nashville, TN, April 7-10, 2000.
11. "Curing optimization of IM7/5250-4 prepregs under field repair conditions", 20th High Temple Workshop, January 24-27, 2000.
12. "Thermal and hygrothermal aging effects on the properties of IM7/BMI composites", 7th Annual International Conference on Composites Engineering, Denver, Colorado, July 2-8, 2000.
13. "Post-Curing Effects on Physical and Mechanical Properties of IM7/5250-4 Composites", *30th International SAMPE Technical Conference*, Vol. 30, 226, 1998.
14. "Hygrothermal Effects on the Thermal and Mechanical Properties of IM7/5250-4 Composites", *44th International SAMPE Symposium & Exhibition*, Vol. 44, 734, 1999.
15. "Short-Term Aging Effects on Thermal and Mechanical Properties of IM7/5250-4 Composites", *44th International SAMPE Symposium & Exhibition*, Vol. 44, 741, 1999.
16. "Physical and Mechanical Characterization of Glass/Vinyl Ester Composite under Environmental Cycling", *12nd International Conference on Composite Materials*, Paper 626.
17. "Study of Thermal and Hygrothermal Behaviors of Glass Fiber/Vinyl Ester Composites", to be published on *Fiber Reinforced Plastics and Composites*.
18. Paul O. Biney, Yang Zhong, and Jianren Zhou, "Hydrolytic Effects on the Properties of IM7/5250-4 Composites", 43nd International SAMPE Symposium & Exhibition, Anaheim, California, May 31-June 4, 1998.
19. Yu He, Yang Zhong, and Jianren Zhou, "Postcuring Effects on the Physical and Mechanical Properties of IM7/5250-4 Composites", accepted by International SAMPE Technical Conference.
20. Rice, B. P. and Lee, C.W., "Study of Blister Initiation and Growth in a High-Temperature Polyimide," 29th International SAMPE Technical Conference, October 1997.

21. Rice, B. P. and Lee, C.W., "Study of Blister Initiation and Growth in a High-Temperature Polyimide Composites," High Temple Workshop XVIII, Jan. 1998, pp. V1-V22
22. Y. He and J. Zhou, "Effect of processing on mechanical properties of BMI polymer matrix composites", Proceedings of the Fifth Engineering & Architecture Symposium, Prairie View, TX, Feb. 6 - 7, 1997, pp. 389 – 392
23. D. Yang and J. Zhou, "Interfacial transfer of polymers and their composite in tribological applications", Proceedings of the Fifth Engineering & Architecture Symposium, Prairie View, TX, Feb. 6 - 7, 1997, pp. 479 - 482.
24. Y. Zhong and J. Zhou, "Fractography of polymeric matrix composites", Proceedings of the Fifth Engineering & Architecture Symposium, Prairie View, TX, Feb. 6 - 7, 1997, pp. 483 - 486.
25. Y. Zhong and J. Zhou, "Effects of fiber/matrix interface on the mechanical properties of polymer matrix composites", Proceedings of the Fifth Engineering & Architecture Symposium, Prairie View, TX, Feb. 6 - 7, 1997, pp. 487 - 490.
26. P. Biney and Y. Zhong, "Manufacturing processes of polymeric matrix composites: an overview", Proceedings of the Fifth Engineering & Architecture Symposium, Prairie View, TX, Feb. 6 - 7, 1997, pp. 153 - 158.
27. Y. He and J. Zhou, "Observation of Structure-Property-Performance Relationship in Polymer Matrix Composites for Elevated Temperature Application," ibid., III-H 1-9.
28. D. Yang and J. Zhou, "Transfer Film Formation and Its Effect on Tribological Properties of Polymer Composites," ibid., V-D 1-10.
29. Carson and R. Jones, "Fluorine Substitution to Improve the Oxidative Stability of High-Temperature Polyimides," ibid., III-F 1-12.
30. Rice, B.P., "Characterization of High Temperature Polyimides," Proceedings of High-Temple Workshop XVII, J1-J23, February 1997.
31. Rice, B. P., "Characterization of High Temperature Polyimides," Proceedings of HITEMP Workshop, April 1997.
32. Rice, B. P. and Lee, C.W., "Study of Blister Initiation and Growth in a High-Temperature Polyimide," Proceedings of 29th International SAMPE Technical Conference, October 1997.

APPENDIX A

FAST CENTER CAPABILITIES & INFRASTRUCTURE BROCHURE